Maritime Research Seminar '99

TECHNICAL RESEARCH CENTRE OF FINLAND ESPOO 2000

VTT SYMPOSIUM 199

Keywords: marine research, marine engineering, meetings, shipbuilding, ice, ships, safety, Finland, design process, ship hulls, fast planing boats

Maritime Research Seminar '99

Espoo, Finland, March 17th, 1999

Edited by

Tapio Nyman

VTT Manufacturing Technology

Organised by

The Maritime Institute of Finland

VTT

TECHNICAL RESEARCH CENTRE OF FINLAND
ESPOO 2000

ISBN 951–38–5275–X
ISSN 0357–9387

JULKAISIJA – UTGIVARE – PUBLISHER

Valtion teknillinen tutkimuskeskus (VTT), Vuorimiehentie 5, PL 2000, 02044 VTT
puh. vaihde (09) 4561, faksi 456 4374

Statens tekniska forskningscentral (VTT), Bergsmansvägen 5, PB 2000, 02044 VTT
tel. växel (09) 4561, fax 456 4374

Technical Research Centre of Finland (VTT),
Vuorimiehentie 5, P.O.Box 2000, FIN–02044 VTT, Finland
phone internat. + 358 9 4561, fax + 358 9 456 4374

VTT Valmistustekniikka, Laiva- ja konetekniikka, Tekniikantie 12, PL 1705, 02044 VTT
puh. vaihde (09) 4561, faksi (09) 455 0619, (09) 456 5888

VTT Tillverkningsteknik, Skepps- och maskinteknik, Teknikvägen 12, PB 1705, 02044 VTT
tel. växel (09) 4561, fax (09) 455 0619, (09) 456 5888

VTT Manufacturing Technology, Maritime and Mechanical Engineering, Tekniikantie 12, P.O.Box 1705,
FIN–02044 VTT, Finland
phone internat. + 358 9 4561, fax + 358 9 455 0619, + 358 9 456 5888

Otamedia Oy, Espoo 2000

Preface

This publication contains the papers given at the seminar 'Marine Research 99'. Seminar was organized by the Maritime Institute of Finland, which is the joint venture between Helsinki University of Technology and the Technical Research Centre of Finland. The aim of seminar was to present to the industry the latest results of the research work done at Otaniemi. This seminar continues and promotes the dialogue between maritime research and industry in Finland.

A modern and competitive ship designer needs today deep knowledge about physical problems in ship and marine structures as the ships are becoming technically more and more complicated. Application of design methods based on 'the first principles' are essential in order to decrease the over dimensioning. Important aspect in the implementation of new methods into the ship design process is that the designer has a clear picture of the contents of the methods and understands the limits of the capabilities of the methods. The iterative nature of the ship design process must be taken into consideration - the accuracy of the design converges stepwise. This means that the methods must accept the limited information at the beginning phase.

The contents of the papers given are divided into several items from ship performance in open water and also in ice to ship safety. The topics are based on the research work carried out during the past years in different research projects. The range of topics covered by the papers of the seminar is broad, which gives a good overview on the research activity in the Institute, but at the same time the broadness inevitably limits the depth of discussion on particular problems. The lecturers are thanked for their valuable contributions.

The seminar was held at Hanasaari in Espoo. The number of participants was about 50 persons. Mr. Martin Landtman, the director of Helsinki New Shipyard, Kvaerner Masa-Yards, gave the opening address. He emphasized the importance of the close contacts and co-operation between the industry and the institute. The discussions during the day gave us evidence that the general direction of the research work carried out in Otaniemi on marine technology is correct. We hope that the participants of the seminar gained some useful ideas. The participants from industry should be thanked for making the time to take part in the seminar.

Otaniemi 26th January 2000 Petri Varsta

Contents

Opening remarks

Martin Landtman, Kvaerner Masa-Yards

Mister Chairman, seminar participants!

At first I would like to take the opportunity to thank you for the invitation to participate in this seminar and for the chance to start it off with a brief address which I do with pleasure. Unfortunately, president and CEO Martin Saarikangas was not able to attend today. I hope that what I have to say to you will serve to compensate for his absence.

Today's seminar is the fifth one organised by the Maritime Institute of Finland. One should point out that the institute has done a commendable job in making its way to the top and securing its position in the field of maritime research in Finland. What is essential from the industry's perspective is the considerable extent to which customers' needs have been taken into consideration. In my view the industry is one of the main customers of the institute. This, more than anything, is a case in point of how resources and expertise need to be joined in Finland. When VTT and the Helsinki University of Technology combine their expertise, theoretical background and practical applications, actual results begin to emerge.

Previously held seminars have focused on specific narrow segments such as "Numerical tools for ship design", "Marine safety" and "Structural design" and related issues.

As Professor Jansson pointed out just a moment ago, the subject matter of today's seminar covers more ground, "something for everyone". This may well be a fitting approach. We are well aware of the fact that an extensive amount of research in various fields is being conducted through the institute and under its management. One of today's subjects is ship damage. This is always a very topical subject. Mechanical resistance of equipment will be discussed and is always a central issue in terms of ship design and use. The agenda today also includes fast boats, which traditionally is a strong area of expertise for both VTT and the University of Technology, and will hopefully continue to be so in the future. I am sure we are going to be pleased to learn of the latest developments in this area. Other subject matters include the dimensioning of propellers and ship hull beams with the help of the latest technology and expertise. In the expertise areas I mentioned, many advancements have surely been made under the institute's management.

The study of ice is also on the agenda. This is one of our expertise areas and we must ensure that it continues as such. I was intrigued to notice that the use of virtual methods is included as one the subjects discussed today. Without a doubt, virtual technology will increasingly be used at shipyards. Appropriately enough, marine safety is also on the agenda today.

It can probably be maintained that all these subjects are essential in terms of the success of our industry. I would also like to talk briefly about our industry, the maritime cluster.

What we have is industry, suppliers, establishments of higher education and other educational institutes, and a research organisation. All these compose our cluster. Combined together, the yield of this cluster results in a remarkable turnover. Naturally, we must work together to ensure the continued success of the entire industry. In this sense, today's seminar is of primary importance.

One of our most essential tasks in Finland is the correct management of resources. Operations that have been decentralised to too large an extent fail to produce results in research as well as within the industry. At present, a proper concentration of resources is one of the main challenges of the institute. As far as I can see, the institute has been fairly successful in selecting a few key areas for deeper focus. In addition, the industry is facing a similar challenge. We at shipyards and the suppliers need to combine our resources on primary issues. This is further emphasised especially during these turbulent times we have once more found ourselves in, not only in European shipbuilding but also globally. We are aware of what is happening in Korea, the situation in Europe as well as globally regarding the subsidising of Far Eastern exchange rates. Furthermore, the expected OECD agreement was not concluded after all.

A plunge in oil prices has resulted in a decline in the offshore sector, container ship prices and cargo volumes. All this presents us with great challenges. One general feature worth mentioning is the present oversupply of shipbuilding capacity, which will not discontinue. There is no indication that the current low price levels would rise in the near future. The current difficult situation is likely to prevail. This is something not to be overlooked by shipyards or the industry. Naturally, our future also depends, to a large extent, on the favourable development of external factors such as exchange rates and the European shipbuilding and industrial policy in general. Structural changes are on the way, not only in Europe but globally as well. In this industrial branch, only the "good students who make their way to and stay at the top" will be able to keep going. In other words, we must do our "homework" diligently.

I would like to mention a few points that are important from our shipyards' point of view. In a wide sense, we must improve the general quality to a level unseen before. It is high time to turn our industry into a methodical one. We must break away from workshop mentality. In many ways, shipbuilding still remains at the level it was in the 1970s and 1960s. Craftsmanship and improvisation are too prevalent. Methodicalness is the most important thing for the industry in case efficiency desired. If one wishes to operate in a first-rate and methodical way, everything depends on basic factors starting from basic design, research and product development and from there onwards. I believe that the above-mentioned combined with the challenge brought on by the new kind of networked operations in Europe constitute our biggest challenges in the near future. In other words, quality must be raised to a new level bearing in mind the fact that, in a networked society, a completely new way of operation is required. This also relates to research, which will no longer be conducted at shipyards. Institutes such as this one are needed for co-operation in matters such as those on the agenda today which will hopefully also give rise to active discussion. The industry should be better able to utilise, for example, the resources that area represented here today. This is an enormous challenge, and is largely dependent on how active the industry is.

Here in Otaniemi, VTT and the Helsinki University of Technology represent the vanguard of know-how. The matter in question is how we can best utilise these expertise areas and skills together. There are still barriers between the industry and the institute. It is high time we removed such hindrances. It is hardly an overstatement to say that we need each other, the industry cannot operate without the support of research organisations and vice versa. As far as we are concerned, we are ready to make this type of investment. Unfortunately, the industry has to grapple with everyday problems and does not always have adequate resources to look into the future and beyond what can already be seen on the horizon. This is the point where supporters are needed, as they force us to focus on problems that are closer at hand and to pay attention to what is behind them. We are part of Europe. We should consider which joint European projects to participate in, and select a few to invest in. We should try to take the lead in the selected projects and strive to influence their development. This is where we stand.

I would like to express my thanks to the leaders of the institute and today's speakers and lecturers for your important contribution to the study of Finnish shipbuilding and our entire industry in general. This work is of essential significance. There are many interesting subjects on the agenda today which can be expected to give rise to interesting discussion. I take this opportunity to welcome everyone to this seminar once again, thank you.

DAMAGE OF SHIP BOTTOM STRUCTURES IN GROUNDING ACCIDENT

Jyri Luukkonen
Helsinki University of Technology, Ship Laboratory
Espoo, Finland

Abstract

This paper summarises some of the main results recently published in the master's thesis of the author. Detailed damage data was gathered from 20 grounding accidents that occurred in Finnish waters after 1980. The characteristics and extent of the damage are analyzed. Simple methods published in literature for predicting forces and energy absorbed due to grounding are discussed and their applicability to grounding accidents is investigated. A brief overview of general grounding statistics of 90's is also presented.

1 INTRODUCTION

The development of safety systems has reduced the risk of accidents at sea. Despite this, safety of the ship, its crew, passengers and cargo can be endangered by rough weather, human error or technical failure. In these situations, the severity and consequences of possible accidents depend much on the structural safety of the ship. In the case of collision or grounding, applicable design of structures and subdivision has a positive effect on preventing possible flooding. The increased amount of double hull tankers is a good example of the development of structural safety.

A grounding accident can be defined as an incident in which the bottom of a ship collides with underwater soil causing scratches, dents or even tears to bottom shell plating. The incident is called a 'bottom touch' when the ship does not become stuck on a rock. This means that its kinetic energy is not totally absorbed. Kinetic energy depends on the ship's velocity and displacement. *Figure 1* illustrates the difference between penetration δ and vertical extent d of bottom damage.

The grounding problem can be divided into external dynamics and internal mechanics. The model for the external dynamics calculates the rigid body ship motion given a force on the hull. The model for the internal mechanics estimates the force on the hull given a certain penetration of the rock into the hull. Internal mechanics includes energy dissipation by plastic deformation and fracture and energy dissipation by friction. Ship motions are normally neglected in the studies concerning damage of structures.

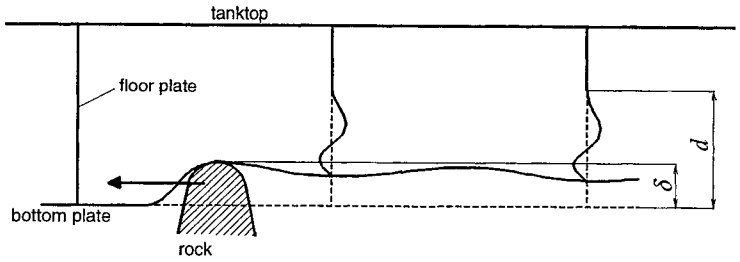

Figure 1. Definition of penetration δ and vertical extent d of damage caused in grounding.

For proper direction in the development of safer ship structures and constructions in the future, it is profitable to know the characteristics of structural damage and their effects on a ship. There are relatively many studies about groundings published in literature but those dealing with damage caused in real grounding incidents are very scarce. The most important part of the analysis made by Luukkonen (1999) was to gather as detailed as possible damage data.

2 GROUNDING STATISTICS OF 90'S IN FINLAND

Collisions are the most frequent of all the major accidents which a ship can experience in Finland. According to the statistics of *Nordic Dama*, which is an accident data base maintained by the Finnish Board of Navigation, over half of all collision incidents were groundings. Forty-eight percent occurred near islands or on a narrow route.

During the years 1990-97 the Finnish Board of Navigation was informed of 274 grounding incidents. The annual number of grounding accidents are given in *Table 1*. The total number of groundings is divided into groups according to the gross tonnage of the ships.

Table 1. Annual number of groundings in Finland.

BRT	1990	1991	1992	1993	1994	1995	1996	1997	Yht.	percentage
-98	7	12	8	4	2	1	5	3	42	15,3 %
99 -498	7	14	10	10	3	7	7	9	67	24,5 %
499 -998	7	5	3	3	2		3	2	25	9,1 %
999 -1998	6	7	4	7	4	3		1	32	11,7 %
1999 -4998	5	2	4	2	3	4	4	5	29	10,6 %
4999 -9998	5	2	3	3	4	3	2	4	26	9,5 %
9999 -	3	2	3	4	2	6	6	2	28	10,2 %
not known	2	3	5	3	4	4	2	2	25	9,1 %
total	**42**	**47**	**40**	**36**	**24**	**28**	**29**	**28**	**274**	

The data of *Table 1* is illustrated in *Figure 2* with a rougher division of ship's size. According to *Figure 2* it seems that the smaller ships have the biggest effect on the variation of the annual number of groundings. The grounding frequency of bigger (>998 GRT) ships has been relatively constant throughout this time period. More statistics on the groundings

which have occurred in Finnish waters are given in the reports of Kaila & Luukkonen (1998) and Luukkonen (1999).

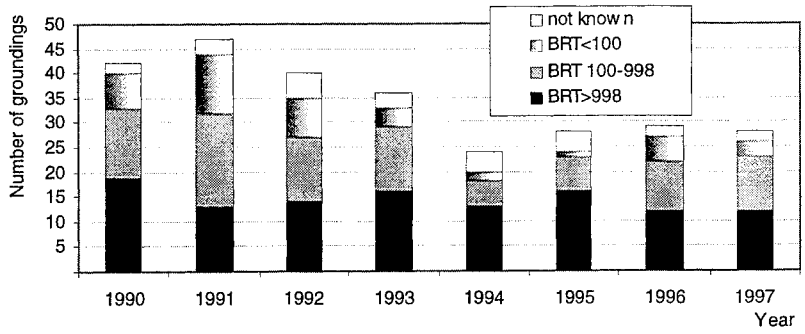

Figure 2. Number of groundings during 1990-97.

3 CHARACTERISTICS OF THE GATHERED DAMAGE STATISTICS

Detailed damage data was gathered from 20 grounding accidents occurring after 1980. The main sources for the data needed for this analysis were the files of shipowners and the Finnish Board of Navigation. Diver's reports, shipyard's work list, survey reports and photos were the documents from which the damage data was mainly collected. Accuracy of the available damage data varies a lot among these grounding cases.

Exact location of the damage was found out from the shipyards' work list and the ships' shell expansion. The actual volume of the damaged steel was not specified, so the extent of damage is defined by the mass of replaced bottom structures. A rough estimate for the ratio of deformed and replaced steel volume is 50-80%, depending much on the extent of damage. The absorbed energy E due to grounding is approximately given as:

$$E = \frac{1}{2} m(1 + C_a)(v_1^2 - v_2^2) \qquad [1]$$

where m is ship's displacement (*tons*), v_1 is the velocity of a ship (*m/s*) before and v_2 after grounding and the added mass coefficient C_a is often taken as 0,1.

The main damage data of the grounding cases is presented in *Table 2*. Vertical extent of damage d is that which extended from the baseline to the uppermost deformation in a structure in way of the ruptured tanks (see *Figure 1*). Respectively, horizontal extent s is the distance between the foremost and the aftermost deformed bottom structure parallel to the ship's symmetry line. The area of replaced bottom plate and total mass and volume of replaced bottom structures are also given in *Table 2*.

Table 2. Main data of the grounding cases.

	Displacement [ton]	Velocities v_1 [kn]	v_2 [kn]	Absorbed energy E [MJ]	Damage data Vertical extent d_{max} [m]	Horizontal extent s_{max} [m]	Replaced structures Area of replaced plate A [m^2]	Bottom plating m [ton]	Inner structures m [ton]	**Total mass m [ton]**	Volume of steel R_T [m^3]
ship#1	21100	15	0	690,9	1,35	93,6	638	82,7	50,3	**133,0**	16,6
ship#2	22700	8	1	208,1	1,50	108,9	475	54,9	40,6	**95,5**	11,9
ship#3	22100	13,5	8	380,3	1,60	101,5	549	70,7	82,8	**153,5**	19,2
ship#4	8980	1,5	0	2,9	0,75	7,2	20	2,7	0,4	**3,0**	0,4
ship#5	8780	18	16	86,9	1,20	50,4	45	4,5	4,6	**9,2**	1,1
ship#6	9830	1,5	0	3,2	0,65	13,6	15	3,8	2,0	**5,8**	0,7
ship#7	12000	14	0	342,3	1,90	92,2	1124	134,0	140,0	**274,0**	34,3
ship#8	57000	2,5	1	43,6	0,98	37,2	152	18,7	2,3	**21,1**	2,6
ship#9	11025	6	0	57,8	0,80	22,5	100	14,0	26,0	**40,0**	5,0
ship#10	12829	19	10	487,3	1,20	107,2	929	115,0	155,0	**270,0**	33,8
ship#11	9800	9	0	115,5	0,95	25,3	79	11,4	10,3	**21,6**	2,7
ship#12	25673	3	0	33,6	0,80	8,8	20	4,4	1,6	**6,0**	0,8
ship#13	14200	10	5,5	144,1	1,00	28,8	120	23,6	23,6	**47,2**	5,9
ship#14	9050	11,5	0	174,2	1,95	50,2	327	44,1	28,7	**72,8**	9,1
ship#15	25580	4	0	59,6	?	8,1	65	11,7	11,3	**23,0**	2,9
ship#16	16100	12	11	53,9	1,10	32,9	35	4,3	2,8	**7,0**	0,9
ship#17	12200	13	0	300,1	2,00	46,8	479	52,8	55,9	**108,7**	13,6
ship#18	8582	14	0	244,8	1,50	60,8	442	62,3	40,0	**102,3**	12,8
ship#19	18700	3	0	24,5	0,60	40,2	61	7,4	10,9	**18,3**	2,3
ship#20	350	9	0	4,1	0,60	9,0	17	1,5	0,7	**2,1**	0,3

3.1 MAIN TYPES OF GROUNDING

Plans of the damaged ship bottom areas are presented in *Figures 3, 4, 5* and *6*. The solid outline refers to the line of the flat bottom and the dashed outline respectively to the tanktop in these figures. Hatched areas are the bottom strakes which have been replaced. According to the location and extent of the damage, three main types of damage can be found:

- *Bow damage*. The damage begins from the area of the stem or bulb and continues aft parallel to the ship's symmetry line. The damage extends only for a length of a few double bottom tanks *(Figure 3)*.
- *Bilge damage*. The damaged area is on SB- or BB-side of a ship and follows the region of bilge/near the flat bottom edge aft. Its initial location is between fore and mid ship *(Figure 4)*.
- *Extensive damage*. The damaged area begins from the bow region of a ship and extends on both sides of the symmetry line over 1/3 of a ship's length. The damage usually contains several ruptures and extensive denting zones. Extensive damage causes an actual risk of ship sinking or capsizing. Typically there is also more than one contact point between the underwater ground and the ship's bottom plating, unlike the case of *bow* or *bilge damage (Figure 5&6)*.

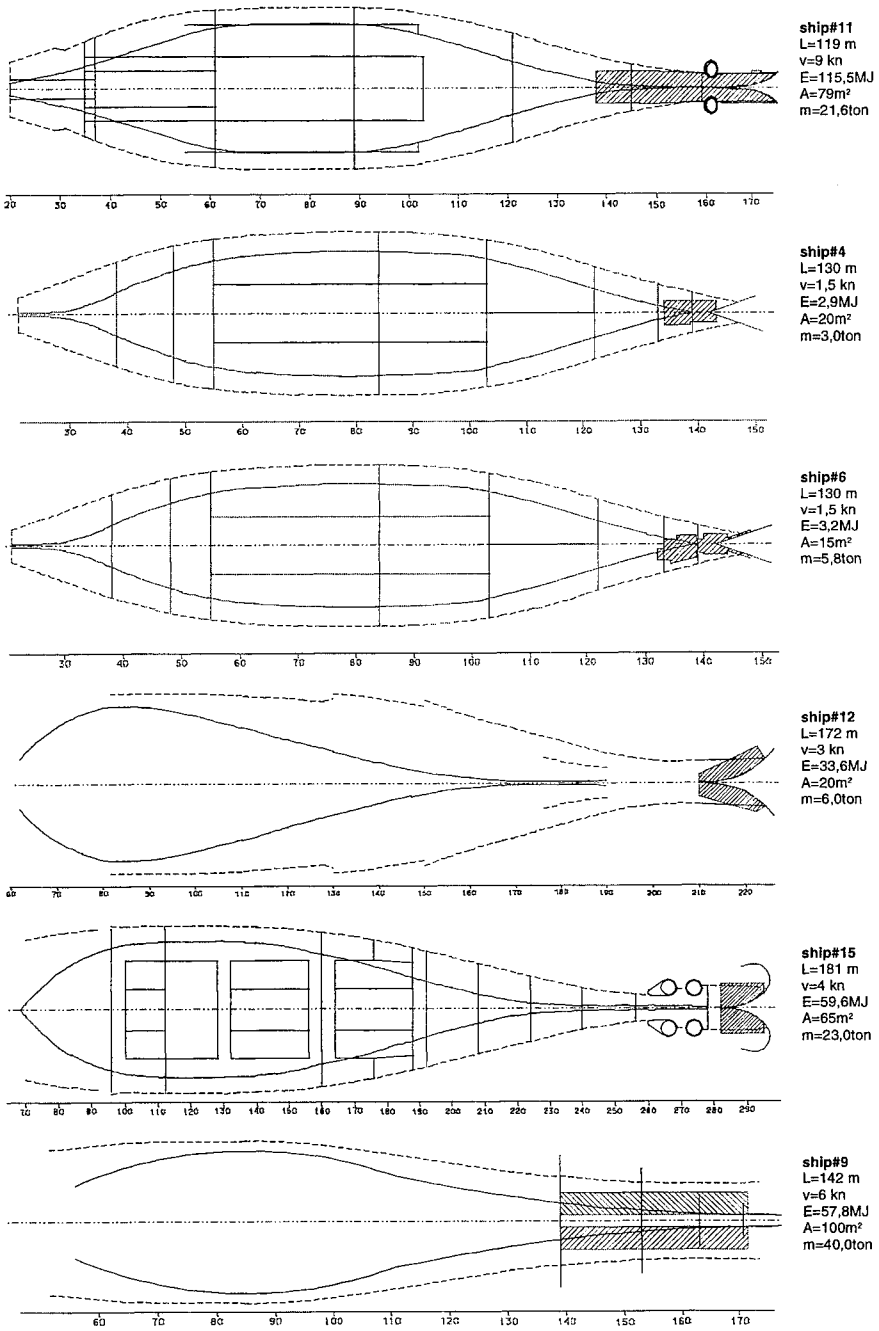

Figure 3. *Ships with bow damage. Ship n:o, waterline length, velocity (and velocity after grounding), absorbed energy, mass and area of replaced shell plating are given.*

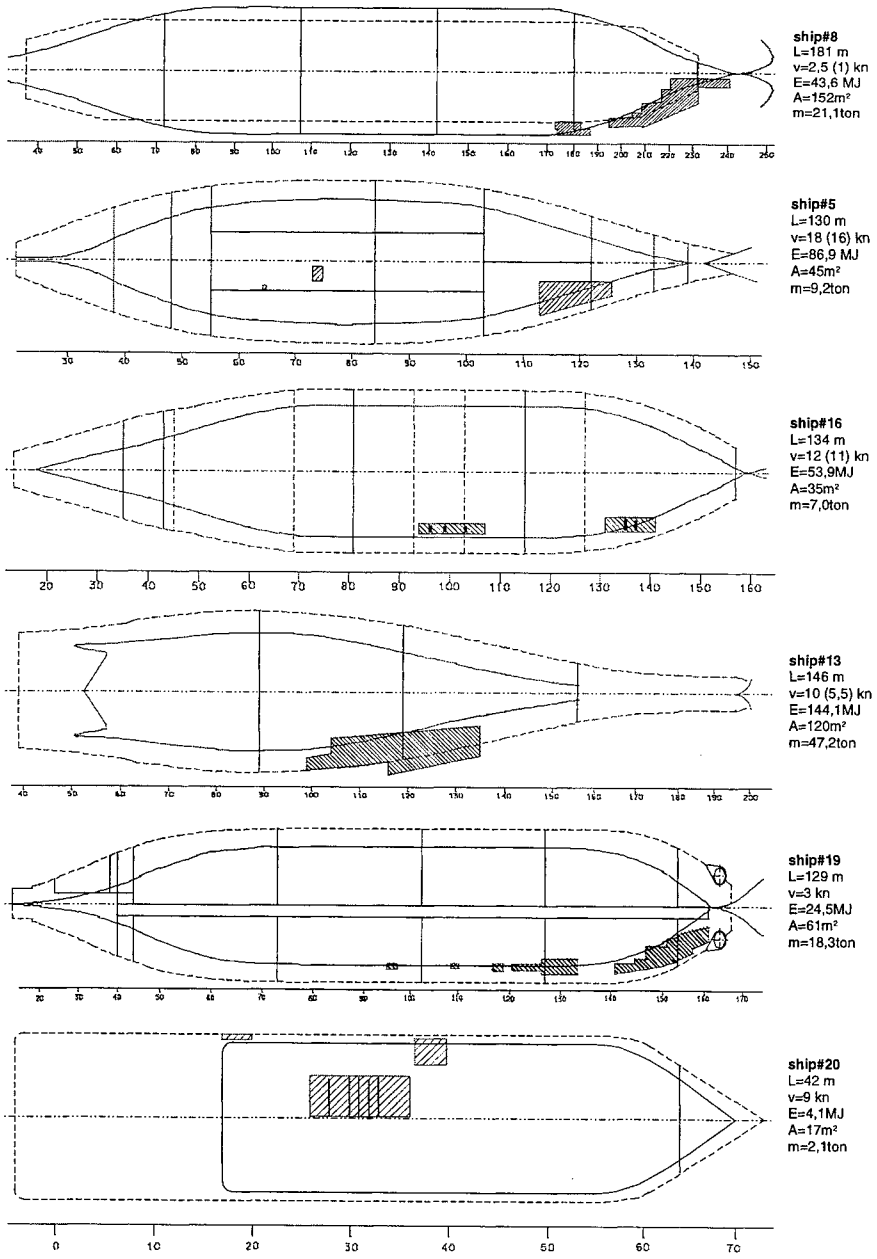

Figure 4. *Ships with bilge damage. Ship n:o, waterline length, velocity (and velocity after grounding), absorbed energy, mass and area of replaced shell plating are given.*

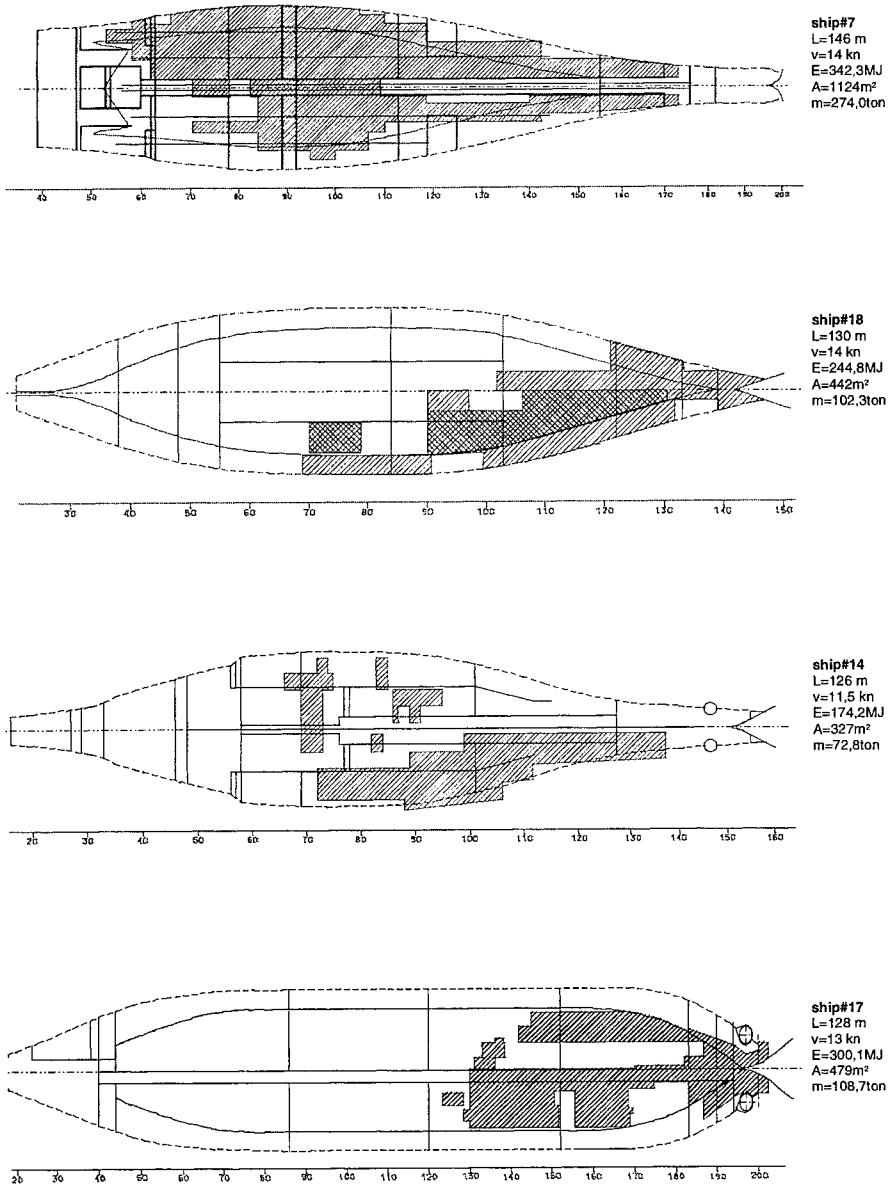

Figure 5. *Ships with extensive damage. Ship n:o, waterline length, velocity (and velocity after grounding), absorbed energy, mass and area of replaced shell plating are given.*

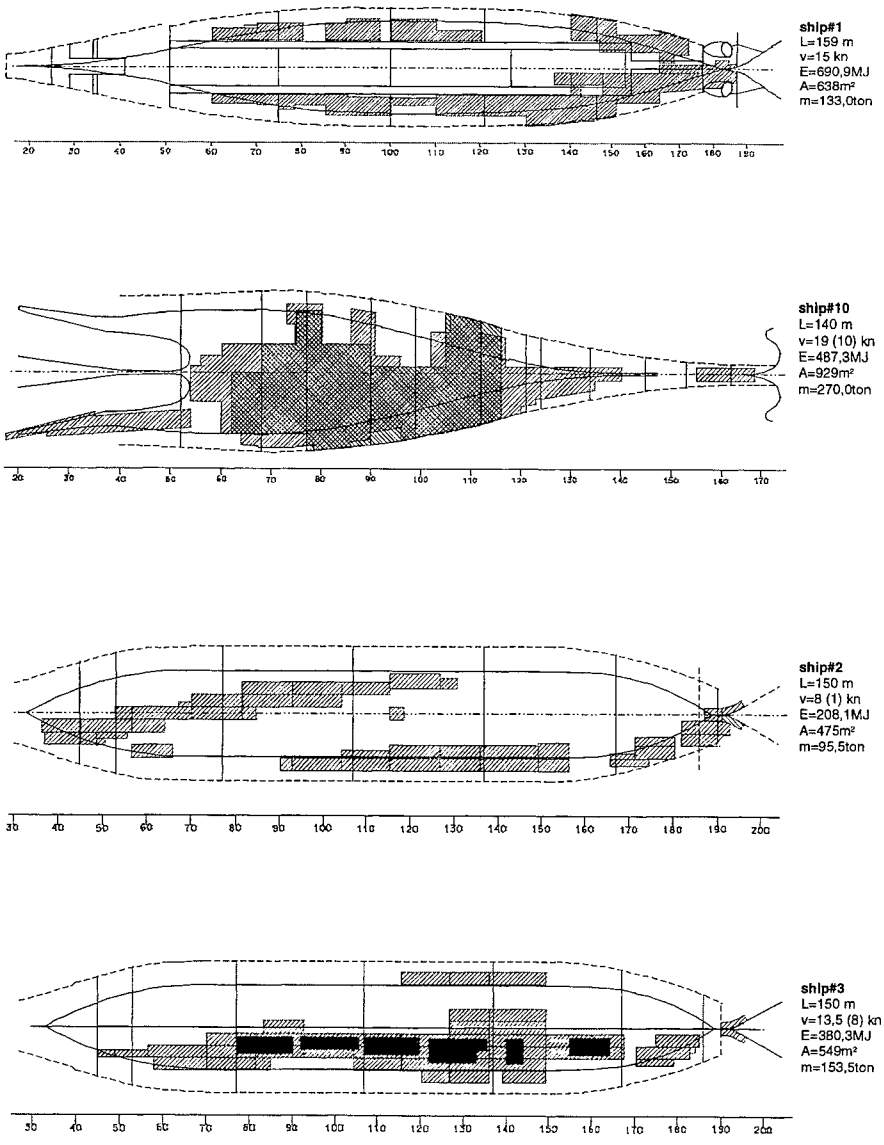

Figure 6. Ships with extensive damage. Ship n:o, waterline length, velocity (and velocity after grounding), absorbed energy, mass and area of replaced shell plating are given.

3.2 SHIP'S KINETIC ENERGY

The amount of energy absorbed in each of the 20 grounding cases is illustrated in *Figure 7.* As can be seen, groundings in which the amount of absorbed energy is small correspond to *bow* or *bilge damage.* All the ships with bow damage has stopped on the rock. This means that a minor amount of the kinetic energy of the ship has been totally absorbed by the region of the bow structures. In the case of a greater amount of kinetic energy *extensive damage* could have occurred instead of *bow damage.*

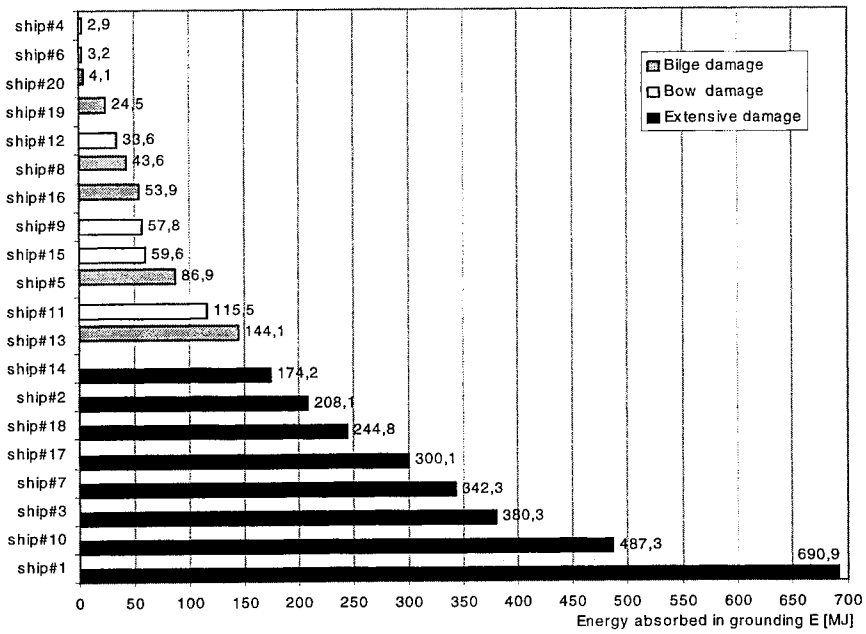

Figure 7. Grounded ships and the amount of absorbed energy.

Four of six ships with *bilge damage* are 'bottom touches'. The kinetic energy of these ships may have been great, but because of the location of the grounding contact point on the bilge or near the edge of the flat bottom, the ship has 'come off' the rock and only a minor amount of kinetic energy has been dissipated.

According to the assumptions and *Figure 7* presented above, a limit for absorbed energy of *extensive damage* can be set to 144MJ (ship#13's absorbed energy, which is the greatest of *bow* and *bilge damage* cases). The ships operating within that limit avoid the possibility of *extensive damage.* A limit curve for 144MJ of absorbed energy is presented in *Figure 8* as a function of ship displacement and velocity.

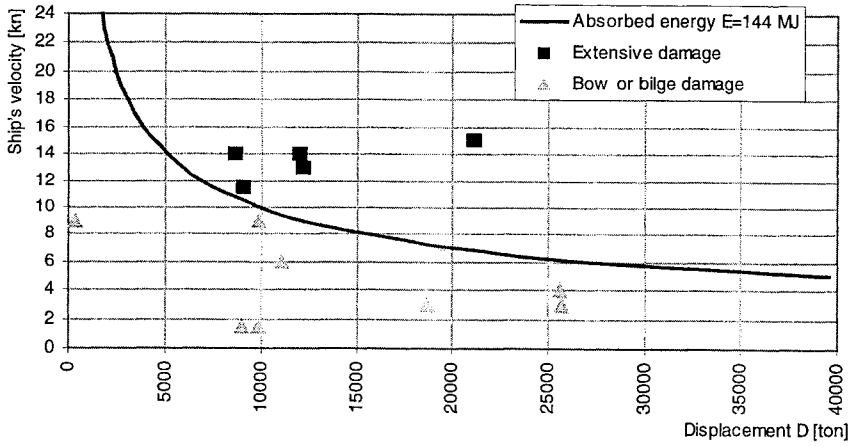

Figure 8. *Limit curve for 144MJ of absorbed energy presented as the function of ship displacement and velocity.*

3.3 SIZE OF DAMAGE

The mass of replaced bottom structures is plotted as a function of absorbed energy in *Figure 9*. A graph was drawn through the points to present a relationship between absorbed energy and replaced steel. The formula of the graph seen in *Figure 9* is

$$E = 2{,}5548 m_r^{0{,}9901} \quad [MJ] \qquad [2]$$

where m_r is the mass of replaced structures in tons.

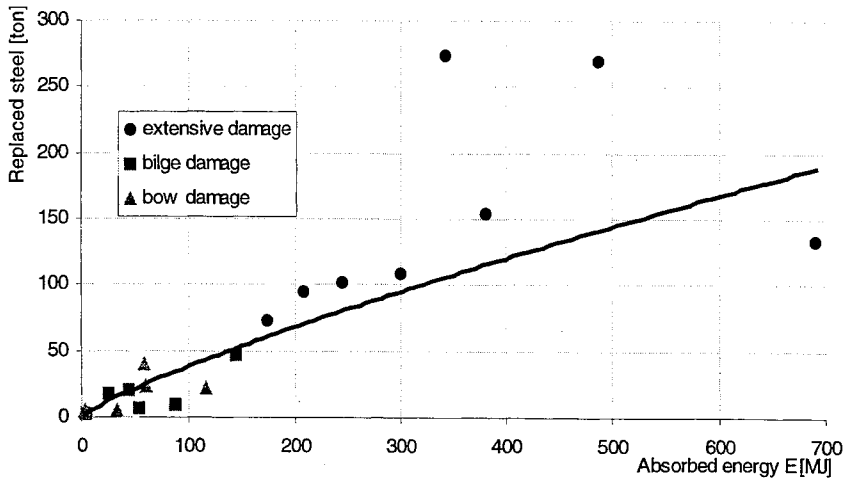

Figure 9. *Replaced steel as the function of absorbed energy.*

It is clearly seen from *Figure 9* that especially with minor and major values of absorbed energy the amount of replaced steel deviates significantly from the graph drawn. This observation supports the fact that energy absorbed in grounding depends not only on the volume of damaged steel but also on the geometry of a structure.

4 PREDICTION OF ENERGY ABSORBED IN GROUNDING

4.1 SIMPLE ANALYTICAL METHODS

A couple of simple analytical methods for predicting forces and energy absorbed due to grounding have been developed. Minorsky's (1959) and Vaughan's (1977) formulas are the most simple and probably the best known in the field of collision and grounding studies. Minorsky assumed that there was a linear relationship between absorbed energy and damaged steel. In the SI-units, Minorsky's formula for the absorbed energy E is

$$E = 47R_T + 32 \quad [MJ] \qquad [3]$$

where R_T is a resistance factor defined as the volume (m^3) of damaged material.

Minorsky's *Formula 2*, which was later modified by Vaughan (1977), was initially developed in 1959 to predict the collisions of a nuclear powered ships. Vaughan analyzed the Japanese plate cutting experiments (Akita 1972) and included a factor of energy absorbed by a cutting wedge in Minorsky's formula. According to Vaughan the energy absorbed by a structure G is

$$G = 352V_S + 126A_S \quad [tons \cdot knots^2] \qquad [4]$$

where V_S is the volume of damaged material in the structure ($m^2 \cdot mm$) and A_S is the area of torn plate ($m \cdot mm$).

More advanced but also more complicated approach to predict the grounding forces are presented by Thomas and Wierzbicki (1992), Ohtsubo (1997) and Simonsen (1997). The geometry of a structure is taken into account in the methods based on the various damage mechanisms of a single structural component. The formulas, assumptions and parameters used on these methods are discussed in greater detail in Luukkonen (1999).

A sufficiently "sharp" rock to cause penetration of the hull is assumed in the method of Thomas and Wierzbicki (1992). In this method the resisting force is expressed as a sum of the fractional contributions due to the primary failure mechanisms of the major structural members. Ohtsubo's

(1997) method considers four primary structural failure modes; behavior of transverse structures such as floors, deformation of the plates and and last two for the torn bottom plate and inner bottom plate. Simonsen's (1997) grounding model includes various damage mechanisms for each individual structural member of the bottom before and after the structure has fractured.

4.2 APPLICABILITY OF THE METHODS

Applicability of the methods is examined by the data gathered. At first, the absorbed energy of each of the 20 grounding cases of the study was assessed with *Formula 2* and the formulas of Vaughan and Minorsky. The ratio of damaged and replaced steel is taken as 0,5. Deviation percentages of assessed energy are illustrated in *Figure 10.* As seen, a moderate correlation in results is found only on a range of 100-400MJ energy absorbed.

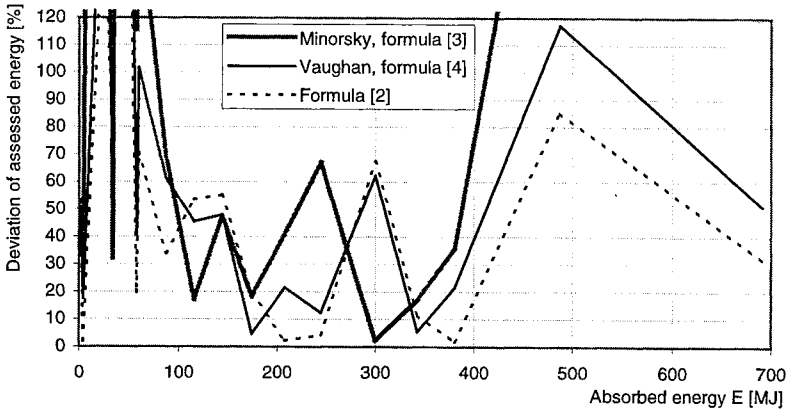

Figure 10. Deviating percentage of assessed and absorbed energy.

Some parameters of Thomas & Wierzbicki's and Ohtsubo's methods are to be found too difficult to define in actual groundings. In addition to that, the damage models described in damage statistics report by Luukkonen (1999b) differ a lot from the models assumed in the methods. Simonsen's method was preferred for prediction of energy absorbed in two different cases chosen; *ship#2 (see Figure 11)* and *ship#20.* a conventional double hull tanker with longitudinal frames and transverse floors at the bottom and, a single bottom transversely framed freighter which suffered relatively minor damage.

The calculations were simplified by taking only deformation of the bottom plates, floors and longitudinal frames into account. Longitudinal frames were treated as a reduced thickness of the bottom plating. Values needed for vertical extent of the damage were found in the shipyard's work lists and the

penetration and width of the damage were estimated from the photos, diver's reports and measurements (in case of *ship#20*).

According to *Table 2*, the kinetic energy dissipated in the groundings of *ship#2* and *ship#20* are 208,1MJ and 4,1MJ. As the calculated values of energy absorbed by the bottom structures are 195,9MJ and 3,7MJ using the Simonsen's method, a satisfactory accuracy of the results is reached; the deviating percentages are 10% for *ship#2* and 6% for *ship#20*.

The energy dissipation in the grounding of *ship#2* is illustrated in *Figure 11*. The graph presents the amount of remaining kinetic energy. As can be seen, energy absorption is relatively great at the bow region of the ship because of the more frequent spacing of the transverse floors.

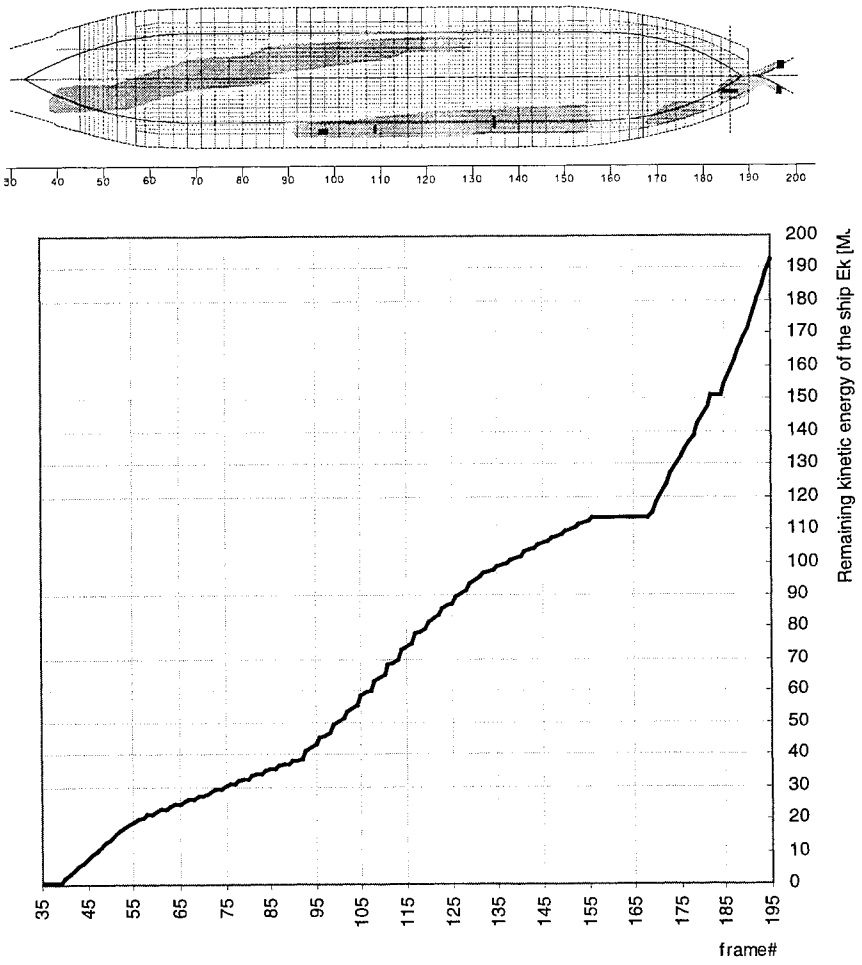

Figure 11. *Energy absorbed by the bottom structures of ship#2 from the bow to the stern. In the ship's plan above the graph, the floors are illustrated as vertical lines and the frames as horizontal lines.*

5 CONCLUSIONS

Detailed damage data was gathered from 20 grounding accidents. The characteristics and extent of the damage was analyzed. Three main types of grounding damage were found; *bow damage*, *bilge damage* and *extensive damage*. *Bow damage*, in which the ship's kinetic energy is wholly absorbed in the structures located at the bow region, is a pre-stage of *extensive damage*. A limit value of absorbed energy of 144MJ was found for these two stages.

Applicability of some simple analytical methods for predicting bottom structure damage was investigated. Assessment of damaged steel volume in the grounding cases of this study with Minorsky's and Vaughan's formulas revealed that there is a moderate correlation in results only on a range of 100-400MJ energy absorbed. Simonsen's method gives a good accuracy in the results.

Despite the fact that relatively accurate results are found, there are still a few difficulties using Simonsen's method. The method includes parameters which are not simple to define in real grounding incidents. Some of them are also too sensitive to the results. Developing a formula which takes into account the penetration of damage and separated volumes of damaged transverse and longitudinal structures into account, could provide a method to predict absorbed energy accurate and quick enough. This would require a continuous maintaining of detailed damage data base.

6 ACKNOWLEDGEMENTS

This paper summarises the study which is a part of a national research project *'Ship grounding and safety'*. That project is financially supported by TEKES, Kværner Masa Yards, Aker Finnyards, FG-shipping, Neste, Silja Line, Viking Line, Merenkulkuhallitus, Merivoimat ja Rautaruukki. This financial support is gratefully acknowledged. In addition the ship owners VG-Shipping and ESL shipping are thanked for helping to collect the detailed damage data.

REFERENCES

Akita, Y.; Kitamura, K., 1972. A study on collision by an elastic stem to a side structure of ships. Journal of the Society of Naval Architects of Japan, Vol. 131, June, s. 307-317

Kaila, J., Luukkonen, J., 1998. Tilastoyhteenveto Suomen aluevesillä tapahtuneista karilleajoista ja pohjakosketuksista. Otaniemi. Helsinki University of Technology, Ship Laboratory. M-233. 47 p.

Luukkonen, J.; 1999. Laivan pohjarakenteiden vauriot karilleajossa. Master's Thesis, Helsinki University of Technology, Ship Laboratory, 81 p.

Luukkonen, J., 1999b. Vauriotilastot Suomen aluevesien karilleajoista ja pohjakosketuksista. Otaniemi. Helsinki University of Technology, Ship Laboratory. To be published.

Minorsky, V.U., 1959. An analysis of ship collisions with reference to protection of nuclear power plants. Journal of Ship Research, No. 4 Dec, p. 1-4

Simonsen, B.C., 1997. Mechanics of ship grounding. Ph.D.thesis, Technical University of Denmark, Department of Naval Architecture and Offshore Engineering, February, 260 p.

Vaughan, H., 1977. Damage to Ships Due to Collision and Grounding. DnV Technical Report No. 77-345.

DESIGN PRESSURES FOR FAST PLANING BOATS

Gunnar Holm, MScTech, Markku Hentinen, MScTech
VTT Manufacturing Technology, Espoo

Abstract

An overview of the available methods for slamming pressure determination is given. Then the results of two different measurements on board fast boats are compared with existing methods. Finally the challenges connected to the high pressures at intermediate speeds are exposed and discussed.

1 WHAT IS THE PROBLEM?

Fast boats gather at present an increased interest through several new projects, where mainly public administrations but also various organisations and private owners are developing and/or purchasing fast 40+ knots boats. The desire to optimise the bottom structures of these and to ensure their reliability put the focus on dimensioning methods for fast boats in this smaller size region.

These planing craft may expose very high vertical acceleration values which are well in excess of those experienced on board fast craft in the 20 - 50 m range. The short duration of these accelerations causes less harm to the crew than on bigger craft and on the other hand, also seats with sophisticated suspension arrangements are used, too. Severe slamming can thus be allowed by the crew.

These factors together with reported structural damages on some boats and the results of measurement data from the fast NV 96 RIB (Rigid Bottom Inflatable) of the Finnish Coats Guard, initiated the efforts to establish some kind of criteria for fast planning craft "flying" from one wave crest to another or landing in between.

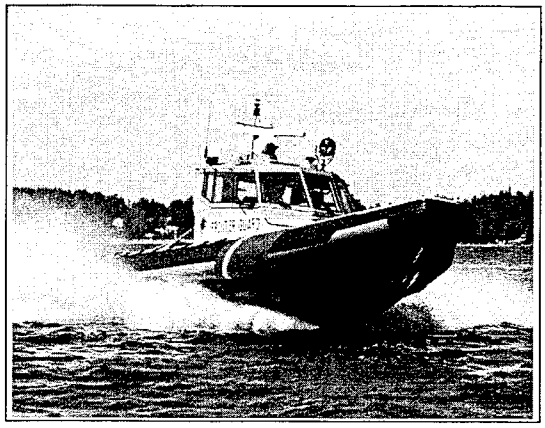

The widely used principle that the bottom pressure is growing in relation to the speed squared is challenged, due to several signals of which some are presented here.

2 THE STATE OF THE DIMENSIONING ART

In the project named SOFT RIDE, where work boat designers, builders and users co-operated with VTT, three basic questions were investigated:

1. Are there feasible calculation methods for slamming loads?
2. Are there methods for estimation of vertical accelerations?
3. Are there seakeeping criteria for these boats to which no ordinary seasickness criteria can be applied?

The study included a survey [1] by which a picture of the field was created on the basis of the following actions.

- conclusions from what is stated in the newest literature sources
- comparison between measured data and calculation methods
- addition of significant data to the picture by further measurements [2]

The literature was studied with the aim of identifying calculation methods, measurement results and slamming loads on fast craft in general. Whipping, springing and the frequency of slamming loads, which are of great importance on slower high speed vessels was not included. The interesting range was limited to Frouds displacement values in excess of 3.0. This means for example for a 10 ton pilot boat, a speed of more than 27 knots.

Corvettes, fast passenger ships and cargo vessels operate in a much lower speed range so the quite extensive literature in this field was only briefly studied.

The study comprised all major data banks, VTTs own literature sources and the Alta Vista search machine.

3 AVAILABLE SOURCES AND METHODS

Generally it can be stated that very little new information is available on the issue of planing boat slamming and accelerations. Most of the new information deals with bigger displacement or slow planing ships.

Rask [3], Faltinsen [4] and Hayman [5] have covered the fundamental principles of the slamming pressure issue and in the two latter ones the problem with high localised pressures is covered. We agree with Hayman that care has to be taken with sandwich structures because of possible high shear stresses due to the very local high slamming pressures. The application dealt with in these sources are bigger craft.

The web sites gave few results as most of the information have the nature of being advertisements of research projects rather than reporting on them. This situation may change day by day, as more and more reports are published on the net as printed.

The issue has also interested experts in Sweden and KTH/FMV have performed measurements and analysis on the Stridsbåt 90 E project. The speed during the measurements was 37 knots and the wave height 1.5 m. At CG the measured acceleration was 17g with 100 Hz filter. The highest pressure was 370 kPa.

3.1 COMPARISON BETWEEN METHODS

The most important methods, for calculation of slamming loads, were identified and studied. In general the problem is connected to the reliable prediction of:

- the relative speed between the water and the hull surfaces
- the coefficient k´s value as a function of steepness of the bottom
- acceleration values for the landing phase of the boat - it is to be noted that due to the light displacement and high speed the motions are highly non-linear.

The different methods are shortly and briefly commented on in the following. Further reading is recommended on the basis of the documents referred to.

FRIDSMA (-71), SAVITSKY ET AL (-72)

Most of the acceleration calculation methods are based on the systematic series made in ref. [7] and the calculation formulae in [8]. The formula for the acceleration is expressed as follows:

$$\bar{n}_{cg} = \frac{0.1175\tau}{4C_{\Delta}}\left(\frac{H_{1/3}}{B_x} + 0.084\right)\left(\frac{5}{3} - \frac{\beta}{30}\right)F_n{}^2\,\frac{L_{wl}}{B_x}$$

where τ = trim angle (4°-6°)

C_{Δ} = load factor = $\nabla / B_x{}^3$ (0,4 - 0,72)

B_x = chine width (1)

$H_{1/3}$ = significant wave height

β = bottom rise (10°-30°)

F_n = Frouds number (0,6 - 1,8)

Note that:
- accelerations are directly proportional to the trim angle
- accelerations are inversely proportional to the bottom rise; however it is to be noted that if the bottom rise angle is increased, the trim will increase thus decreasing seakeeping characteristics
- accelerations are also inversely proportional to the load factor
- accelerations are proportional to the speed squared.

It has to be noted, that spray rails and the shape of the cross sections of the hull can be used to affect both the trim and the time history of the slamming pressure, thus influencing the accelerations a lot.

SPENCER (1975)

The method presented by Spencer [9] is based on Fridsma (1971) acceleration values, Heller-Jasper maximum pressure formula and Allen-Jonesin pressure reduction formula line. The parameter range for the method is presented in Table 1 together with corresponding values for NV-96.

Table 1. Parameter range for Spencer´s method.

Parameter tai -ratio	range	NV-96 -measurements
L_{wl}/B_{ch}	4 - 5	3.1
β [°]	12 - 21	26
LCG % aft from L/2	5 - 9	9
$H_{1/3}/B_{ch}$	0.3 - 0.5	0,5
Lwl [m]	18 - 36	8.0
V [kn]	18 - 30	30 - 40

The pressure formula has the following form:

$$P_i = C_1 + C_2\Delta^{1/3} + C_3 L + C_4 V^2 + C_5\sqrt{VL} \tag{2}$$

Koelbel [10] indicates that this straightforward "cookbook" type formula has been widely used by designers and that it has been the base for Coast Guard approval. Some discussion on the applicability of the approach is going on, however.

DNV HSLC, DESIGN LOADS

The rules of the classification societies are made for dimensioning purposes and thus usually the included physical phenomena are not easily separated from the empirical information.

DnV´s Rules and Regulations for High Speed Light Craft [11](1996) have this character. The acceleration is taken as:

$$a_{cg} = \frac{V}{\sqrt{L}}\frac{3{,}2}{L^{0{,}76}} f_g g_0 \tag{3}$$

The speed and wave height can then be derived from the acceleration value. This, however, gives too low values for small fast boats and the use is thus restricted.

The pressure formula has the format of:

$$p_{sl} = 1{,}3k_l\left(\frac{\Delta}{nA}\right)^{0{,}3} T_O^{\,0{,}7}\,\frac{50-\beta_x}{50-\beta_{cg}}\,a_{cg} \tag{4}$$

The effect of T_o is high and difficult to determine in small fast boats where trim angle and draft may change considerably.

LLOYD'S SSC

Lloyd's Special Service Craft -rules are intended for boats above 24 m with a speed of ($V \geq 7.19\nabla^{1/6}$) and a displacement of ($\Delta = 0.04(L_R B)^{1.5}$), but can be used for smaller boats, too.

The acceleration takes the form of

$$a_v = 1{,}5\theta_B L_1 (H_1 + 0{,}084)(5 - 0{,}1\theta_D)\Gamma^2 10^{-3} \tag{5}$$

where Γ is Taylor's number, $L_1 = (L_{wl}B_c^3)/B_w\Delta$, $H_1 = H_{1/3}/B_w$ ($H_1 \geq 0.2$, $H_{1/3}$ according to Service Group:n 0.6-4.0 m) θ_D bottom rise ($\leq 30°$) and θ_B dynamic trim angle ($\geq 3°$). The formula is close to Savitskys.

Slamming pressure for craft with a Taylor's number $\Gamma \geq 3$ is calculated by:

$$P_{dlv} = \frac{\nabla_d \Delta \Phi (1 + a_v)}{L_{WL} G_O} \text{ kPa} \tag{6}$$

where ∇_d = 54 (monohull), Φ = 1.0 and G_o chine width. The pressure is directly proportional to acceleration and displacement.

ISO TC 188 SMALL CRAFT

Under this technical committee there is a work group, WG 18, which is devoted to hull scantlings. The work is not finished but some signs of the outcome are visible.

Draft ISO CD 12215-5.17 formulae are as follows:

$$P_{bl} = \frac{0.1\Delta}{L_{WL} B_C}(1 + n_{cg}) k_{ar} k_L \text{ kPa} \tag{7}$$

where n_{cg} is the dynamic load factor or the mean value of the highest 1/100 accelerations:

$$\bar{n}_{cg} = 0{,}078(\frac{f_{wl} L_{wl}}{10 B_c} + 0.084)(50 - \beta)\frac{v^2 B_c{}^2}{\Delta}\tau \quad [\mathrm{g}]$$

missä τ = trim angle ($\geq 4°$)
Δ = displacement(ton)
L_{WL} = waterline length
B_x = chine breadth
β = bottom rise ($\leq 30°$)
k_L = longitudinal factor of pressure (8)
k_{ar} = area reduction
v = speed
f_{wl} = *designcategoryfactor*;
1.0 *A & B*
0.75 *C*
0.50 *D*

Also this is close to Fridsma and Savitsky approach.

NBS-VTT EXTENDED RULE

Based on the Nordic Boats Standard (NBS) VTT has developed a new practical rule with applicability up to 24 m including pressure reduction. The rule includes also dimensioning principles for new materials.

The base pressure (p_{base}, kPa) is presented in a graph as a function of speed and length of boat. A polynom fitting the curve can be expressed as:

$$p = 0{,}001(15 + L_{oa} + 0{,}24 * \sqrt{\nabla_{ref}} + 0{,}11 V_{\dim}{}^2 - 0{,}0025(24 - L_{oa})V_{\dim}{}^2$$
$$\nabla_{ref} = 1000(\frac{L_{wl}}{4{,}1 + 0{,}04 L_{wl}})^3 \quad (9)$$

The slamming pressure is calculated at three different speeds namely maximum speed, maximum speed in full load condition and reduced speed in waves corresponding to the selected design category. The design pressure is then calculated by:

$$P_{slam} = k_l k_v k_\beta k_\nabla p_{base} k_{dc} \quad (10)$$

where k_l and k_v are pressure distribution longitudinally and transversally, k_β coefficient for bottom rise, k_∇ displacement factor and k_{dc} design category factor (in the reduced speed condition).

The pressure is thus proportional to the speed squared and the square root of the displacement. The design pressure is derived at, by multiplying with a pressure area reduction factor.

3.2 MEASUREMENTS AND CALCULATIONS

The slamming pressures according to the different methods have been calculated and compared to the NV-96 measurements [14]. Table 2 shows the values used.

Table 2. Initial values in the slamming pressure calculations.

Loa [m]	10,1	Δ [kg]	4090, 4455, 4725
Lwl [m]	8,00	V [kn]	30, 35, 40
B_{ch} [m]	2,60	β [°]	26
T [m]	0,60	H_s [m]	1,3
T_O [m]	0,30	s [m]	0,35

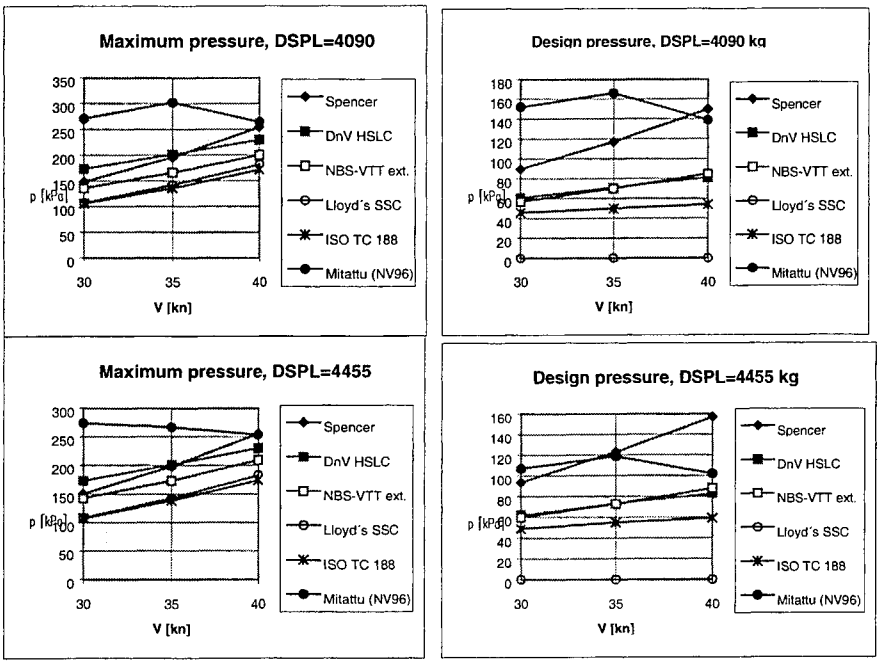

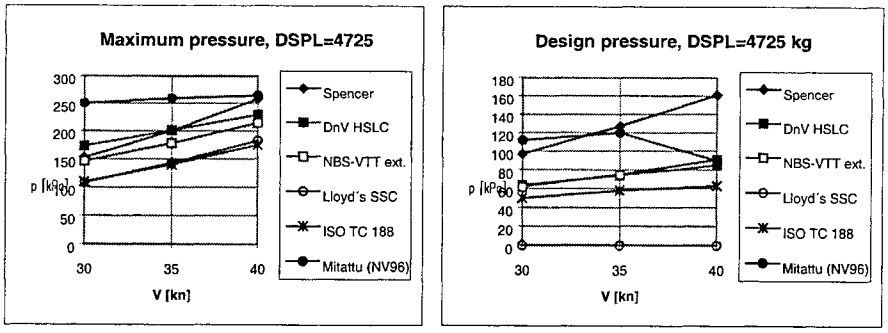

Figure 1. Calculated and measured slamming pressures.

The results presented in Figure 1 show that the measured maximum pressures at 40 knots are clearly higher than estimated by the methods. The situation is even worse for the lower speeds.

The design pressure values are mean values measured from several pressure gauges representing different areas. The areas correspond well with the design areas in the NBS-VTT method and the DnV method.

The general conclusion of these results reinforce the initial expectation that the present methods do not reflect the real pressures correctly as a function of speed. The phenomena can be described as in Figure 2. "By accident" it may, however, be possible to arrive at the right level at higher speeds.

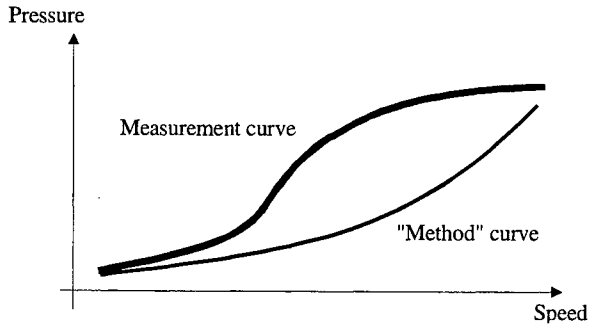

Fig 2. It seems that the actual pressure is much higher at intermediate speed values, than it is according to the different methods.

The comparison for the acceleration values is shown in Figure 3. Here all the calculated values are well above the measured. The difference between the methods is also here considerable although it seems to decrease at lower speeds.

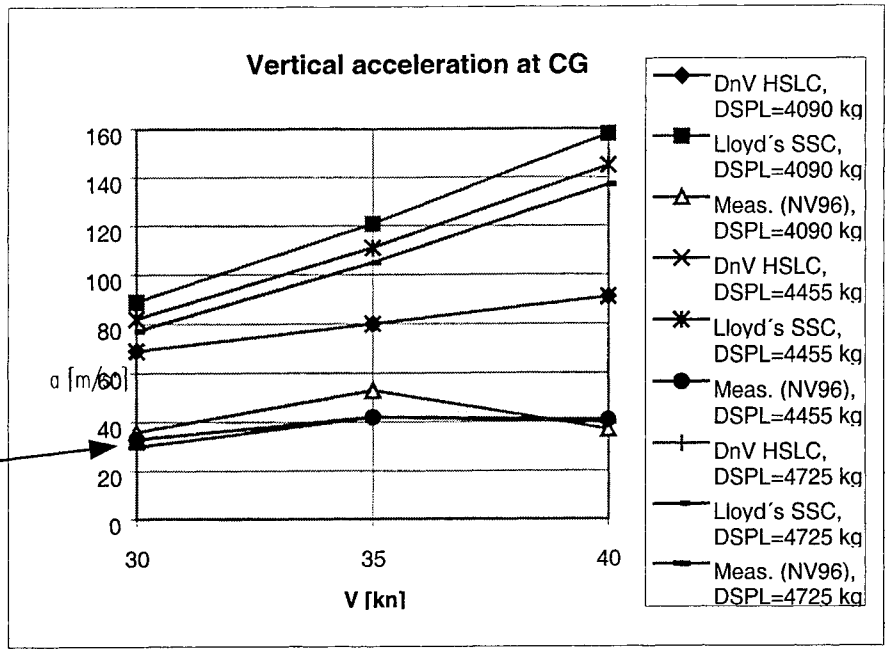

Fig 3. Comparison of the calculated and the measured acceleration values.

4 PILOT BOAT MEASUREMENTS

To investigate the pressures on a heavier and slower type boat and to expand the information base, measurements were performed on a fast pilot boat. The different parameters for the boats can be seen in Table 3.

Table 3. Parameter comparison between NV-96 and Pilot boat. Note that Frouds displacement (Fndspl) value of 3.3 is reached already at a speed of 26 knots with the NV-96. The top speed is much higher while for the pilot boat Fndspl = 3.28 represents the top speed.

	Pilot boat	NV-96
DSPL	11.5	4.7
V (kn)	30	26
Fndspl	3.28	3.3
Bch	3.1	2.6
V (kn)	30	28
Fnb	2.8	2.85

The boat characteristics are as follows .

Length overall Loa	14,21 m
Hull length Lh	13,00 m
Breadth overall Boa	4,3 m
Chine breadth Bch	3,25 m
Bottom rise β	22°
Lightweight about.	9500 kg
Loaded weight about.	11,5 m³
Power	610 kW
Maximum speed about.	30 kn

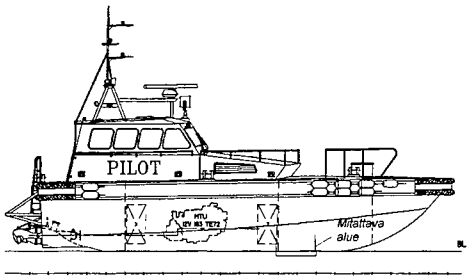

The pressures were measured using calibrated longitudinal stiffeners with shear gauges and the actual measurements were performed both as controlled test run measurements and long term measurements during normal use.

Figure 4 shows typical time histories of the calculated pressure from several gauges.

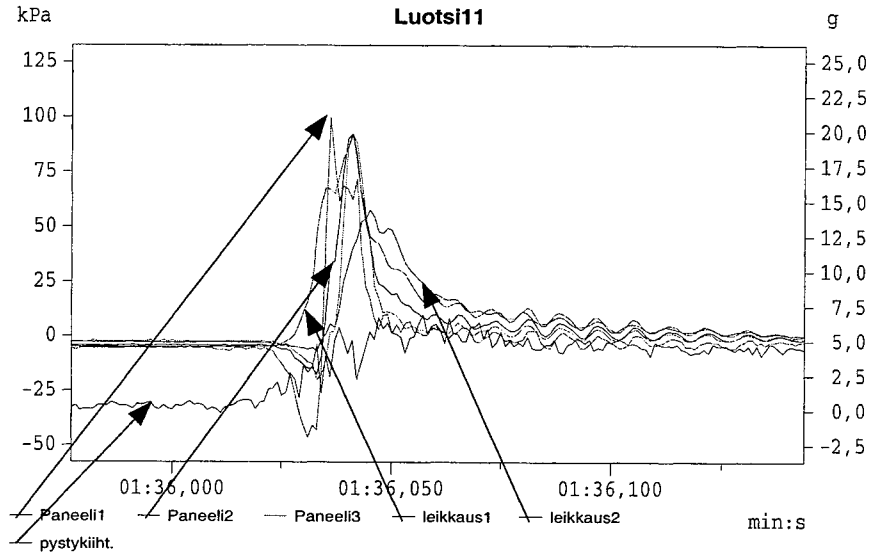

Figure 4. Slamming pressure during a typical slamming situation calculated from bending stresses of the panel, shear stresses of the stiffeners. Vertical acceleration near the panel is also shown.

The results are compared to some calculated values in Table 4.

Table 4. Calculated and measured pressure values for the pilot boat. The design speed of the boat (29 kn) was used as input value in the calculations.

	pslam [kPa]	pdesign [kPa]
Spencer		85
DnV HSLC		55
NBS-VTT ext.	127	70
Lloyd's SSC	143	
Measured 17.6.		appr. 160
Measured 16.10		appr. 100
Measured long term.		appr. 80

It can be noted that during normal operation severe slamming is avoided. Thus maximum pressures are only to be expected in very special conditions or when trying to push the boat to its limits.

5 CONCLUSIONS

It appears to be clear that the available slamming information for very fast small boats still is limited. This may be due to lack of resources in this area and the nature of the small and medium size companies building these boats. Due to increased interest in this type of boats, some important steps toward a better understanding of the phenomena have recently been taken. The measurements and the survey reported here is one important step in this direction.

From the results and information above one can draw the following technical conclusions.

1. The variations between the different available methods is much too high for design pressure estimations. (Note! The scantling determination methods may well work for dimensioning purposes but this was not included in this study!)

2. The methods seem to underestimate the pressures and overestimate the accelerations.

3. There seem to be a significant problem in the intermediate speed range. The wave and motion conditions may, in this speed range, be of higher importance than the speed of the boat.

4. Normal operation seem to be more tender than test runs for maximum slamming. The differences in terms of pressure is in the order -50%. This is important when establishing fatigue load information for the structures

5. Further work is needed to formulate a solution which explains the apparent S-shape of the pressure curve.

The co-operation of the following parties is much appreciated: Finnish Maritime Administration, The Finnish Frontier Guard, the Finnish Naval Headquarters, Boomeranger Boats Oy, Marine Alutech Oy, Gulf of Finland Ship Inspection Division and TEKES

REFERENCES

1. Hentinen, M: Slamming-kuormien ja pystykiihtyvyyksien määritys liukuvisssa veneissä, kirjallisuusselvitys. VTT VALB327, Espoo 1998

2. Hentinen, M: Slamming-kuormat nopeassa luotsiveneessä. VTT VALB355, Espoo 1998.

3. Rask, I: Slamming pressure in short-crested and oblique seas. SSPA Research report no 105, 1986

4. Faltinsen, O: Wave Loadings and Motions of Ships and High-Speed Marine Vehicles. "Mathematical approaches in hydrodynamics", SIAM, 1991

5. Hayman, B: Recent research at Det Norske Veritas concerning fast craft. Int. Conf High speed passenger craft - future developments and the Nordic initiative. RINA, London 1993.

6. Rosén, A: Fullskalemätningar genomförda på Stridsbåt 90 E, hösten 1997. KTH, Stockholm 1998

7. Fridsma, Gerard: A Systematic study of the rough-water performance of planing boats. Davidson laboratory, report SIT-DL-71-1495, New Jersey 1971

8. Savitsky, D., Roper, J.K. & Benen, L: Hydrodynamic development of planing hull for rough water. 9th Symp. Naval Hydrodynamics, Paris 1972.

9. Spencer J. S., Structural Design of Aluminium Crew Boats, Marine Technology, Vol 12, No.3, July.1975.

10. Koelbel, J: Comments on the Structural Design of High Speed Craft, Marine Technology, Vol 32, No2, April 1995, pp. 77-100.

11. Rules and Regulations for High Speed Light Craft, Part 3, Ch. 1. Det Norske Veritas 1996)

12. Rules and regulations for the classification of special service craft, Part 5, Ch. 2. Lloyd´s Register of Shipping 1996.

13. NBS-VTT Extended Rule, VTT Technical Report VALB172, Dec. 1996, Espoo, 43 p.

14. Slamming-kuormat nopeassa vartioveneessä, VTT raportti VALC 342, luottamuksellinen.

FINFLO RANS SOLVER VALIDATION CALCULATIONS FOR PROPELLER OPEN WATER FLOW AND SHIP HULL FLOW

Jaakko V. Pylkkänen, Senior Research Scientist, VTT
Antonio Sánchez-Caja, Research Scientist, VTT
Tom Sundell, Research Scientist (formely), VTT
Heikki Piippo, Research Scientist (formely), VTT

Abstract

This paper gives an outline of the work at VTT in applying the FINFLO code to the hydrodynamic analysis of marine screw propellers and ship hull flow. In Section 2 the numerical method is briefly described. Section 3 presents propeller open water flow predictions for three marine screw propellers. In Section 4 the results of double model and free surface viscous flow calculations are compared with measurements.

Predicted propeller open water thrust and torque for a propeller of simple geometry are within 1.5 percent of the experimental values for advance numbers close to the design value. For off-design operation points and for propellers with unconventional features, the differences in thrust and torque are higher.

The hull flow computations predict the limiting streamlines in the stern region and flow separation satisfactorily. Some details of the wake field are not reproduced well. The computed total resistance coefficient and wave profiles for the Wigley hull model agree well with the experimentally obtained ones. For the Series 60 hull form model the total resistance coefficient is under-predicted and the calculated wave profiles show stronger dissipation than the measured wave profiles.

1. Introduction

The development of the FINFLO RANS (=Reynolds-Averaged-Navier-Stokes) equation code was started at the Department of Aerodynamics of the Helsinki University of Technology (=HUT) and has been continued at the Departments of Aerodynamics and Applied Thermodynamics of HUT. Presently VTT is working together with HUT to apply and extend the FINFLO code to the analysis of rotating fluid machinery and free surface flow around ship hulls. These two projects form parts of the Finnish National CFD Technology Research Programme. This paper is slightly revised version of the previous review papers of VTT Maritime and Mechanical Engineering [1][16]. More detailed descriptions of FINFLO can be found in the references of this paper [2][3][4].

2. Numerical method

The flow simulation in FINFLO is based on the solution of Reynolds-Averaged-Navier-Stokes equations together with the equations for turbulent kinetic energy and dissipation of turbulence. FINFLO has the possibility to use different turbulent models: algebraic turbulence models (Baldwin-Lomax, Cebeci-Smith), the low-Reynolds' number k-e model proposed by Chien, the explicit Reynolds-stress model of Speziale et al. and the Reynolds-stress model of Shima. The concept of artificial compressibility is implemented in FINFLO to seek the solution of the equations for incompressible flows.

A finite volume technique is used for solving the equations. The differential equations are integrated over a computational cell and the summation is extended over the faces of the computational cell. A multigrid method is used to accelerate the convergence. In a rotating frame the functional form of the flux equations is similar to the case without rotation [4]. The difference is that in a rotating frame the motion of the cell faces is taken into account in the evaluation of energy flux and convective velocities.

3. Propeller calculations in homogeneous onset flow

3.1. Grids and boundary conditions

The geometry of the computational grid is obtained using a commercial grid generator program.

The space between two contiguous propeller blades is modelled to take full advantage of the symmetry of homogeneous flow and geometry. Groups of two blocks representing the space

near and far away from the hub are located upstream, downstream and in-between the propeller blades.

In most of the earlier calculations the dimensions of the blocks closer to the hub in the I, J and K directions were 48*72*80, 64*72*80 and 56*72*80 for the blocks located upstream, downstream and in-between the propeller blades, respectively. I stands for the axial direction, J for the circumferential direction, and K for the radial direction. The outer blocks had the same dimensions except for the maximum K index that is 32. The total number of cells was 1354752. Figure 1 depicts the second level grid for DTMB Propeller 4119. Presently about 700000 cells are used.

The hub and blade surfaces of propeller are rotating solid walls. The lateral surfaces adjacent to the propeller blades have a periodic boundary condition. Block boundaries, where two adjacent block surfaces are coincident, are defined as connectivities. Uniform flow conditions are applied for the inlet and external boundary surfaces, and the streamwise gradients of the velocities are set to zero on the outlet surface. The k-e turbulence model was used in the propeller calculations.

3.2. Results of DTMB P4119 open water analysis

DTMB propeller P4119 is a 0.305 m diameter, three-bladed propeller with no skew or rake, and with an almost constant pitch ratio. The blade sections are of NACA 66(modified) thickness form and have NACA a=0.8 meanlines. The design advance number is J=0.833.

The uniform inflow calculations were made for the rotational velocity of 10 rps. The inflow speeds were adjusted to correspond the advance numbers of J=0.3, 0.5, 0.833, and 1.1. Table 1 gives the comparison of the calculated and measured performance [5][6]. The performance predictions were not much affected by the FINFLO version used. The predictions of thrust and torque are accurate for the design advance number. Differences lower than 1.5 percent were found. The corresponding efficiency was calculated with an error rate lower than 3 percent. At low advance ratios, i.e. J=0.3-0.5, the differences from the experimental values were greater for the thrust and torque coefficients, however the efficiency was predicted with reasonable accuracy. This seems to be a common feature of many RANS codes. Furthermore, the distribution of C_p at r/R=0.7 and the distribution of circumferentially-average dimensionless velocities at x/R=0.3281 are presented in Figures 2-3.

Table 1. Comparison of the calculated and measured performance of DTMB P4119. The asterisk (*) indicates that the calculations were stopped at the 2000th iteration. The letters (p-c) indicate that the calculations were made with the pseudo-compressible version of FINFLO and with a more accurate leading edge representation.

J	0.3	0.5	0.833	1.1	0.833 (p-c)
K_T (calculated, 1st grid level)	0.399*	0.294*	0.144	0.0203	0.143
K_T (experimental)	0.375	0.288	0.146	0.035	0.146
K_Q (calculated, 1st grid level)	0.0626*	0.0495*	0.0284	0.0107	0.0278
K_Q (experimental)	0.0587	0.0474	0.0280	0.0107	0.0280
η_0 (calculated, 1st grid level)	0.304*	0.473*	0.673	0.331	0.681
η_0 (experimental)	0.305	0.484	0.692	0.573	0.692

3.3. Results of old icebreaker propeller open water analysis

The old icebreaker propeller is a four-bladed propeller with no skew or rake, and with an almost constant pitch ratio. The thick section shapes differ distinctly from those of a conventional propeller. The propeller diameter is 0.189 m in model scale. The uniform inflow model tests and the present calculations were made for the rotational velocity of 18 rps. The Reynolds number at the 0.7 non-dimensional radius of the model propeller is higher than 0.9*10E6. For most propeller models this Reynolds number is sufficiently high for the flow on the blade to be turbulent.

The comparison of the calculated and measured performance is given in Table 2 [8]. The calculated thrust and torque coefficients at the advance number of J=0.55 were about 8 percent higher than the experimental values. The corresponding efficiency was underestimated by less than 1.5 percent. The values of y+, the non-dimensional sub-layer scaled normal distance from the surface, were lower than 1.0 for most of the blade. These y+ values are acceptable for the k-e turbulence model.

The shear stress on the suction side was also negative close to the trailing edge for 20 per cent of the chord at the inner radii, which is indicative of flow separation. The pressure contours and streamlines give indications on how this particular propeller geometry could have been improved, i.e. the results of the analysis can be used as a tool in iterative propeller design.

Table 2. Comparisons of the calculated and measured performance of the old icebreaker propeller and Troost BB Series propeller with thick hub. The letters (p-c) indicate pseudo-compressible calculations.

J for old icebreaker propeller	0.35	0.55	0.75	J for BB-H	0.800 (p-c)
K_T (calculated, 1st grid level)	0.272	0.178	0.086	K_T (cal)	0.155
K_T (experimental)	0.243	0.166	0.089	K_T (exp)	0.156 W
K_Q (calculated, 1st grid level)	0.0413	0.0299	0.0186	K_Q (cal)	0.0291
K_Q (experimental)	0.0374	0.0275	0.0177	K_Q (exp)	0.0289 W
η_0 (calculated, 1st grid level)	0.366	0.522	0.551	η_0 (cal)	0.676
η_0 (experimental)	0.365	0.529	0.600	η_0 (exp)	0.687 W

3.4. Results of Troost BB Series propeller open water analysis

The calculations for a Troost BB Series propeller with a thick hub were made with the pseudo-compressible version of FINFLO. The comparison of the calculated and measured performance is given in Table 2. The hub of this Troost BB Series model propeller was modified for later use in AZIPOD model tests. The thick hub lowered propeller performance compared from that of a standard Troost BB Series propeller.

4. Ship hull flow calculations

4.1. Free surface calculations and boundary conditions

A free surface boundary model has been implemented in FINFLO to compute the free surface waves around ship hulls [11][13][14]. A moving grid concept is employed where the mesh is following the free surface evolution. The grid is updated during the computations to match both the free surface and the hull surface boundary conditions. Two boundary conditions must be satisfied on the free surface. The kinematic condition simply states that the flow at the free surface must be tangential to the surface. The dynamic boundary condition states that the normal and tangential stresses across the free surface are continuous.

At the outer boundaries the standard free stream condition is imposed. This means that the waves cannot travel through the outer boundary. For this reason the waves are damped when moving towards the boundary. The stretching of the grid gives a dissipation zone to secure a non-reflecting boundary. On the symmetry plane a symmetry boundary condition is imposed.

4.2. Double model flow calculations

Validation computations for double model flow were made for the HSVA-1 and HSVA-2 tankers [9]. Two different grid topologies were used in the computations: an O-O topology grid with 884736 cells and a C-O topology grid with 1327104 cells. The grid on the hull surface was the same in these two cases.

Flow boundaries consist of the upstream inlet, downstream outlet, free surface, symmetry plane, hull surface, grid bottom and grid wall boundary. On the symmetry plane and on the free surface a symmetry boundary condition is imposed. The Reynolds number was 5.0*10E6. Both k-ε and Cebeci-Smith turbulence models were used. The distance from the hull surface to the center of the first cell, expressed as the non-dimensional value y+, was less than one.

Table 3 compares the computed double model resistance values. Both the turbulence model and the type of grid affect the predicted stern flow. The computed limiting streamlines and especially the computed resistance values were close to the measured ones obtained from wind tunnel tests [10]. The characteristic hook-shape in the axial velocity contours in the propeller plane, caused by the bilge vortices, was not reproduced.

Table 3. Computed double-model viscous resistance coefficients for the HSVA tankers. The letter (k) refers to the three dimensional form factor on flat plate.

Grid topology & turbulence model	HSVA1	HSVA 2
Computed, OO-grid, k-ε	3.96*10E-03	4.16*10E-03
Computed, OO-grid, C-S	4.02*10E-03	4.22*10E-03
Computed, CO-grid, k-ε	4.13*10E-03	
Computed, CO-grid, C-S	3.96*10E-03	
Measured $(1+k)C_F$ (CETENA)	4.11*10E-03	
Measured $(1+k)C_F$ (Dyne)		4.25-4.38*10E-03

4.3. Free surface flow calculations for Wigley model

As the first free surface test case a simple Wigley hull form was chosen [11]. A O-H topology grid having 786432 (256*128*24) cells was used for the Wigley hull.

Baldwin-Lomax turbulence model was used in all the free surface calculations. The value of y+ at the center of the first cell of the Wigley model was about one. The computed wave profiles were compared with experimental results presented at the 1983 DTNSRDC workshop [12]. In Figure 4 the wave profiles are drawn from bow (x=-1.0) to stern (x=1.0). The correlation of the profiles along the hull is very good. The amplitudes and phases of the computed profiles coincide with those observed in model tests. The computation also reproduced the Kelvin wave

pattern and the Kelvin angle. Figure 5 shows that the computed resistance is close to the measurements at IIHR and SRI.

4.4. Free surface flow calculations for Series 60 hull form

As the second test case a Series 60 hull form of CB=0.60 was chosen [13][14]. A O-H topology grid, shown in Figure 6, having 786432 (256*96*32) cells was used for the Series 60 hull. The value of y+ at the center of the first cell of Series 60 model was about two. The main features of the flow patterns are well captured.

The even keel predictions for F_n=0.316 and R_n=2.564*106 were compared with experimental results of Toda et al. [15]. Figures 7-10 compare axial and total head velocity contours at a section close to stern. Figures 11-12 show computed transverse wave cuts against measured transverse wave cuts and figures 13-17 compare the wave heights at longitudinal wave cuts. The computed wave field shows good agreement with the experimental ones in regions close to the hull. In regions far from the hull the wave heights were under-predicted. The calculated zero height contours agree well the measurements. The predicted total resistance coefficient was C_T=5.4*10-3, whilst the measured one for a free floating model was C_T=5.96*10-3.

5. Conclusions

Predicted propeller open water thrust and torque for a propeller of simple geometry are within 1.5 percent of the experimental values for advance numbers close to the design value. For off-design operation points and for propellers with unconventional features, the differences in thrust and torque are higher.

The computations predict the limiting streamlines in the stern region and flow separation satisfactorily. Some details of the wake field are not reproduced well. The computed total resistance coefficient and wave profiles for the Wigley hull model agree well with the experimentally obtained ones. For the Series 60 hull form model the total resistance coefficient is under-predicted and the calculated wave profiles show stronger dissipation than the measured wave profiles.

Ongoing propulsor work deals with time accurate interaction between the propeller and the housing of the azipod. Furthermore, present hull form calculations concern the HSVA2 tanker free surface calculations.

Figure 1. Grid for P4119.

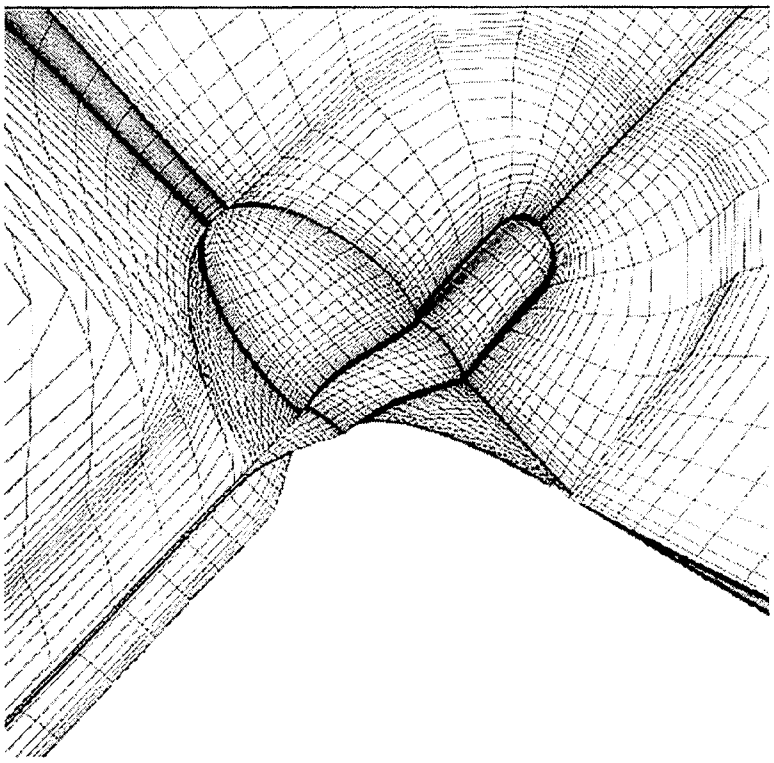

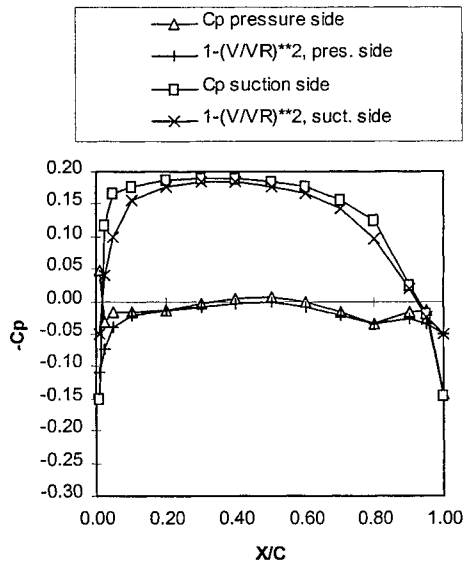

Figure 2. P4119 at J=0.833: Chordwise distribution of -Cp based on the relative velocity at r/R=0.7.

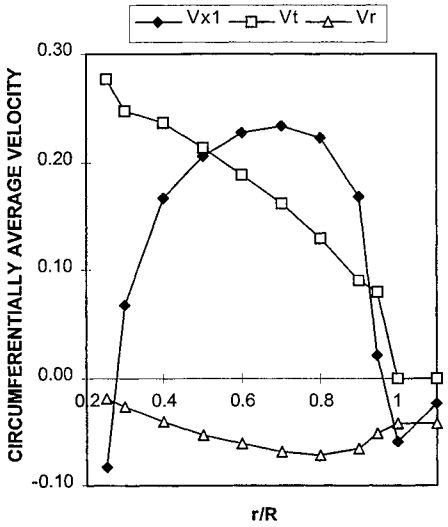

Figure 3. Radial distribution of circumferentially-average dimensionless velocities at x/R=0.3281.

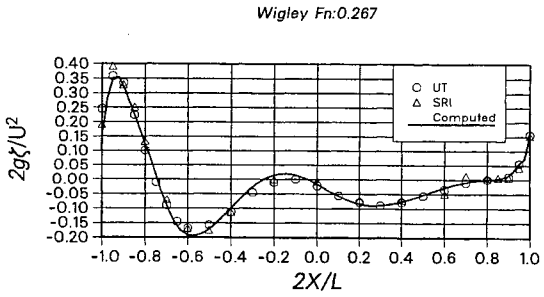

Figure 4. Computed and measured wave profiles for Wigley hull at F_n=0.267.

Figure 5. Comparison of total resistance coefficients for Wigley hull

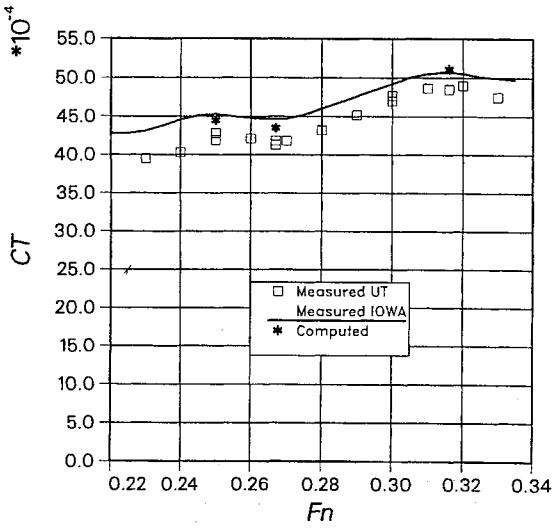

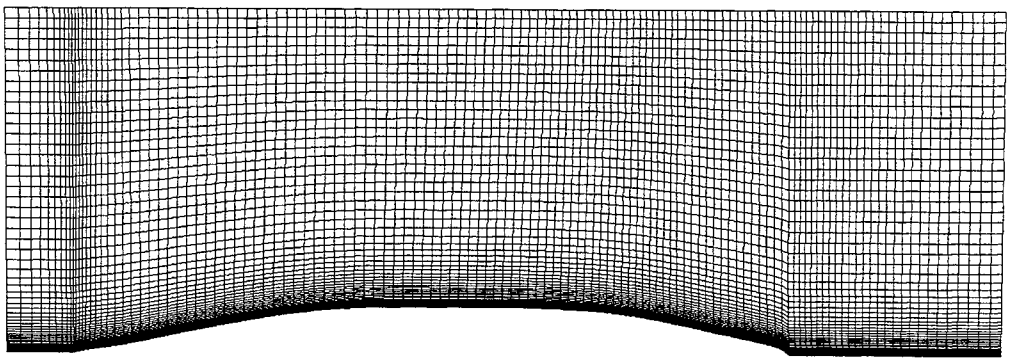

Figure 6. A part of the free surface grid for Series 60 hull (16≤i≤140, 1≤j≤97).

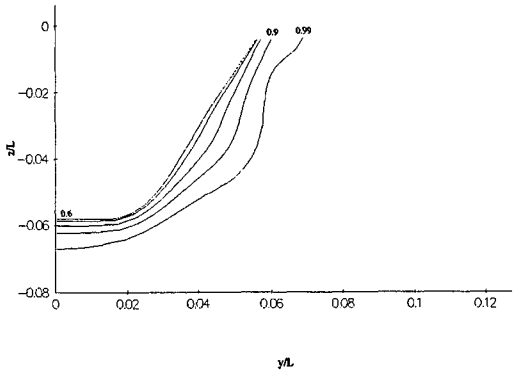

Figure 7. Series 60 calculated total head velocity contours at x= -0.2 (Piippo, 1998).

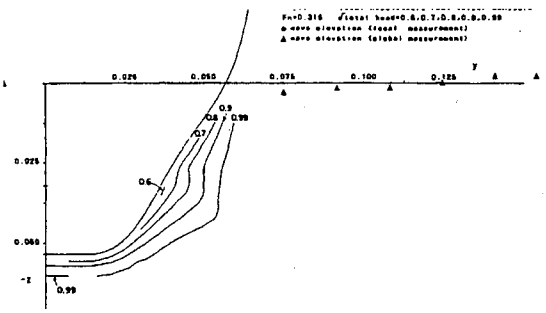

Figure 8. Series 60 measured total head velocity contours at x= -0.2 (Toda et al., 1991).

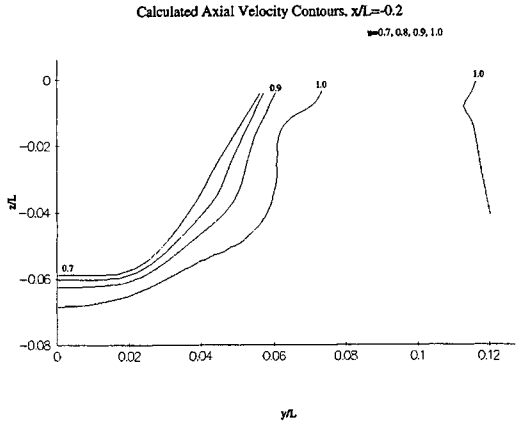

Figure 9. Series 60 calculated axial velocity contours at x= -0.2 (Piippo, 1998).

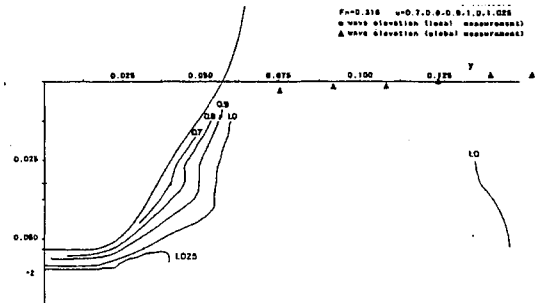

Figure 10. Series 60 calculated axial velocity contours at x= -0.2 (Toda et al., 1991).

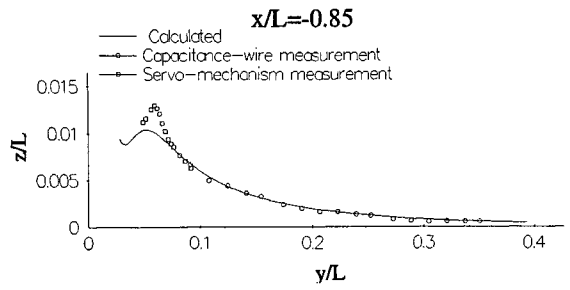

Figure 11. Computed transverse wave cut at x/L=-0.85 compared with measurements by Toda et al. (Toda et al., 1991).

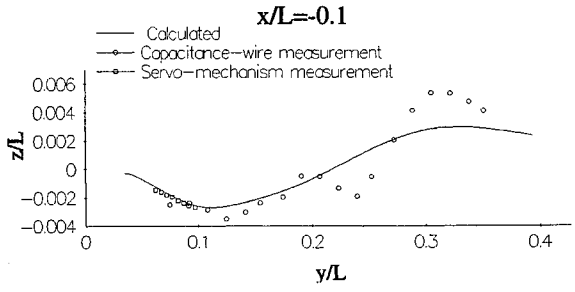

Figure 12. Computed transverse wave cut at x/L=-0.1 compared with measurements by Toda et al. (Toda et al., 1991).

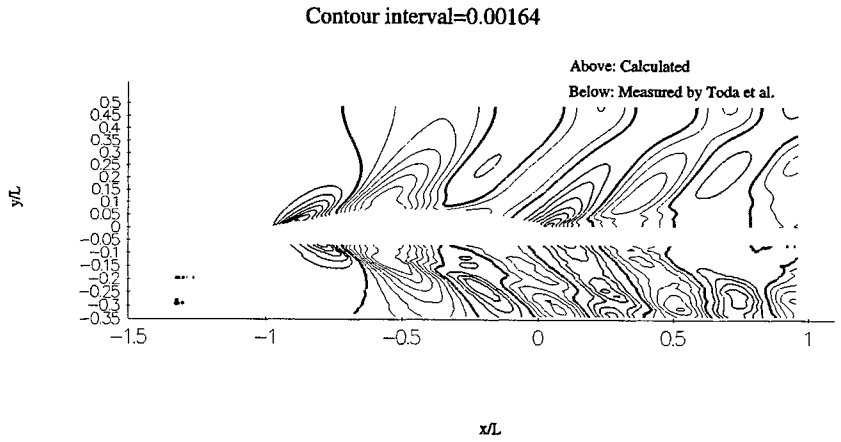

Figure 13. Series 60 computed wave field at F_n=0.316, Rn=2.564*10^6 compared with measurements by Toda et al. (1991). The thickest, mediocre and thinnest lines represent the zero, positive and negative free surface elevation contours, respectively.

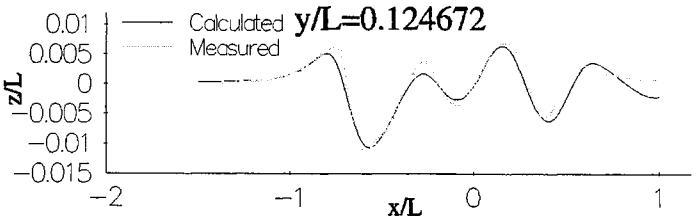

Figure 14. Computed longitudinal wave cut compared with measurements by Toda et al. (Toda et al., 1991).

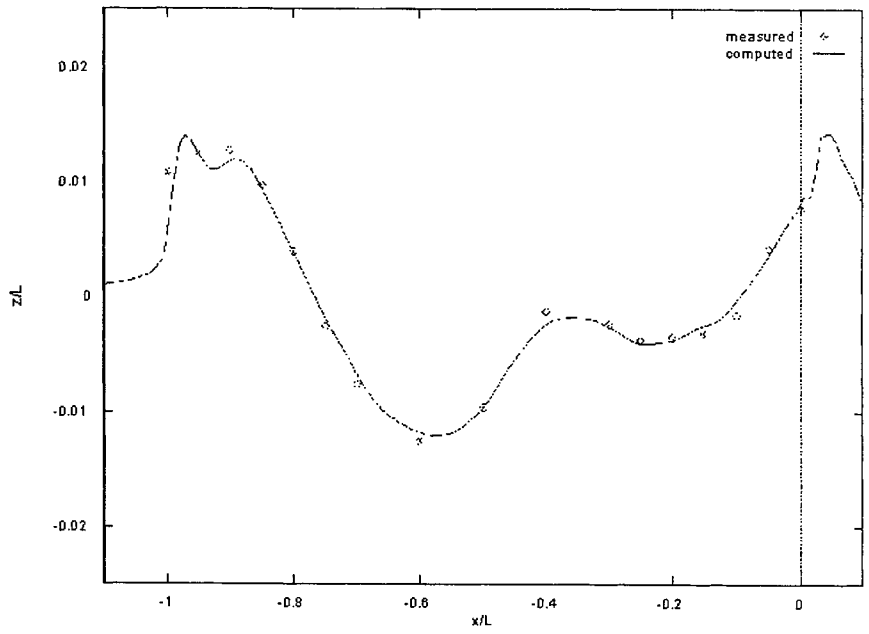

Figure 15. Series 60 computed wave profile at hull and symmetry plane at F_n=0.316 compared with measurements by Toda et al. (1991).

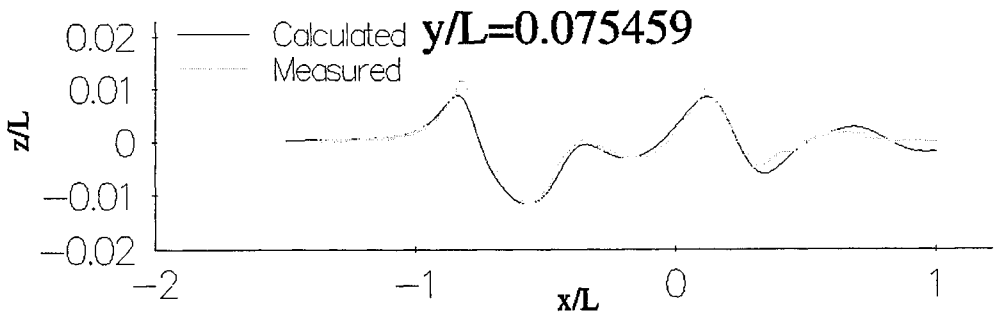

Figure 16. Series 60 computed longitudinal wave cut compared with measurements by Toda et al. (1991).

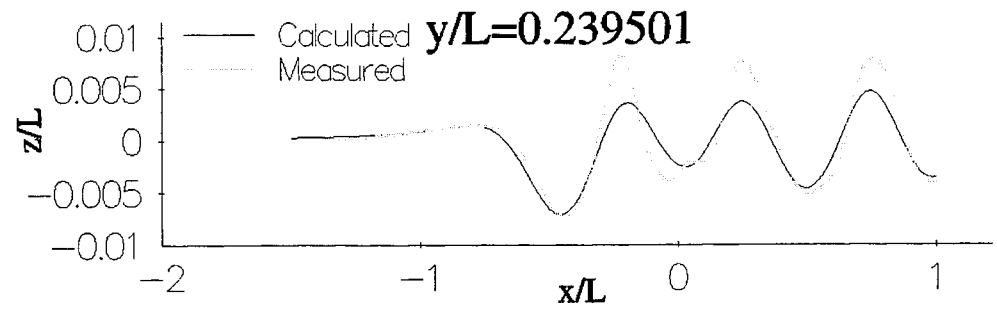

Figure 17. Series 60 computed longitudinal wave cut compared with measurements by Toda et al. (1991).

References

1. Pylkkänen, J.V., Sánchez-Caja, A., Sundell, T. Applications of FINFLO RANS Solver to Naval Hydrodynamics. The International CFD Conference, Ulsteinvik, 29-31 May, 1997. 16 pp.

2. Siikonen, T., Hoffren, J., Laine, S. A Multigrid LU Factorization Scheme for the Thin-layer Navier-Stokes Equations. 17th ICAS Congress, Stockholm, 1990. ICAS-90-6.10.3, pp. 2023-2034.

3. Lehtimäki, R., Laine, S., Siikonen, T., Salminen, E. Navier-Stokes Calculations for a Complete Aircraft. 20th ICAS Congress, Sorrento, 1996. ICAS-92-4.2.1, 8 pp.

4. Siikonen, T., Pan, H.-C. An Application of Roe´s Method for the Simulation of Viscous Flow in Turbomachinery. First European CFD Conference, Brussels, 7-11 Sep 1992. Pp. 635-641.

5. Sánchez-Caja, A. Numerical Calculation of Viscous Flow around DTRC Propeller 4119 for Advance Number Range 0.3-1.1 Using FINFLO Navier-Stokes Solver. Espoo, 1996. VTT Report VALB141A. 36 pp.

6. Sánchez-Caja, A. DTRC Propeller 4119 Calculations at VTT. 22nd ITTC Propulsion Committee Propeller RANS/Panel Method Workshop, Grenoble, 5-6 April 1998. (Espoo, VTT Report VALB304. 13 pp.)

7. Jessup, S.D. An Experimental Investigation of Viscous Aspects of Propeller Blade Flow. Washington, D.C., The Catholic University of America, 1989. Ph.D. Dissertation. 249 pp.

8. Sánchez-Caja, A., Pylkkänen, J.V. Numerical Calculation of Viscous Flow Around an Old Icebreaker Propeller for a Wide Advance Number Range Using the FINFLO Navier-Stokes Solver. Espoo, 1997. VALC335.

9. Saisto, I., Sundell, T. Computation of the Viscous Flow Field around the HSVA Tankers. Helsinki University of Technology, 1996. Technical Report M-206. 57 pp.

10. Hoffmann, H.P. Untersuchungen der 3-dimensionale turbulenten Grenzschicht an einem Schiffsdoppel-modell im Windkanal. Institut für Schiffbau der Universität Hamburg, 1976. Technical Report 343.

11. Sundell, T. Computation of the Free Surface Flow Around a Ship Using the NS Solver FINFLO. Espoo, 1997. VTT Manufacturing Technology Technical Report VALB279. 24 pp.

12. DTNSRDC Workshop on Ship Wave-Resistance Computations. Bethesda,16-17 November 1983. 71 pp.

13. Piippo, H. Computation of Steady Flow of Series 60 Ship Model. Espoo, 1998. Ms. Thesis HUT. 158 pp.

14. Piippo, H. Computation of Steady Flow of Series 60 Ship Model in a Towing Tank. Espoo, 1998. VTT Manufacturing Technology Technical Report VAL3A-010.

15. Toda, Y., Stern, F., Longo, J. Mean-flow Measurements in the Boundary Layer and Wake and Wave Field of a Series 60 C_B=.6 Ship Model for Froude Numbers .16 and .316. IIHR, 1991. Report No. 352, 182 pp.

16. Pylkkänen J., Sanchez-Caja A., Sundell T., Piippo H., FINFLO RANS Solver Validation Calculations for Propeller Open Water Flow and Ship Hull Flow. International Shipbuilding Conference - ISC' 98, St. Petersburg, November 24-26, 1998

WAVE LOADS OF SIX BOW VARIATIONS BY SEGMENTED SHIP MODELS

Timo Kukkanen
VTT Manufacturing Technology
Espoo, Finland

Abstract

Model tests were carried out by segmented ship models for six different bow versions. Discussion of the results and predictions of sagging and hogging moments are given. Hogging moments were in the same order of magnitude for all of the bow version, but differences existed in sagging moments. The sagging moment for the smallest flare angle model was about 20% higher than for the sharpest bow form.

1 INTRODUCTION

Ultimate strength of the hull girder is mainly determined by the wave induced and still water vertical bending moments. Responses are linear with respect to excitation, if a change in the magnitude of the excitation (input) induces the same magnitude change for responses (output). In high waves, the linearity assumption of wave loads with respect to the wave height is not usually valid. For example, sagging moments are clearly larger than hogging moments for ships in a heavy sea. The sagging moment can be twice as high as the hogging moment in extreme waves. The difference between sagging and hogging wave bending moments can be due to the non-vertical sides of the hull. Typically the difference is larger if the block coefficient of the ship is low, and if the flare angle at the bow is large. Also impact type wave loads can induce non-linearities for the vertical bending moments.

Seakeeping model tests were carried out to investigate wave loads, and seakeeping characteristics of a fast Ro-Ro ship. Experiments were conducted for six different bow versions in co-ordination with Kvaerner Masa-Yards Technology. The aim of the model tests was to determine extreme values of the wave induced vertical bending moments, and to investigate the effect of bow geometry on bow forces and global hull girder loads. The tests were carried out with segmented ship models. Background of the methods and applications of the segmented models can be found from Karppinen et

al. (1998). The models have different flare and stem angles, and a different angle of entrance. Bow angels of the ships are given in Table 1.

Table 1. Bow angles of the fast Ro-Ro ship versions in the model tests.

	Bow version:		A	B	C	D	E	F
Angle of entrance	α	[°]	9	6.75	14	9	9	9
Flare angle	β	[°]	65	65	65	52	40	85
Stem angle	γ	[°]	90	90	90	70	50	105

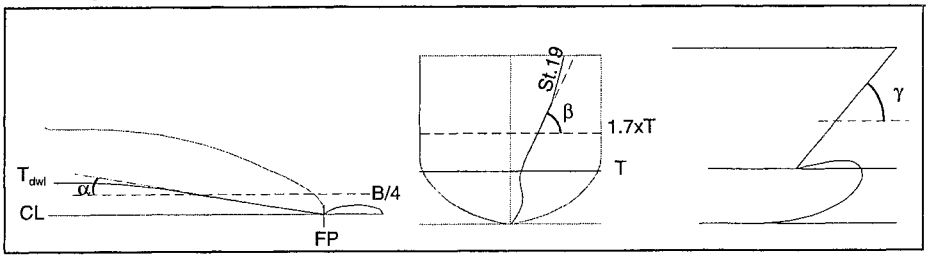

2 MODEL TESTS

The ship models were segmented to four parts from midship to bow, Figure 1. The stern part was the same in all of the six models. Four foremost segments were attached to a rigid backbone by force transducers. The force transducers measured vertical forces. In addition of the segment forces, the vertical bending moment and shear force were measured at midship by strain gauges. Ship motions, heave and pitch, were measured also. Acceleration transducers were installed at each segment and at the aft perpendicular.

The model tests were carried out in irregular and regular head waves with two different speeds. In irregular waves one sea state was approximately the severest sea state where the ship can maintain her service speed. The characteristic significant wave height and zero crossing period of this sea state were H_s = 5 meters and T_z = 8 seconds, respectively. The other sea state was an extreme condition where the speed of the ship was considerable lower than the service speed. This sea state was described by H_s = 7.5 meters and T_z = 9 seconds. Two-parameter ISSC- wave spectra were applied generating long-crested irregular waves. In regular waves several different wave lengths were used, and also three different wave amplitudes.

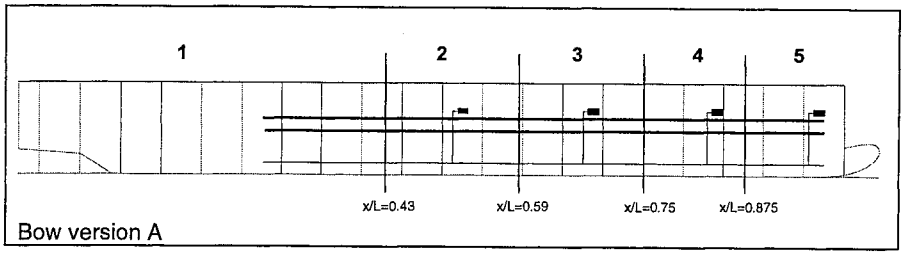

Figure 1. Schematic drawing of the segment divisions, and backbone with force transducers. Strain gauges measuring the vertical bending moments were installed between segments 1 and 2.

3 RESPONSES IN REGULAR WAVES

Regular wave test results were analysed to obtain the transfer functions of the responses. The amplitudes of the transfer functions of heave and pitch are given in the Figure 2, and vertical bending moments at midship are given in Figure 3.

The hull geometry of the models were similar below the still water line, except the somewhat different longer and shorter versions B, and C. Thus, the linear transfer functions should be relative close to each other. Most of the values were within couple of percentage, but larger differences existed near the resonance. One reason is the non-linearities in the responses. However, the differences in the linear transfer functions between the different bow versions were relatively small in all cases.

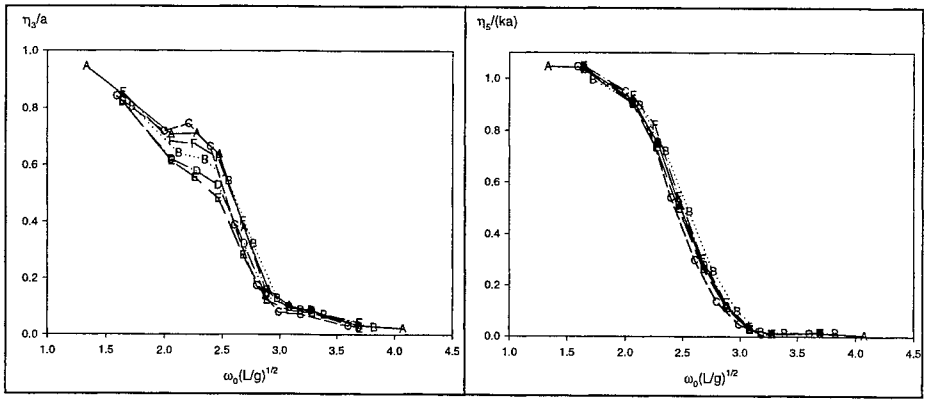

Figure 2. Non-dimensional heave (left) and pitch (right) amplitudes of the six bow versions. Fn = 0.36, head seas.

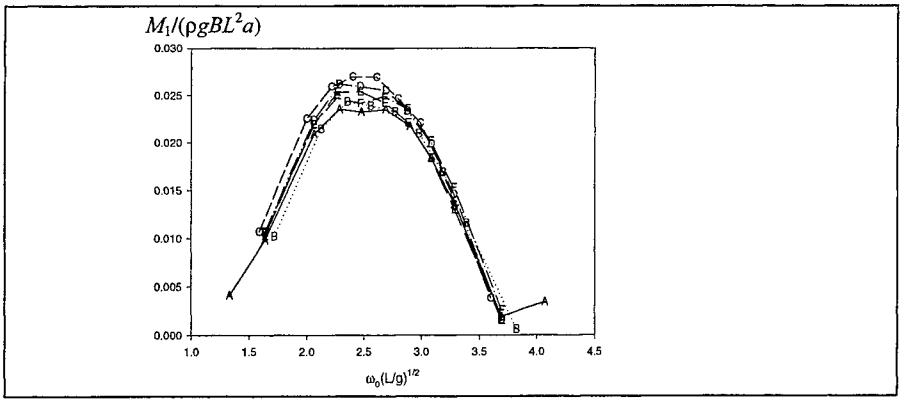

Figure 3. Non-dimensional vertical bending moment amplitudes (M_1) of the six bow versions. Fn = 0.36, head seas.

In order to investigate more detail of the non-linear sagging and hogging bending moments, harmonic analyses were carried out to obtain first and second order amplitudes of the moments. The total vertical bending moment were divided into the following parts

$$M_T = M(x)_{sw} + M_{ss}(x,U) + M_w(x,U,t)\,. \tag{1}$$

where M_{sw} is a still water bending moment, M_{ss} is a steady state bending moment, and M_w is a wave induced bending moment. All the bending moment components are dependent on the longitudinal co-ordinate of the ship hull. The still water bending moment is induced by the buoyancy and weight distributions of the ship, and it is independent of time and speed of the ship. The steady state bending moment is dependent on speed, and it is induced by the wave elevation due to forward speed of the ship. The steady state bending moment is typically sagging-type moment because there exists wave crest at the bow and stern, and hollow at midship. The wave induced bending moment depends on time and speed.

It is assumed that there is no interaction between the steady state and the unsteady flows. Hence, the steady state bending moment and the wave induced bending moment can be analysed separately and superposed to obtain the total bending moment. This might be questionable assumption when the responses are strongly non-linear.

The bending moments without still water bending moments can be expresses as follows

$$M(x,U,t) = M_{ss}(x,U) + M_w(x,U,t)\,. \tag{2}$$

Further, the wave induced bending moment can be expressed by first and second order components (see, e.g. Juncher Jensen & Dogliani, 1996)

$$M_w = M^{(1)} + M^{(2)}, \tag{3}$$

where $M^{(1)}$ is the first and $M^{(2)}$ is the second order component. Higher order components are neglected. In regular waves, first and second order moments can be expressed by multiples of the fundamental wave encounter frequency. The amplitude of the first order moment, M_1, is the same as the amplitude of the linear transfer function. The second order moment includes second order amplitude M_2, and also mean shift M_0. M_1 and M_2 are the two first amplitudes of the Fourier harmonic components. The mean shift M_0 for different wave lengths is determined by calculating first the total mean value from the time histories of the regular wave test data. After that, the steady state component M_{ss} is subtracted to obtain the mean shift M_0. Steady state bending moment M_{ss} is independent of the wave amplitude and frequency, but the mean shift M_0 is not.

An example of time histories in the model tests are given in Figure 4. In the figure, magnitudes of the different components of the vertical bending moments are given also. Second order expansions were close to the measured values, and much better than first order moment only. In this case, the steady state bending moment had large influence on the differences between the sagging and hogging moments.

Sagging and hogging moment amplitudes were determined also by analysing separately positive and negative peaks from time histories. Non-dimensional sagging and hogging moments, at three different wave amplitudes, are presented in Figure 5. At the higher wave amplitude, there exist scatter, especially in sagging moments, near the peak values. In shorter and longer waves, both hogging and sagging moments were almost the same for the different bow versions. Differences in hogging moments between the bow versions were generally smaller than in sagging moments.

Hogging:	M_w / M_1	0.54
Sagging:	M_w / M_1	–1.79
1. harmonic:	M_1 / M_1	1.00
2. harmonic:	M_2 / M_1	0.30
Mean total:	$(M_0+M_{ss}) / M_1$	–0.38
Steady:	M_{ss} / M_1	–0.26

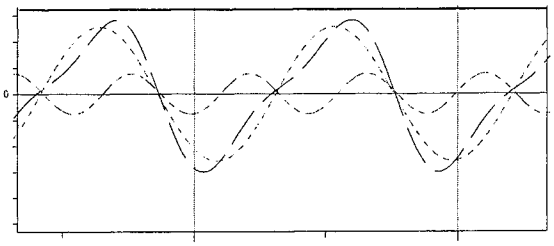

1. harmonic (-----), 2. harmonic (— - -), Second order without mean shift (— —).

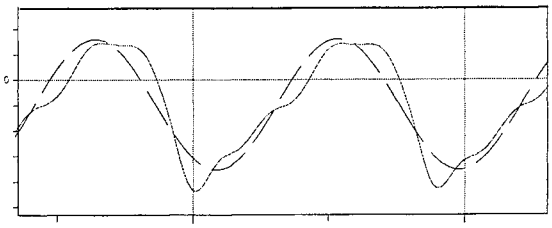

Measured (——), 1. harmonic + mean shift (— —).

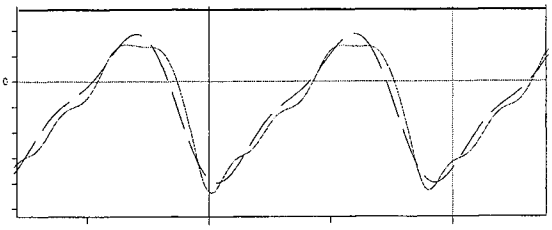

Measured (——), Second order (— —).

Figure 4. Time histories of midship vertical bending moments and analysed harmonic components in regular waves, Fn = 0.36, head seas, wave length is λ/L_{pp} = 1.04. The moments at the top of the figure are non-dimensionalized by the amplitude of the first order moment (linear part).

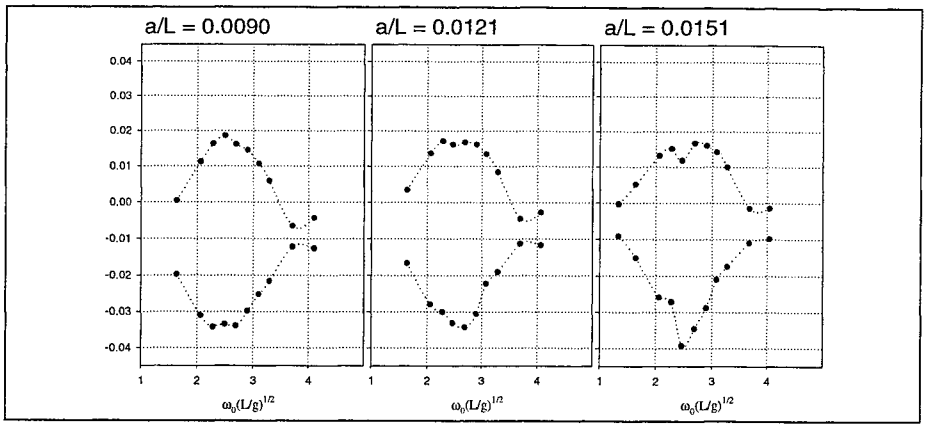

Figure 5. Non-dimensional hogging and sagging moment amplitudes ($M/(\rho g B L^2 a)$). a is the wave amplitude. Fn = 0.36, head seas.

4 RESPONSES IN IRREGULAR WAVES

Spectrum analyses were used to obtain characteristic values of the vertical bending moments in irregular waves. Vertical bending moments in terms of linear standard deviations in irregular waves were relative close to each other for the six bow versions.

Applying time history analyses, the difference between sagging and hogging moment can be determined. The ratios of hogging to linear were the same order of magnitude for all of the bow versions. The sagging moment increased as the flare angle decreased. The shorter and longer ship models clearly deviated from the models of the same length. The differences between sagging and hogging moments were rather large.

Peak distributions of external hydrodynamic forces for the six models are given in Figure 6. External hydrodynamic forces mean that the inertia forces of the segments are subtracted from the measured forces. The external hydrodynamic forces acting on the bow were largest for the bow version E that has the largest flare. The smallest measured forces were at the bow version F. Despite the facts that the differences in bow forces were relatively large, the differences in the sagging bending moments between the bow versions were smaller. Extreme peaks were more like impact loads and they can induce whipping moments but not necessary rigid body bending moments.

In the early design stage, the sagging and hogging moments can be estimated using so called modelling factors, see, e.g. Guedes Soares & Schellin

(1996). First linear methods can be used to calculate the vertical bending moments and then using the modelling factors, the sagging and hogging moments can be determined. In the simple formulas, modelling factors depends on block coefficient only. In the rules of the classification societies, the difference of the sagging and hogging moments is taken into account by block coefficient also. The ratios of sagging and hogging moments can be determined from the irregular wave test results. These ratios can be applied to take into account the difference between sagging and hogging moment. However, strictly speaking the ratios are valid only for the speed, heading angle and sea state where they are determined. More accurate model has been developed where the factors depend on the significant wave height, heading angle, and wave frequency (Guedes Soares & Schellin 1996). The dependence of wave frequency is taken into account by using transfer functions of amplitudes seprately for sagging and hogging moments, see Figure 5.

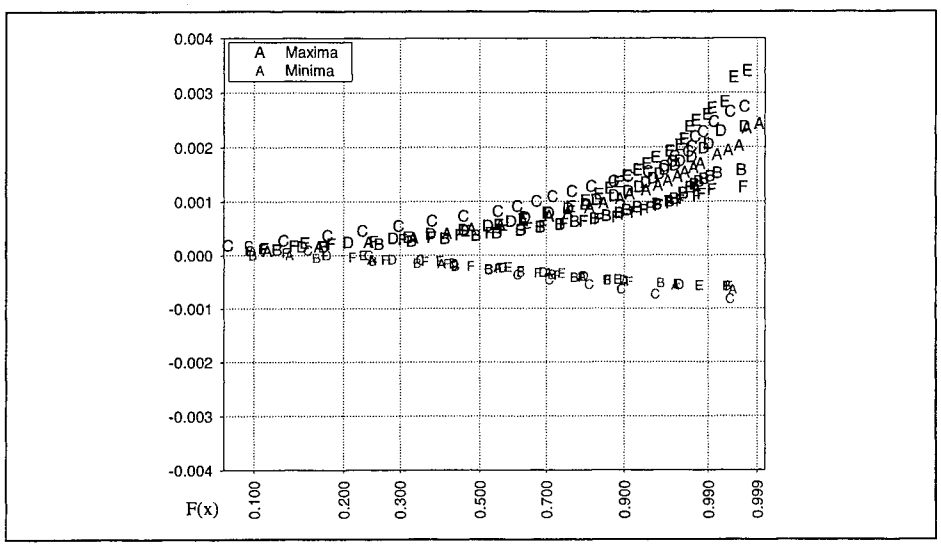

Figure 6. Peak distributions of external hydrodynamic forces ($F/(\rho g B L^2)$) at the foremost segment, Segment 5. Models A ... F, Fn = 0.36, head seas, and H_s = 5 meters.

5 SAGGING AND HOGGING MOMENTS

Design values of the bending moments depend on the intended operation of the ship. For unrestricted service, the sea area in wave load analyses is typically the North Atlantic and only an involuntary speed reduction may be allowed. The design moments are defined as an extreme value that can occur

once during the service time of the ship. Service time in wave load analyses is typically 20 years. However, for the safe operation of the high speed ship, normally service area restrictions and sea state limits have to be defined. For example, HSC code defines the following specific conditions to operate the ship (HSC code 1994):

- Normal operation conditions. No limits of safe operation.
- Worst intended conditions; specified environmental conditions within which the intentional operation of the craft is provided. Operations at all headings may not be possible.
- Critical design conditions; limiting specified conditions chosen for design purposes.

The limits for the operational and environmental conditions are defined in the code by vertical and horizontal accelerations. In the normal and worst intended conditions, limiting criteria can be based on passenger comfort and safety of cargo. Critical design conditions are more severe than the worst intended conditions. The design loads can be based on involuntary and/or voluntary speed reductions, and a change of course in severe sea states. All the different operational and environmental conditions have to be checked to determine the design loads. This means that several different, speeds, headings, and combinations of wave periods and wave heights are needed to obtain predictions for the maximum values of the responses.

To obtain design sagging and hogging moments in different sea states statistical predictions were applied. The predictions were determined by applying second order statistics and regular wave test results. Short-term extreme values and probability distributions of peaks were based on Hermite moment model, see Winterstein (1988), Mansour & Juncher Jensen (1995), and Juncher Jensen & Dogliani (1996). Applying the peak distributions or extreme values, the predictions for sagging and hogging moments can be calculated in the certain short term conditions, i.e. for different sea states H_s and T_z for certain speeds and headings.

The design load is assumed to be defined as the extreme value that will occur during a sea state of three hours with exceedance probability of 1%. Most probable extreme responses in 3 hours sea state with exeedance probability 1% can be obtained from the equation

$$\hat{x} = \delta\sigma\sqrt{2\ln(N)}, \tag{4}$$

where σ is a standard deviation of the process, N is a number of encountered response cycles during the short term sea state, and δ is a non-linearity parameter (Mansour & Juncher Jensen 1995). Generally, the non-linearity parameter for sagging is greater than one, and for hogging less than one. In the linear theory, the non-linearity parameter is unity (δ = 1.0). The non-

linearity parameter depends on skewness and kurtosis coefficients. The skewness coefficients increased in higher waves and affected the differences between sagging and hogging.

The applied second order statistics have been developed for weakly nonlinear responses but the bending moments were more like strongly nonlinear for these ship models and in these model test conditions. For example, at Froude number of $Fn = 0.36$ the large part of the bow area was out of water in higher waves in regular and irregular waves, and moderate bow impacts occurred frequently. However, applying the second order statistics it was possible to analyse the sagging and hogging moments more reliable in different sea states, H_s and T_z, than where the model tests were carried out. It is also improvement on the linear methods.

Verifications of the predictions were carried out by using the irregular wave test results. The correspondence was reasonable. The sagging moment was somewhat underestimated and hogging moment underestimated. The same trend can be seen in the time histories of the regular wave test results, see Figure 4. This explains partly of the differences in predictions comparing to the irregular wave test results. In the final predictions, the differences between measured and calculated peak distributions were taken into account by applying calibration coefficients. The coefficients were obtained from irregular wave test resultss. In other sea states, than used in the model tests, the calibration coefficients might overestimate or underestimate the predictions.

Model test results in irregular waves include also uncertainties due statistical scattering due to random phenomena of the responses in irregular waves. Thus, the uncertainties in the extreme peaks at the low probability level include rather large uncertainties. In the design value predictions, this was partly taken into account by using exceedance probability level of 1%.

The sagging and hogging bending moments at two different speeds were determined in different sea states by applying the second order statistics. The differences of the midship bending moments among the six bow versions were detectable. However, the differences are relative small. The sagging moment was about 20% higher for the bow version E than for the A version. Hogging moments were in the same order of magnitude for all of the ship models. Bending moments of the longer and shorter versions B and C were consistent with the other ship models.

6 SUMMARY AND CONCLUSIONS

Model tests were carried out by segmented ship models for six different bow versions. The ship models were fast Ro-Ro ships with different bow designs. The models had a different flare and stem angles, and a different angle of entrance. The ship models were segmented to four parts from mid-ship to bow. The model tests were carried out in irregular and regular head waves with two different speeds.

Seakeeping characteristics were similar for the six bow versions. Heave and pitch transfer functions were almost identical. The hogging moments were in the same order of magnitude for all of the bow version, but differences were relatively larger for the sagging moments. The sagging moment was highest for the largest flare bow version.

ACKNOWLEDGMENT

Experiments were conducted in co-ordination with Kvaerner Masa-Yards Technology.

REFERENCES

Guedes Soares, C. & Schellin, T. E. 1996. Long term distribution of non-linear wave induced vertical bending moments on a container-ship. Marine Structures, Vol.9, pp. 333-352.

HSC Code. 1994. International code of safety for high speed craft. IMO Resolution MSC.36(63) adopted on 20 May 1994.

Juncher Jensen, J. & Dogliani, M. 1996. Wave-induced ship hull vibrations in stochastic seaways. Marine Structures, Vol.9, pp. 353-387.

Karppinen, T. Rantanen, A. & Hellevaara, M. 1998. Wave loads on fast monohulls. In symposium on Structural Design'98, Espoo, Finland 1998.

Mansour, A. E. & Juncher Jensen, J. 1995. Slightly non-linear extreme loads and load combinations. Journal of Ship Research, Vol. 39, No. 2, pp. 139-149.

Winterstein, S. R. 1988. Non-linear vibration models for extremes and fatigue. Journal of Engineering Mechanics, Vol. 114, No. 10, pp. 1772-1790.

ICE FORCE MODEL TESTS OF A FPSU SYSTEM

Sami Saarinen, Kaj Riska, Ilkka Saisto
Helsinki University of Technology
Espoo, Finland

Abstract

The aim of the model test series carried out on the FPSU-system was to obtain the design values of forces on the yoke used in the system. The tests were divided into three different FPSU-ice interaction situations. One where the ice meets the stern of the tanker first and then forces it to turn around into the normal weather vaning position. The other test situations included the weather vaning position and one where the ice meets first the side of the tanker. The model tests were done with a range of sheets of thicker ice than the design level was. The extrapolation of forces into the design case was done then by first fitting an expression on the measured maximum forces, then the expression was extrapolated into full scale and then the values in the design case were calculated.

1. INTRODUCTION

The purpose of the project was to clarify ice forces and design features in ice of the FPSU system and to develop design criteria for FPSU in ice conditions using model test results. Also a basis to rationally evaluate ice resistance of the FPSU system of SZ 36-1 field was provided. The aim of the tests was to search for the critical ice-FPSU interaction scenarios that produce the highest loads.

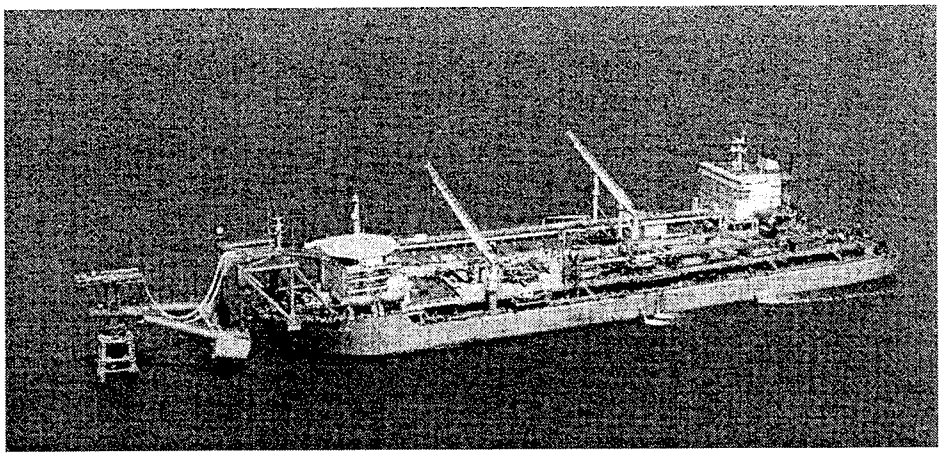

Figure 1. The FPSU at SZ 36-1 oil field.

The FPSU is located in the Bohai Bay (China) east from Tianjin. Maximum current in the area is 1.76 m/s in northerly or southerly direction. The following full-scale ice data with 25 years return period was provided by COOBC as a basis to simulate the ice conditions at SZ 36-1 location:

Level ice thickness	24.0 cm
Rafted ice thickness	44.0 cm
Flexural ice strength	650 kPa

The design level ice thickness of the FPSU unit was very thin, 24 cm. As in AORC model ice cannot be produced to specified properties when ice was thinner than 20 mm, this would have led to a scale of 1:12. This scale would mean a 17.5 m long tanker model. Because this size of models cannot be used in AORC, it was decided that the model tests have to be performed in three larger ice thickness and then the results are to be extrapolated to the design ice thickness. The used scale was chosen so that the model would be as large as possible and thus a scale of 1:30 was selected.

The tests were done by pulling or pushing the jacket and FPSU through level ice. During a test the yoke and FPSU was allowed to turn freely around the jacket. In the tests there were three different pulling directions (0°, 90°, 180°) and two different speeds (0.5 and 1.0 m/s at full scale).

The forces affecting on the whole FPSU system were measured using six force gauges and the forces affecting to the yoke were measured with three force gauges, which were installed to the rotating head. Also the pulling force of mooring legs were measured with force gauges. The relative movement of the yoke system compared to the jacket was also recorded.

1.1 GENERAL DESCRIPTION OF FPSU

The FPSU system consists of five rigid elements: Mooring tower, yoke, two mooring-legs and FPSU. The mooring tower is piled jacket structure and it is about 60 m high from seabed. The water depth is about 32m. The joint between the rotating head of yoke and the tower is about 18 m above the water line.

Yoke is 32 m long and this from above "Y" shape structure is 24 m wide. At the FPSU end of the yoke is 162 tons ballast. The mooring legs connect the yoke and the FPSU with universal joints at both ends.

The length of the floating production and storage unit, FPSU, is 210 m, the draft is 11.7 m and the displacement is 75 335 tons when full loaded. The mooring structure is above the deck at the bow of the FPSU. The produced fluids are transmitted through the tower via piles of the jacket so there are no flowlines or

risers at the center of the jacket structure. Transmission from the tower to FPSU is arranged via free-hanging flowlines, which are above the yoke.

1.2 GENERAL DESCRIPTION OF THE MODEL

The model was constructed in AORC. At the model scale 1:30 the properties of the ice were within achievable range and the size of the model suitable for testing. The basic model principle in constructing the model was to reproduce the parts of the system according to scale. Thus the yoke system is geometrically similar to that in full scale and also the mass is scaled ($M \sim \lambda^3$). The forces were measured in principle at three locations:

- Tension at the mooring legs attaching the yoke to the FPSU.
- All force components between the yoke and the jacket.
- All force components of the total load acting on the jacket.

Also the position of the yoke relative to the jacket was measured by three angles. This array of signals leaves the positions of mooring-legs and thus the position of FPSU undetermined. A sketch of the measurement arrangement is in fig. 2.

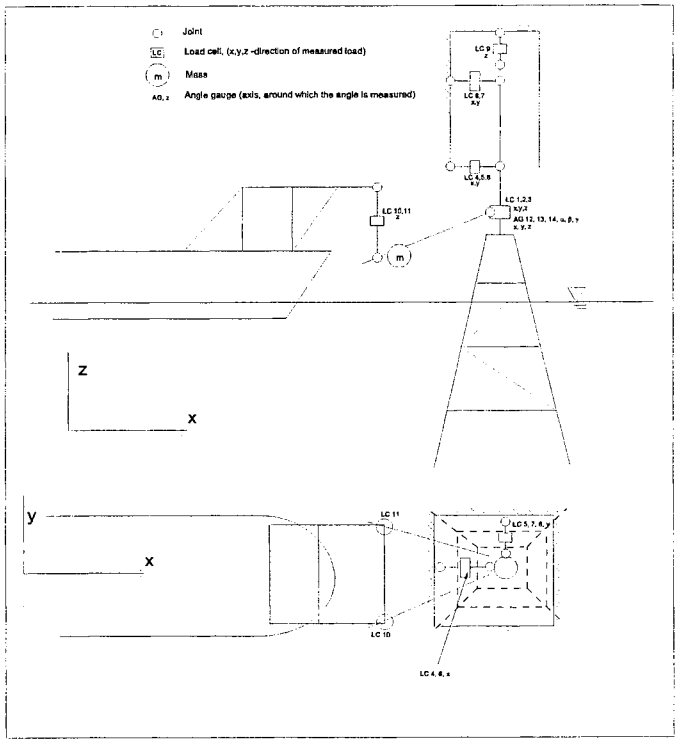

Figure 2. A sketch of the measurement arrangement

1.3 THE YOKE MECHANISM

The yoke mechanism is also studied in order to understand how it responds for different loads. All joints between the elements of whole FPSU -system allow free turning around all axes. Thus this "yoke - mooring-leg -mechanism" behaves like a progressive spring between the jacket and the FPSU. Ballast masses at the yoke's FPSU -heads increases the stiffness of the spring-mechanism. A simplified sketch of this structure is presented in fig. 3.

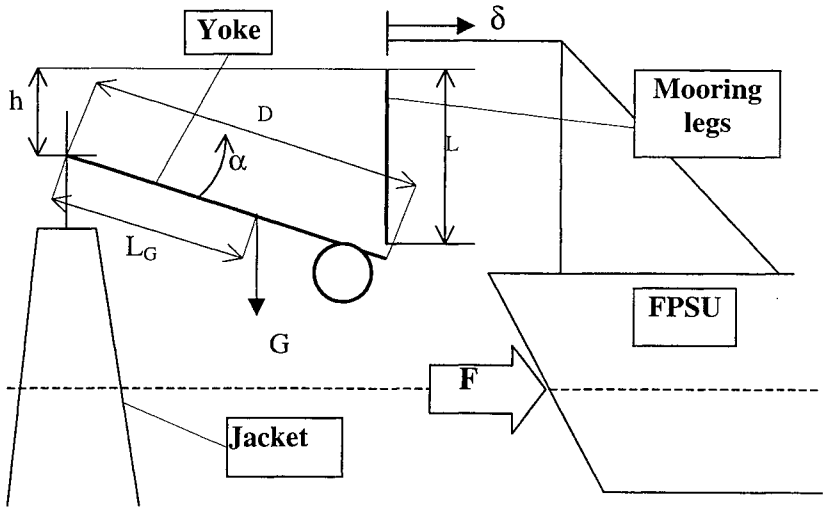

Figure 3. A simplified sketch of the FPSU with yoke angle α ,deflection δ and the external ice force F.

When the system freely settles to its equilibrium (when there is no external forces acting to the system) the potential energy reaches minimum. From the geometry of the structure it can be easily seen that it happens when mooring legs stand exactly vertically.

When load is applied on the tanker, the mooring legs turn towards vertical position and the yoke is lifted up. The resistance of the yoke increases when the deflection δ increases. When δ increases, also α increase. Using statistical analysis we can get the stiffness of the yoke versus the deflection and the stiffness as a function of the angle α. When the FPSU is in full load we get the stiffness curve of the yoke as a function of δ that is plotted in the fig. 4.

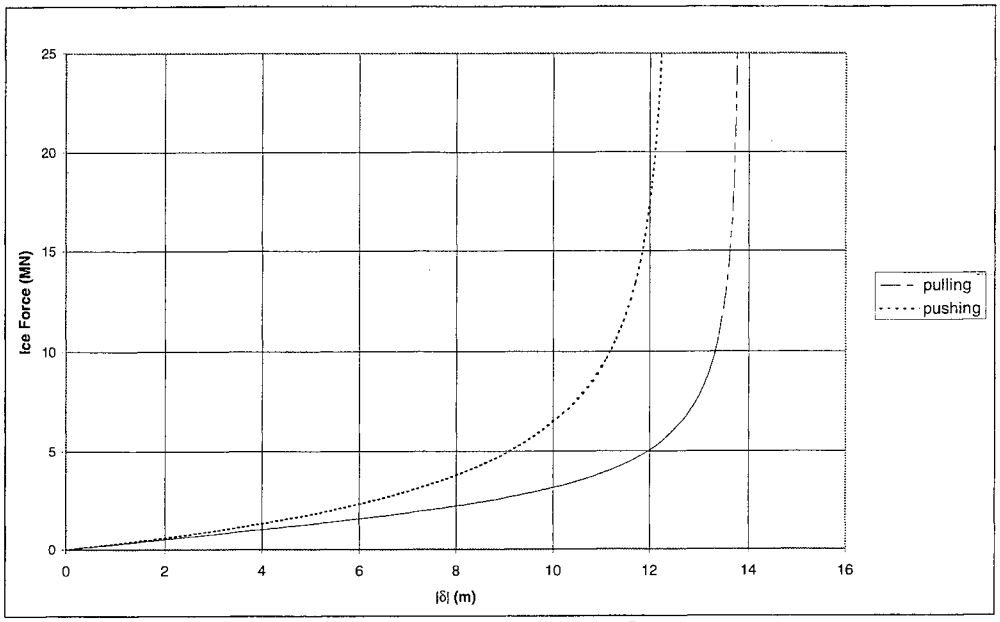

Figure 4. The ice force of the FPSU as a function of δ.

The ice force has to grow beyond any limit, when α and δ are about to reach their geometrical maximum values. α and δ have two maxims depending on the situation. When the tanker is pulled away from the jacket and the yoke-mooring leg -mechanism is completely straightened out, the maxims are α=21.0° and δ=13.9m and when the tanker is pushed against the jacket the maxims value for α are 29.2° and δ= -12.5m.

2. MODEL TESTS

2.1 TEST PROGRAM

The original test program suggested three different loading conditions. Since the amount of the ice sheets was limited to six, only full load condition was tested.

Each test was done by pulling the jacket and the FPSU through ice and the forces on the jacket and the yoke were measured. The jacket was moved instead of pushing the ice field. This way the water flow around the tanker and the jacket is similar to the full scale situation. Since it was not clear if the phenomena are speed dependent, some tests were done with normal speed (in full scale 0.5 m/s) and some with double (1.0 m/s) speed.

Three test types (directions of pulling) were selected:

1. The counter vaning position (test T1):

   The ice is pushed against the stern of the tanker. The initial motion of ice is parallel to the tanker.

2. The weather vane position:

   Weather vaning position where the tanker is parallel to the ice movement. Ice first hits the jacket and then the bow of the tanker. Test labels T2 (full scale speed 0.5 m/s) and T3 (1.0 m/s)

3. The transverse position:

   The tanker has penetrated ice and then the ice starts to move perpendicular to the length of the tanker. Ice hits thus the side of the tanker. In test T4 the FPSU-system was in the ice channel and T5 (full scale speed 0.5 m/s) and T6 (1.0 m/s) ice was only in the one side of the tanker.

A view how one ice sheet was used making tests T1 – T6 is presented in appendix A.

The tests were decided to be done in three different ice thicknesses and in three different ice strengths. Since the number of ice sheets was limited to six all the nine possible h -σ combinations were not measured. The ice properties of all ice sheets are presented in Table 1.

Table 1. The ice properties during FPSU-model tests.

Ice sheet	Date	σ_f (kPa)	σ_c (kPa)	h (mm)	E (Mpa)
1	040398	24.4	15.0	30.0	65.6
2	060398	51.3	19.6	22.0	224.5
3	100398	16.6	15.8	38.0	28.6
4	120398	18.8	16.0	22.0	82.1
5	250398	25.0	18.8	22.0	21.9
6	310398	10.7	6.3	30.0	3.8

3. TEST RESULTS

The preliminary tests with the system proved that the speed of ice sheet motion has a large effect on the forces. Thus it was decided that the tests are run with a full scale speed of 0.5 m/s. Only the tests in weather vaning position are run in two speeds; 0.5 m/s and 1 m/s, in order to clarify the speed dependency.

3.1 RESULTS FROM THE BACKING TESTS (T1-SERIES)

The T1-type of test starts by pushing the tanker stern to the ice sheet. The test can be divided into three distinct phases; the starting phase, turning phase and final phase.

The results obtained include a qualitative description of events taking place in each FPSU-ice interaction scenario. Especially the sequence of events in the counter vaning position were clarified. First the turning rate of the tanker is relatively slow and the stern of the tanker crushes ice. After a while the tanker starts to turn quickly and almost on the spot. The maximum forces occur in the beginning of this second phase i.e. when the tanker has turned about 40°. Further the maximum horizontal force on the yoke system in this set-up was 17 MN in the design condition. The yoke system was seen to rotate much in this test. As large as 25° angles were observed. These occur when the tanker is not aligned with the yoke. The mooring legs experienced even larger forces, the maximum force in the design condition being 30 MN.

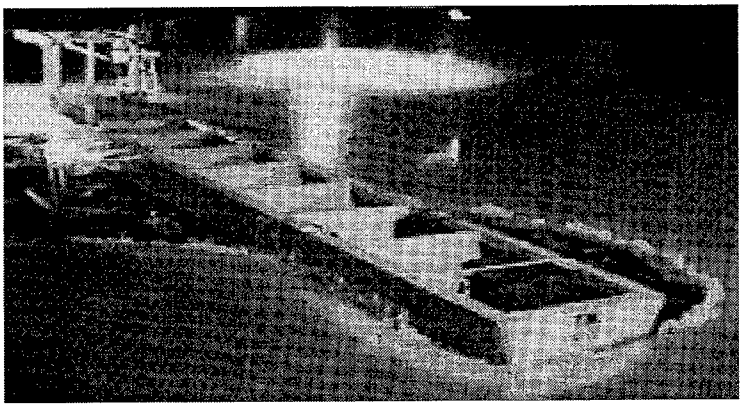

Figure 5. The turning phase

As a qualitative conclusion of the this test type it can be said that the moment on the tanker causes a large moment on the yoke and makes it rotate much. All the flexibility of the yoke system was consumed in almost all the ice sheets; only in

the last, very soft ice sheet, the angle α was smaller than the structural maximum. Examples of the quantities measured in test T1 is presented in figs. 6 and 7.

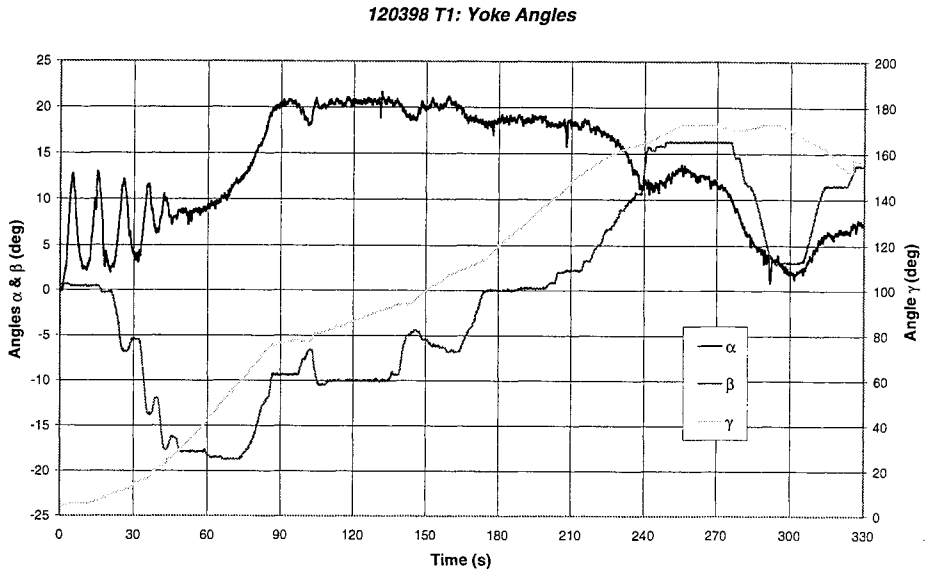

Figure 6. Examples of the yoke angles measured in test T1.

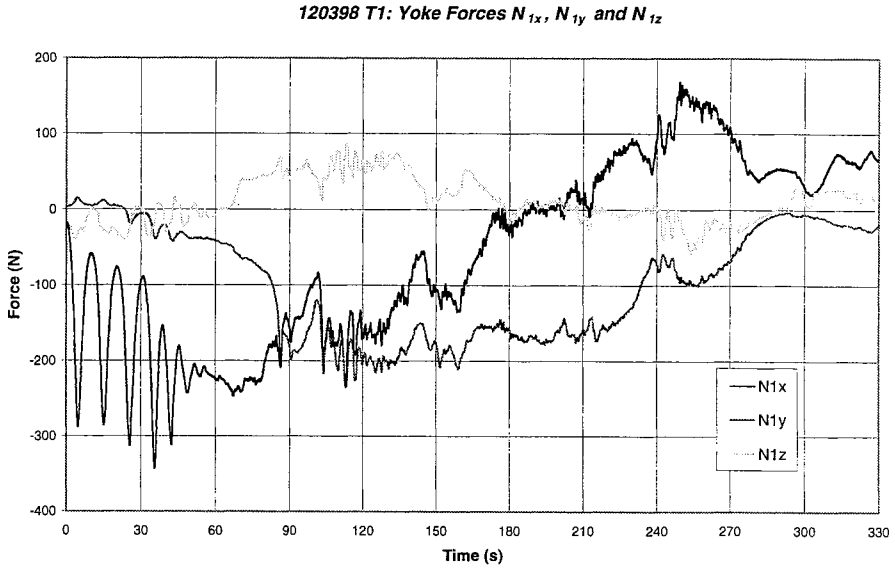

Figure 7. Examples of the forces measured in test T1.

3.2 RESULTS FROM THE TESTS FORWARD (T2- AND T3)

The weather vaning scenario gave naturally the least forces. Typical for this test was that even a small change of the tanker position sideways in relation to the jacket led to large difference in the forces on the mooring legs. This suggests that it cannot be assumed that the mooring legs share the force but might carry all the force alone at some time instant. The speed dependency of the forces proved to be linear, doubling the speed led to doubling of forces. It is, however, uncertain to how large a speed range this conclusion is valid.

3.3 RESULTS FROM THE TESTS OF 90^{O} ICE MOTION (T4-, T5- AND T6)

The test where the tanker–yoke–jacket -system is first aligned and then pulled in the direction of the normal of the symmetry axis may be performed in a variety of ways. In the present test series, two types of tests were done: T4 -series and T5/T6 -series (series T6 is similar to T5, but done with a double speed).

The situation where the ice meets the side of the tanker first was much different in the case when the tanker was in the ice channel and when only an ice floe hit the side. The forces were clearly larger in the first case. This is natural, as when the tanker turned, it had to break ice at the stern also. The maximum horizontal yoke force was 9.1 MN and 5.0 MN in the first and second case, respectively. The forces on the mooring legs were smaller than the horizontal yoke force; being 5.2 MN and 4.1 MN, respectively.

The situation where the ice meets the side of the tanker first was much different in the case when the tanker was in the ice channel and when only an ice floe hit the side. The forces were clearly larger in the first case. This is natural, as when the tanker turned, it had to break ice at the stern also.

4. ANALYSIS OF THE TEST RESULTS

The analysis is carried out by investicating the measured maximum values from the model tests.

In order to widen the range of applicability of these results, it is here assumed that the maximum values are set mainly by the ice parameters. The parameters considered to influence the maxima are the ice thickness h, ice compressive strength σ_c and ice flexural (bending) strength σ_f. The ice force or angle, in case of α, is assumed to take the following form stemming from bending, crushing and submersion (sinking) force components:

$$F = C_1 \cdot \sigma_f \cdot h^2 + C_2 \cdot \sigma_c \cdot h + C_3 \cdot \rho_{ice} \cdot g \cdot h \qquad (1)$$

where ρ_{ice} is ice density and g is acceleration of gravity. The constants C_1,C_2 and C_3 are determined with regression. The regression gives the possibility to extrapolate the results to the values of ice strength and thickness in full scale given in the design case. The Equation 1 assume that the force has three components. These components describe ice behaviour when the offshore structure is breaking it. The first part is related to ice bending, the second part to ice crushing and the third part to ice sinking below the waterline. These three ice breaking components are presented in fig. 8.

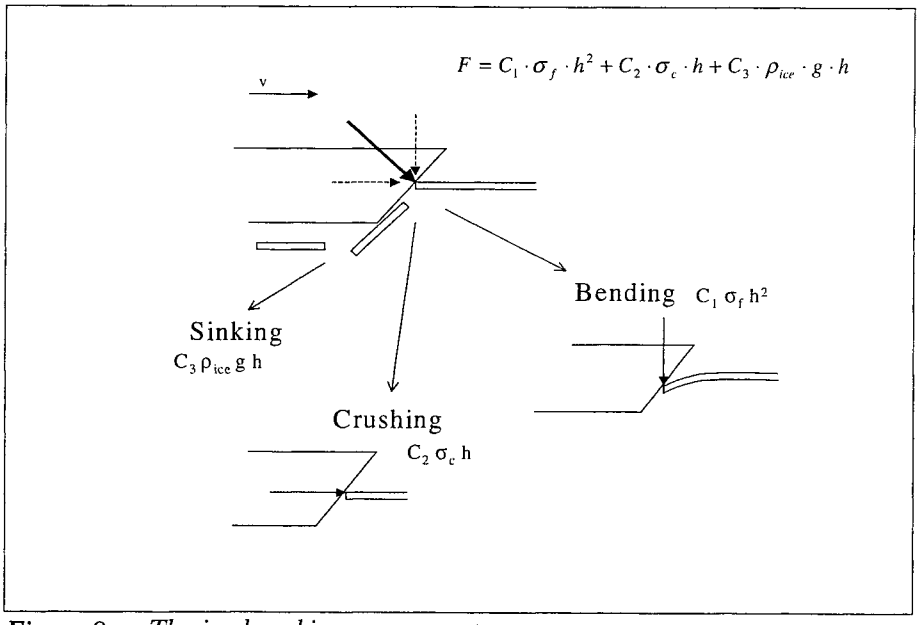

Figure 8. The ice breaking components.

The regression gives different values for C_1, C_2 and C_3 for each test type. Some of these values may be nearby zero (or even negative) which usually means that the corresponding ice breaking component is not involved (or is very small) at the present test. In this case the regression must be solved again but this time without the zero-constants. The solved constants for each test type are presented in Table 2.

Table 2. The coefficients and the ice breaking prosess for each test type

Test 1	C_2	crushing
Test 2	C_1 , C_3	bending and sinking
Test 3	C_1 , C_3	bending and sinking
Test 4	C_1 , C_2	bending and crushing
Test 6	C_1 , C_2	bending and crushing

In extrapolating the maxima to full scale we have to first scale the coefficients to the full scale. C_1 is dimensionless so model and full scale values are the same. C_2 has a dimension of length so it must multiply by the scale factor λ (=30) and C_3 has a dimension of length squared so it must be multiplied by λ^2 (=900). After this we can put the wanted full scale ice property values to the equations to get the final full scale forces. These values are calculated according to the ice properties of original test-plan and according to the ice properties of design point.

5. CONCLUSION

The aim of the model test series carried out on the FPSU-system was to obtain the design values of forces on the yoke used in the system. The tests were divided into three different FPSU-ice interaction situations. One where the ice meets the stern of the tanker first and then forces it to turn around into the normal weather vaning position. The other test situations included the weather vaning position and one where the ice meets first the side of the tanker. These last situations were tested in to variations: One where the tanker was in an ice channel made by the previous tanker weather vaning motion and other which correspond to a situation where an ice floe hits the tanker on the side.

The design point of the FPSU-system is in very thin ice, h_i=0.24 m. As the tanker itself is relatively large, L=210 m, the model tests were carried out in scale of 1:30. Model ice cannot be produced reliably in this thickness. Thus it was decided that the model tests are run with a range of sheets of thicker ice. The extrapolation of forces into the design case is done then by first fitting an expression on the measured maximum forces, then extrapolating the expression into full scale and then calculating the values in the design case.

The tests achieved the targets set for them. There are, however, clearly many things open still if a more general design basis is needed for SPM-loading systems. The estimates made based on existing force formulations showed that none are directly applicable to this situation. Still at present, the only reliable way

to obtain the design forces in any configuration is to carry out model tests. When advances are made in the simulation of the breaking pattern around ships and structures, numerical methods may give answers for design. These tests might serve as a starting point for this kind of research.

Appendix A

Testing plan for one ice sheet.

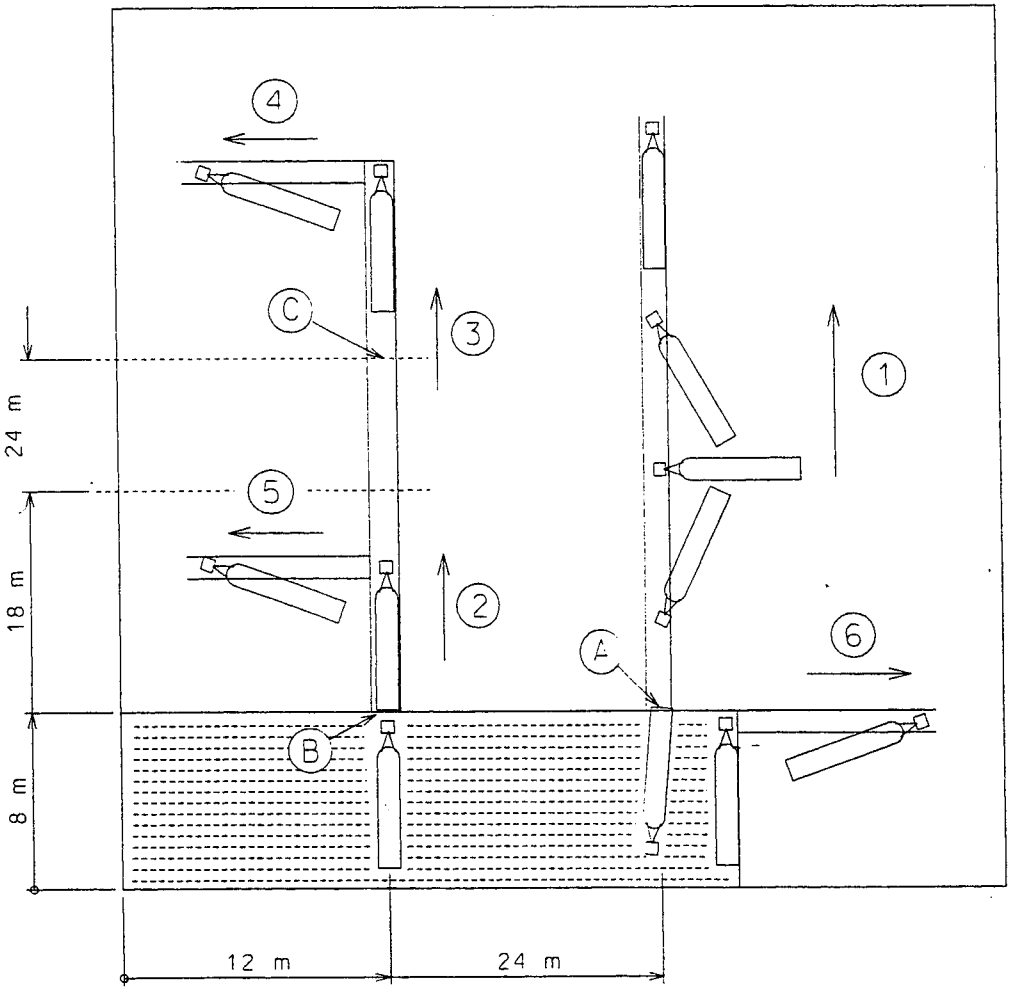

LABORATORY TESTS ON FORMATION OF ICE RIDGES

Jukka Tuhkuri, D.Sc. (Tech.)
Mikko Lensu, M.Sc.
Helsinki University of Technology, Ship Laboratory
Espoo, Finland

Abstract

One of the mechanisms that limit ice forces on structures is the capability of an ice cover to transmit horizontal forces; The force cannot be higher than the force needed to fail the ice sheet away from the structure. If the failure initiates ridging or rafting, these processes determine the force level as long as they go on. In order to find out this force level, ridging and rafting processes have been studied in an ice model basin. During a test, a sheet of model ice was pushed against another similar ice sheet and the pushing force was measured. Two types of ice sheets were used. Ice sheets of uniform thickness did not form ridges, they only rafted, but in ice sheets of non-uniform thickness the initial rafting process transformed into a ridging process. Thus, pressure ridges were formed and ridging forces were measured for the first time in laboratory conditions.

1. INTRODUCTION

Ice forces on a structure are due to relative movement between the structure and ice and sequential failure of the ice. Figure 1 shows an example of ice cover failure against a marine structure. In this problem four different processes are identified: crushing, flexural failure, pile-up, and ridging. When a floe edge strikes the structure, the ice edge crushes locally until the vertical contact force is large enough to cause a shear or flexural failure and a new contact edge forms. Pile-up refers to the process of building a rubble pile against the structure. It can be assumed that the ice load cannot grow to infinity as the force on a structure cannot be higher than the horizontal force needed to fail the ice sheet away from the structure. Thus the load carrying capacity of the ice sheet is defined by the ridging and rafting processes. This force has also been called the pack ice driving force.

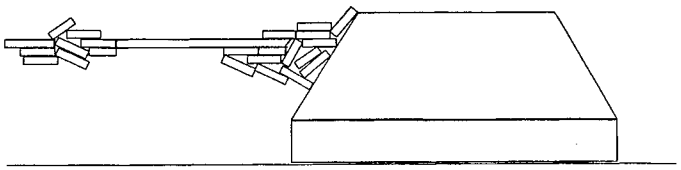

Figure 1. Ice sheet failure against an inclined offshore structure (Riska et al., 1994).

The ice deformation and failure mechanisms active in a ridging event and the related forces are not fully known, and several models have been proposed. Parmerter and Coon (1972, 1973) considered a process where two ice sheets move toward each other closing a lead filled with broken ice pieces. The weight and buoyancy of this rubble load the ice sheet and may break it by bending. This model simulates the ridge growth and suggests that ridges have a limiting height which is a function of the thickness and strength of the ice sheet. By using the model, the ridging force for a 1 m thick ice can be estimated to be about 10 kN/m.

Kovacs and Sodhi (1980) studied shore ice pile-up and ride-up and suggested that when a moving ice sheet hits an obstacle (a pre-existing ridge or a thicker sheet) the ice sheet will first (i) buckle and thus form ice blocks which then (ii) pile up to form a small ridge. In the later stages the moving ice sheet will either continue piling up in front of the ridge, (iii) ride up the face of the ridge, or (iv) push its way through the rubble. Kovacs and Sodhi (1980) concluded that the pressure in an ice sheet during ridging or pile-up is on the order of 10 to 350 kPa.

Sayed and Frederking (1984, 1986, 1988) modelled ridges as two-dimensional wedges and assumed that a critical state of the wedge simulates an actively forming ridge. The ridge is thus assumed to be a rubble pile and the ice sheet is not assumed to enter into the ridge but only to apply a load to the boundary of the rubble pile. Ice thickness is not a parameter in the Sayed and Frederking model, but the ridging force is related to the ridge depth instead: a 150 ... 200 kN/m force is needed to produce about 15 m thick ridge.

Ridge formation has been studied also by using simulations. Hopkins (1994) used a two-dimensional discrete element method to study ridge formation when thin lead ice was driven against a thick floe. Initially, the ice sheet buckled and formed a pile in front of the thick floe. In later stages the sheet was also observed to ride up the slope of the ridge. Recently, Hopkins (1998) extended that work to longer simulation lengths to study the evolution of ridge profile and ridging forces. He observed that the ridge depth growth stops when the force needed to continue the growth reaches the buckling strength of the ice sheet. For a 1 m thick ice with a 1 GPa modulus, Hopkins obtained a maximum average ridging force of 300 kN/m with peaks of 900 kN/m.

Laboratory experiments on ridge formation are rare, and there seems to be no reports on pressure ridge formation from two ice sheets driven against each other. Abdelnour and Croasdale (1986) report on laboratory experiments which consisted of pushing an ice sheet onto an opposite ice sheet or onto a rubble pile. In tests where there were no ice rubble between the two ice sheets, the sheets rafted when pushed against each other. In the other type of tests, when an ice sheet was pushed onto a rubble pile, the sheet either rode up or down the pile. In order to avoid this rafting, Timco and Sayed (1986) did not use two ice sheets but a single one which was compressed against a vertical plate. Initially, the ice sheet failed against the plate, usually in buckling. After formation of a rubble pile, the ice sheet failed either against the rubble or slid over the rubble to fail against the vertical plate. A similar test set-up was used by Lensu and Green (1995) because also their attempts to initiate ridging from the head on impact of two ice sheets were not successful but only simple rafting or finger rafting were observed.

To summarise, two basic types of ridging models can be identified: models analysing deformation of a rubble pile and models analysing failure of an ice sheet against an obstacle (vertical wall or an existing rubble pile). To study initiation of ridging from two ice sheets of equal or roughly equal thickness is one of the aims of the research described here. This paper will first review the main results from laboratory experiments performed to study ridging and rafting, and then discuss the ridging processes observed and the ridging forces measured. The experiments are reported in detail by Tuhkuri and Lensu (1998) and Tuhkuri, Lensu and Hopkins (1998). Parallel to the laboratory work reported here, also discrete element simulations (Hopkins and Tuhkuri, 1998) and field work (Lensu, Tuhkuri, and Hopkins, 1998) have been performed to study ridging and rafting.

2. EXPERIMENTAL

The ice tank of the Ship Laboratory at the Helsinki University of Technology was used in the tests. The tank is a 40 m x 40 m water basin equipped with a cooling system and an xy-carriage. Water depth in the basin is 2.8 m. The x-carriage, or bridge, has a span of 40 m and is mounted on rails along the two sides of the basin. A smaller y-carriage hangs under the bridge and is mounted on round steel rails. The model ice currently used is granular fine grained ice (Jalonen and Ilves, 1990; Li and Riska, 1996). The flexural and crushing strengths and the Young's modulus of each ice sheet used in the tests were measured. The flexural strength was determined from cantilever beam tests. Also the crushing (or compressive) strength is determined by using cantilever beams. The crushing strength was therefore measured only in-plane. The Young's modulus was determined by the plate deflection method.

The test program to study ridging consisted of two parts. In the first part a 40 m x 40 m model ice sheet was cut into two 20 m x 40 m ice sheets and one of the sheets was pushed against the other at a low velocity (~ 1...2 mm/s). Only visual observations and no force measurements were made during these initial tests. Six ice sheets with different thicknesses and mechanical properties were produced and tested. The second part of the test program was more extensive and included 17 tests. Figure 2 shows a sketch of the experimental set-up. A 6.0 m wide area of ice was cut loose from the surrounding ice sheet by cutting parallel slots, leaving the far end uncut. Then the strip was divided into equal parts by making a transverse cut. A 5.3 m wide pusher plate was placed against the free end. During an experiment a strip was compressed at a constant velocity with the pusher plate and the ridging and rafting processes were monitored. The ridges initiated at the initial transverse cut. The load on the pusher plate and its displacement were measured.

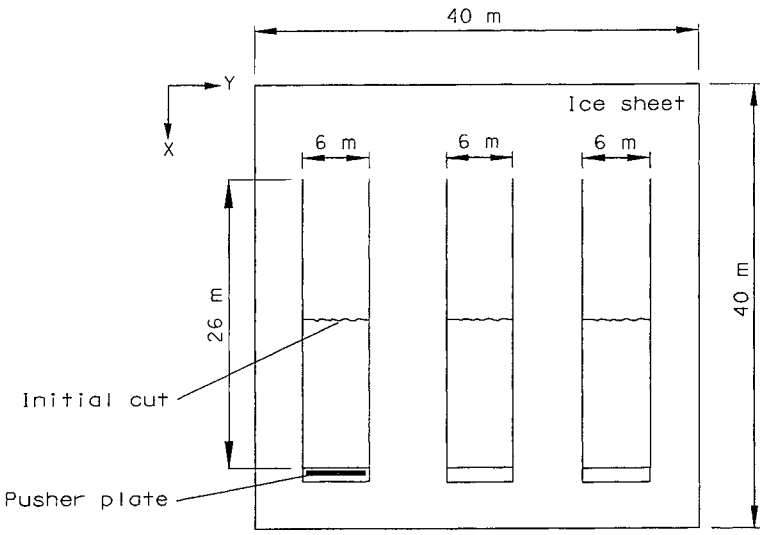

Figure 2. The test set-up used in the tests with ice sheets of non-uniform thickness.

A key aspect of the experiments was the use of model ice with non-uniform thickness. These ice sheets consisted of floes (thick ice) of thickness t_1 and thin ice of thickness t_2 connecting the floes. Such ice sheets were produced in two stages. First an ice sheet of thickness t_i was broken into approximately square shaped pieces which were randomly distributed. No ice was removed from the channel, but as some of the floes were pushed on top of the others, areas of open water were created. Then another ice sheet was produced on top of the floes. Table 1 summarises the main parameters of the tests.

Table 1. Test variables. In the first test series (Tests A - F) the ice thickness t was uniform, and in the second (Tests 1 - 17) non-uniform. $\sigma_{f\downarrow}$ and $\sigma_{f\uparrow}$ are flexural strengths upwards and downwards, E is elastic modulus, and v is pushing velocity. Type is the deformation type are described in Figure 3.

Test	t_1	t_2 / t_1	Initial ice sheet		Floe size	v	Type
			$\sigma_{f\downarrow} / \sigma_{f\uparrow}$	E			
	[mm]		[kPa]	[MPa]	[mm]	[mm/s]	
A	31	1	41.0 / 32.5	-	-	~ 1.0	C
B	53	1	68.4 / 67.1	103.7	-	~ 2.0	C
C	60	1	65.1 / 98.6	214.0	-	~ 1.0	C
D	60	1	31.6 / 42.7	80.0	-	~ 1.0	C
E	34	1	11.3 / 8.1	36.3	-	~ 1.0	C
F	58	1	31.3 / 46.5	100.2	-	~ 1.0	C
1	69	0.36	39.9 / 27.9	-	500	10.5	B2
2	69	0.36	39.9 / 27.9	-	500	35.9	A
3	68	0.35	46.2 / 38.1	65.2	500	10.2	A
4	68	0.35	46.2 / 38.1	65.2	500	10.1	A
5	68	0.35	46.2 / 38.1	65.2	500	10.1	A
6	62	0.39	54.7 / 38.8	53.0	100	10.6	B1
7	62	0.39	54.7 / 38.8	53.0	200	10.5	B1
8	62	0.39	54.7 / 38.8	53.0	300	10.4	A, B1
9	62	0.66	28.8 / 51.1	4.9	500	10.9	C
10	62	0.66	28.8 / 51.1	4.9	500	34.5	B2
11	62	0.66	28.8 / 51.1	4.9	500	61.7	B1
12	61	0.38	41.8 / 25.7	27.8	500	10.3	B1
13	61	0.38	41.8 / 25.7	27.8	500	37.7	B2
14	61	0.38	41.8 / 25.7	27.8	500	24.5	B1, A
15	69	0.36	25.4 / 15.7	11.3	500	10.3	B1
16	69	0.36	25.4 / 15.7	11.3	500	21.9	B1
17	69	0.36	25.4 / 15.7	11.3	500	34.6	B1, A

3. TEST RESULTS

During each experiment the two ice sheets at first rafted at the initial cut. In some cases this was finger rafting and in other cases simple rafting. However, in tests performed with the ice of non-uniform thickness, this rafting process changed into a ridging process. Figure 3 shows the different deformation types observed. These can be characterised as follows:

Type A: After initial finger rafting, a ridging process started and formed both a sail and a keel. Both normal and shear stresses were active. The horizontal shape of the ridge was similar to those seen in the field: the ridges were curvilinear.

Type B1: The deformation started as finger rafting and this formation was stable. A rubble pile formed under each finger. No distinct sail formed, the rubble piles grew under intact ice sheets which naturally were lifted upwards due to buoyancy of the keel.

Type B2: The deformation started as simple rafting. Similarly to Type B1, a rubble pile formed under an intact ice sheet and no sail formed.

Type C: Only simple rafting, no rubble formation.

Type A can be called a ridging process, Type C a rafting process, while Types B1 and B2 are processes between these simple ridging and rafting modes. A similar classification has been earlier suggested by Fukutomi and Kusunoki (1951). As Types A and B were observed only for non-uniform thickness, the thickness ratio t_2/t_1 was a key parameter in defining whether an ice sheet ridges or rafts. This result does not support the crossover thickness between rafting and ridging suggested by Parmerter (1975). The thickness, bending strength, and elastic modulus of the uniform ice sheets were such that, according to Parmerter's model, ridging should have occurred. Hopkins and Tuhkuri (1998) have studied this ridging-rafting transitional behaviour further by using discrete element simulations. The simulations show that the important parameters include thickness t, thickness ratio t_2/t_1, elastic modulus, and ice-ice friction coefficient.

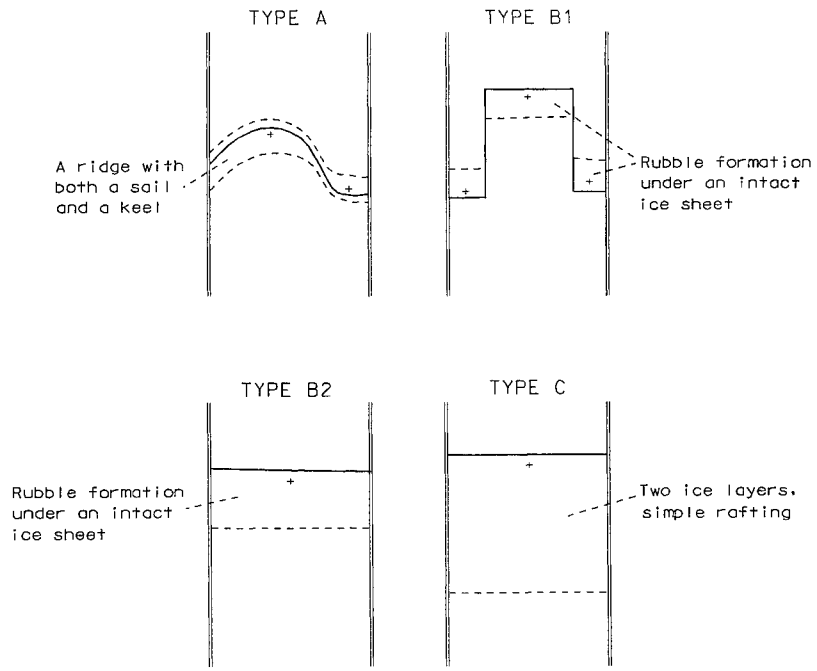

Figure 3. Deformation types observed. Extent of ridge keel (Types A, B1, and B2) or lower ice sheet (Type C) is shown with the dashed line. + refers to an ice sheet on top.

Figure 4 gives an example of the force-displacement, or $F(x)$, records with features characteristic of this test series: After an initial force peak, the force increases about linearly. This linear relationship does not start from the origin. Later the linear increase of the force ceases, but the load appears to continue growing at a lower rate. It also appears that close to the end of the test, the force levels and fluctuates around an average value. In some tests all these features were clearly identifiable while in others only part of them were present. Especially, the change from an increasing trend into a more a less constant force so clear in Figure 4, was not observed in all the tests. However, it is suggested that the above features are characteristic of the ridging and rafting processes observed

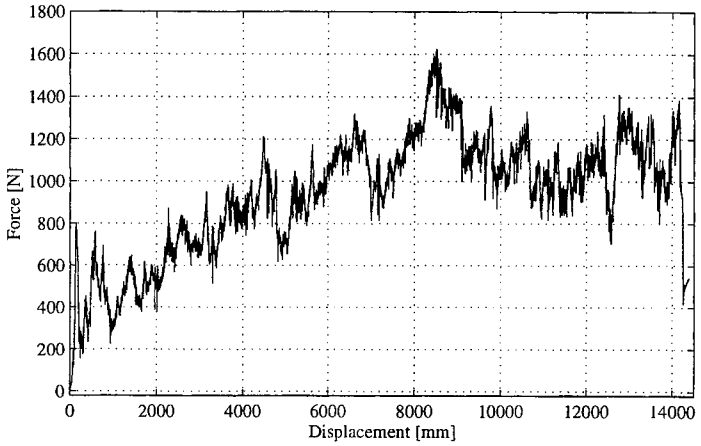

Figure 4. The force-displacement record from Test 3.

4. RIDGING PROCESS

Figure 5 shows the force-displacement records of Type C (Test 9) and Type B2 (Tests 1, 10, and 13) processes. As only simple rafting was observed during Test 9, the slope $\partial F/\partial x$ was constant for the whole test. It is also seen that initially the slopes $\partial F/\partial x$ of Type C and Type B2 processes are equal, but after some displacement l_R the forces of Type B2 processes deviate from linearity. For Test 10, $l_R \approx 10$ m which is also the length of the ridge profile. For Tests 1 and 13, $l_R \approx 5$ m which is again about the length of the ridge profiles. It is therefore hypothesised, that during Type B2 processes the force was increasing linearly as long as only simple rafting was taking place, and this continued until the force was high enough to break the ice sheet and initiate rubble formation. It is noteworthy, that the ice sheet used in Test 10 was stronger ($t_2/t_1 = 0.66$) than the ice sheet used in Tests 1 and 13 ($t_2/t_1 = 0.36$) which might explain why l_R was longer for Test 10.

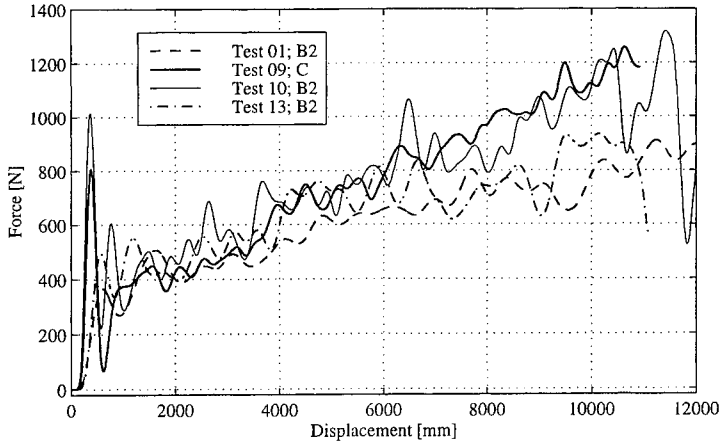

Figure 5. The force-displacement records from Tests 1, 9, 10, and 13. The signals are low pass filtered at $0.005 f_N$, where f_N is the Nyquist frequency.

This hypothesis is sketched in Figures 6 and 7. After a threshold force value F_0 is reached, the initial rafting starts and continues as long as the sheets sustain the pushing force, which increases linearly with displacement ($\partial F/\partial x = \alpha$). It is assumed, that after displacement of l_R the lower ice sheet starts to fail and pile down near the edge E, because the stresses at the lower sheet are highest there. In addition, due to the curvature needed to raft the two sheets, the lower sheet may be pre-broken. When the block piling starts, a Type C rafting process transforms into a Type B2 ridging process. With continued movement the keel may grow as sketched in Figure 6(c). The exact pile down process is not known, but it may include rafting a third layer and especially sheet ride down along the keel slope. A few ice blocks have also been observed to ride up to form a small sail. It can be assumed that with increasing depth of the rubble, higher force is needed to add blocks into the keel. At some stage this piling force may become high enough to break the ice sheet at another location and initiate ridging there, or alternatively the keel may start growing laterally. This stage defines the maximum force F_{MAX}.

In this model, the ridging force is assumed to be below the line defined by F_0, α, and F_{MAX}. A key element of this model is that it suggests that a maximum ridging force F_{MAX} exists, and that F_{MAX} is set by properties and failure process of the ice sheet surrounding the ridge and not by deformation of the ridge itself. This model has common features with other ridging models but also novel features. Especially, the assumption that ridging initiates as rafting grew from the experiments. The relation between ridging force, ice thickness, and keel depth has been suggested also earlier.

What are then the parameters that determine whether initial finger rafting transforms into ridging? In the laboratory test the key parameter was the non-uniform thickness. However, it is not claimed that ridges form only

from ice sheets with non-uniform thickness, but rather that some sort of inhomogeneity of ice is an important factor. Thus the non-uniform thickness should be seen as a test method to model real inhomogenous ice sheets. Inhomogenous ice may have rough surfaces, weak zones, and discontinuities in stress distribution, all contributing to short length of overlap before keel formation. In the experiments, one obvious effect of the non-uniform thickness was that the areas of thinner ice acted as weak zones in the ice sheets.

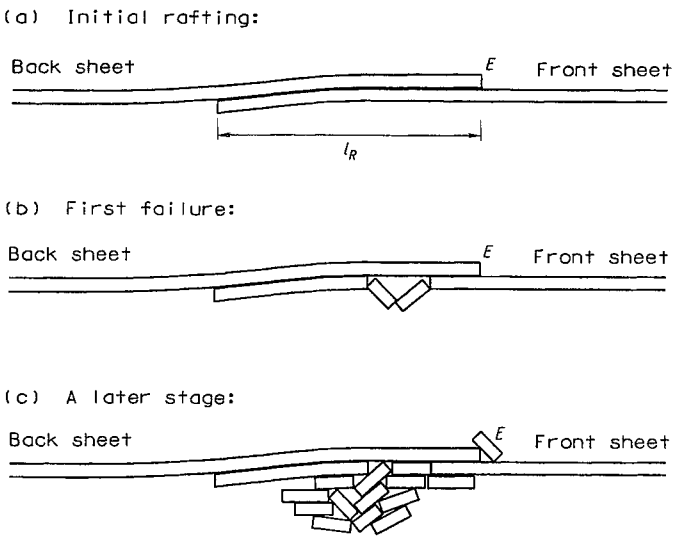

Figure 6. Cross-sections of different stages of a Type B2 ridging process.

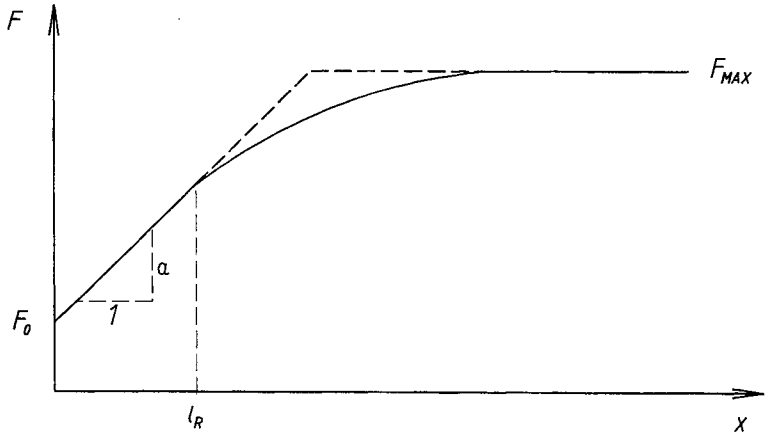

Figure 7. Schematic presentation of the force-displacement relation $F(x)$ according to the proposed ridging model.

5. RIDGING FORCE

One of the important features of the present laboratory experiments was that ridge building forces were measured. Forces have been measured also in the earlier laboratory tests, but in those tests the ice sheets piled-up against obstacles (vertical wall or existing ice rubble). In the present tests series, however, the forces during formation of a rubble pile between two ice sheets were measured. In order to compare the laboratory results with field data and ridge building models, the model test results should be scaled up. Assuming Froude scaling, the forces scale as λ^3, where λ is the scale.

Table 2 shows estimates of ridge building forces from different models and tests. The attempt has been to show estimates of ridging force for 1 m thick ice. The models were discussed already in Section 1. At least partly, the different forces reflect the different assumptions made in the models. Interesting field data has been published by Croasdale et al. (1992). Based on several field measurements of pack ice stresses, they have estimated the ridging forces to be about 40 ... 300 kN/m for 1 m thick ice. An important aspect of the field data is that the instruments measured local stresses and that stress data was then used to estimate the force per unit width at a floe edge. Also based on field data, Croasdale et al. (1992) have estimated the ice forces on the Molikpaq caisson structure loaded by multi-year ice floes frozen within first year level ice. That estimate of pack ice driving forces was obtained by dividing the global load estimate by the ice thickness and the floe boundary length. Ridge building behind the floe was observed.

In their laboratory tests, Timco and Sayed (1986) used different ice thicknesses which in this comparison is taken as different scales. When scaled to 1 m thick ice, their ridging force varied from 130 kN/m to 500 kN/m. In the present tests the model ice thickness was about 70 mm and the highest measured force about 330 N/m. From that value a ridging force of 70 kN/m for 1 m thick ice is obtained. Table 2 gives also a result from discrete element simulations performed parallel with the laboratory tests (Hopkins and Tuhkuri, 1998). These simulations were two-dimensional versions of the three-dimensional tank tests, but otherwise the same dimensions and material parameters were used. The ridging force obtained from the simulations was about half the level measured in the model experiments. This difference is assumed to be due to the nature of the two-dimensional simulations where the force often drops to zero, when a block fails off the sheet. In contrast, in the three-dimensional model tests a failure at a point on the leading edge of a sheet does not coincide with failure across the entire width. In other respects the model tests and simulations gave similar results.

The data in Table 2 shows that the ridging forces during the present laboratory tests were at the low end of the ridging forces estimated earlier. It is possible that this is because the maximum force defined in Figure 8 was actually not reached; If the model ridges did not reach their maximum depth, higher forces could be expected if more ice had been pushed into the

ridge. On the other hand, if the maximum ridging force was reached in the experiments, the value of this F_{MAX} depends on the mechanical properties of the ice sheet. If the maximum ridging force is defined by buckling of the ice sheet, as Hopkins (1998) suggests, the ice thickness t and elastic modulus E are the key parameters. Obviously, the ice with non-homogenous thickness has a smaller buckling strength than a uniform ice sheet with the same average thickness. It can thus be hypothesised, that the ridging force is limited simply by the buckling load. The load needed to buckle a semi-infinite bar resting on Winkler foundation is

$$F = \sqrt{\rho_W g \frac{Et^3}{12(1-\nu^2)}}$$

where ν is Poisson's ratio, and ρ_W is water density (Hetényi, 1946). Taking ρ_W = 1000 kg/m^3, ν = 0.3, E = 1 GPa, and t = 1 m, the buckling force per unit width becomes about 950 kN/m.

Table 2. Ridging force F per unit width in [kN/m] by different models and experiments. For details, see text. t is ice thickness and h is ridge depth.

Pile up against an obstacle:			
Parmerter and Coon (1973)	Model	t = 1 m	10
Kovacs and Sodhi (1980)	Model	t = 1 m	10 ... 350
Hopkins (1998)	DEM	t = 1 m	300
Croasdale et al. (1992)	Field data	t = 1 m	40 ... 300
Croasdale et al. (1992)	Molikpaq	t = 1 m	85 ... 550
Timco and Sayed (1986)	Lab. Data	t = 1 m	130 ... 500
Deformation of a rubble pile:			
Sayed and Frederking (1986)	Model	h = 15 m	150 ... 200
Two ice sheets pushed together:			
Tuhkuri and Lensu (1998)	Lab. Data	t = 1 m	70
Hopkins and Tuhkuri (1998)	DEM	t = 1 m	35
Reference value:			
Buckling	Model	t = 1 m	950

6. SUMMARY AND CONCLUSIONS

This paper has described laboratory experiments on ridging and rafting of an ice cover and discussed the ridging process and the ridge building force. The main results can be summarised as follows:

- All the experiments started as rafting.
- Ice sheets of uniform thickness did not form ridges, they only rafted.
- When ice sheets of non-uniform thickness were used, the initial rafting process transformed into a ridging process.

- Initially, the measured force increased linearly and it was suggested that this linear force increase was defined by rafting. The experiments also suggested that there is a threshold force value which must be reached before the rafting starts.
- The ridging force continued to grow also after the initial linear trend, albeit at a lower rate. A further characteristic of the measured $F(x)$ plots was that in some tests the force appeared to cease increasing and reach a plateau value. This levelling of the force was observed to be connected with either onset of failure of the surrounding ice sheet against the ridge or onset of rafting at a new site.

ACKNOWLEDGEMENTS

This work described here is a part of the project "Local Ice Cover Deformation and Mesoscale Ice Dynamics" or "Ice State" (Contract No MAS3-CT95-0006) supported by the European Commission, DG XII, through the Marine Science and Technology programme 1994-1998 (MAST III). The project is coordinated by the Ship Laboratory, Helsinki University of Technology, Finland and the partners are: Nansen Environmental and Remote Sensing Center, Norway; Scott Polar Research Institute, University of Cambridge, UK; Department of Geophysics, University of Helsinki, Finland; and Engineering Research Institute, University of Iceland, Iceland.

REFERENCES

Abdelnour, R. and Croasdale, K. 1986. Ice forces associated with ridge building: Model tests and results compared with theoretical models. In: Proc. of *IAHR Ice Symp.* 1986, Iowa City, USA, Vol. 3, pp. 227-245.

Croasdale, K.R., Frederking, R., Wright, B., and Comfort, G. 1992. Size effect on pack ice driving forces. In: Proc. of *IAHR Ice Symp.* 1992, Banff, Alberta, Canada, Vol. 3, pp. 1481-1496.

Fukutomi, T. and Kusunoki, K. 1951. On the form and the formation of the hummocky ice ranges. *Low Temperature Science*, 8: 59-88. (In Japanese with English summary.)

Hetényi, M. 1946. *Beams on elastic foundation.* The University of Michigan Press. 255 p.

Hopkins, M.A. 1994. On the ridging of intact lead ice. *Journal of Geophysical Research*, 99, C8, 16351-16360.

Hopkins, M. and Tuhkuri, J. 1998. Simulation of ridging and rafting in first-year ice. Proc. of the 14th International Ice Symposium, *IAHR '98*, Vol 1, Balkema, Rotterdam. pp. 623-630.

Hopkins, M.A. 1998. Four stages of pressure ridging. *Journal of*

Geophysical Research, 103, C10, 21883-21891.

Jalonen, R. and Ilves, L. 1990. Experience with a chemically-doped fine-grained model ice. In: Proc. of the *IAHR Ice Symp.* 1990, Espoo, Finland, Vol. 2, pp. 639-651.

Kovacs, A. and Sodhi, D.S. 1980. Shore ice pile-up and ride-up: Field observations, models, theoretical analyses. *Cold Regions Science and Technology*, 2, 209-288.

Lensu M. and Green J. 1995. Ice tank tests on pressure ridge formation. Espoo, *Helsinki University of Technology, Ship Laboratory*, Report M-202. 83 p.

Lensu, M. Tuhkuri, J. and Hopkins, M. 1998. Measurements of curvilinear ridges in the Bay of Bothnia during the ZIP-97 experiment. Espoo, *Helsinki Univ. of Technology*, Ship Laboratory, Report M-231. 64 p.

Li, S. and Riska, K. 1996. Preliminary study of physical and mechanical properties of model ice. Espoo, *Helsinki University of Technology*, Ship Laboratory, Report M-212. 100 p + App.

Parmerter, R.R. and Coon, M.D. 1973. Mechanical models of ridging in the Arctic sea ice cover. *AIDJEX Bulletin* 19. 112 p.

Parmerter, R.R. 1975. A model of simple rafting in sea ice. *Journal of Geophysical Research*, 80, 15, 1948-1952.

Riska, K., Cangbo, Z., and Saarikoski, R. 1994. Structure-ice interaction for a Bohai Gulf oil production project. Proc. of 93's *International Symposium on Sea Ice*, Beijing, pp. 230-246.

Sayed, M. and Frederking, R.M.W. 1984. Stresses in first-year ice pressure ridges. In: Proc. of the 3rd *OMAE* Symp., New Orleans, USA, Vol. III, pp. 173-177.

Sayed, M. and Frederking, R.M.W. 1986. On modelling of ice ridge formation. In: Proc. of *IAHR Ice Symp.* 1986, Iowa City, USA, Vol. 1, pp. 603-614.

Sayed, M. and Frederking, R.M.W. 1988. Model of ice rubble pileup. *Journal of Engineering Mechanics*, 114, 149-160.

Timco, G.W. and Sayed, M. 1986. Model tests of the ridge-building process of ice. In: Proc. of *IAHR Ice Symp.* 1986, Iowa City, USA, Vol. 1, pp. 591-602.

Tuhkuri, J. and Lensu, M. 1997. Ice tank tests on ridging of non-uniform ice sheets. Espoo, *Helsinki University of Technology, Ship Laboratory*, Report M-236. 130 p.

Tuhkuri, J., Lensu, M., and Hopkins, M. 1998. Laboratory and field studies on ridging of an ice sheet. Proc. of the 14th International Ice Symposium, *IAHR '98*, Vol 1, Balkema, Rotterdam. pp. 397-404.

THE BACKGROUND OF THE POWERING REQUIREMENTS IN THE FINNISH-SWEDISH ICE CLASS RULES

Kaj Riska, Dr. Tech.
Arctic Marine Technology
Helsinki University of Technology

Abstract

The background of the requirements for the propulsive power of merchant vessels in the Baltic is described in this article. The background work included observations of the operational mode and the encountered ice conditions of a set of vessels navigating in the northernmost Baltic. These observations showed that merchant vessels mostly operate assisted by an icebreaker in an old channel. These two factors were decided to form the design point of the performance of merchant vessels. Thus the ice resistance in channels forms the basis of the determination of the propulsive power. In order to improve the existing formulation of channel resistance, an extensive model test series was carried out where ship particulars were varied. Based on this series, a formulation of ice resistance was developed and finally a powering equation formulated. The powering requirement was, as the last task in the project, validated using the knowledge of performance from existing vessels as a reference set.

1. INTRODUCTION

The decision to keep a number of ports along the whole coastline open throughout the year was made in Finland in the 70's. As all the Finnish ports are ice bound at least during a part of the year, this decision must be accompanied with decisions about winter navigation support. The principle of winter navigation is that all vessels are offered icebreaker assistance into and out of these winter ports. In order to ensure safe and continuous navigation, the authorities place rules for ship strength and performance. These are the Finnish-Swedish Ice Class rules placed and maintained by the Finnish and Swedish maritime administrations. The background of the performance requirements is that once icebreaker escort is

offered, the vessels should be able to follow icebreakers with adequate speed so that vessel delays and icebreaker waiting times are minimized. These performance requirements in the rules have been under revision and Helsinki University of Technology, Ship Laboratory has carried out a project to provide the basis of this revision. The project included first an extensive field campaign during which the basic data about the winter navigation system was collected. This was followed by development of ice resistance and powering formulation. The project was completed by carrying out a verification of the developed formulations using the existing vessels as a test set. The results of these project phases will be described briefly here.

2. THE BALTIC WINTER

During an average winter the whole northern Baltic is ice covered from the line Stockholm - Estonian Hiiumaa island northwards. Even in a mild winter the Gulf of Finland and the Gulf of Bothnia are ice covered. Thus only the port of Hanko and the ports Rauma and Pori on the Bothnian Sea are ice free in a mild winter. The number of annual ice days in the north is about 120 and along the coasts of southern Finland the length of the ice season varies between two and three months. The first ice forms in the beginning of November and sometimes there is still some ice floes in the north in June.

The ice thickness in the Gulf of Bothnia may reach 1.2 m in the shorefast ice but out at sea the thickness of level ice seldom exceeds 0.8 m. The corresponding figures for the Gulf of Finland are 0.8 m and 0.5 m. The thickness of level ice is a good general indication of the severity of the winter but for ship navigation the amount of ridged ice must be taken into account in judging the severity of the winter. Ridging occurs when winds and currents break the ice cover and push it against the fixed ice next to a coast line. Ridging in the Baltic is mostly controlled by winds and thus, as westerly winds prevail, the ice along the Finnish coast is heavily ridged outside the northernmost ports (Kemi, Oulu, Raahe). Likewise the ice is pushed towards the end of the Gulf of Finland and the entrance of the ports of Kotka and Hamina are thus heavily ridged.

The ice cover closer to land i.e. inland from about the 15 m isobath is stationary throughout the winter. This inmovable ice is called the shorefast ice zone. As the Finnish coast is quite shallow, this zone can be very wide. The ship fairways leading to and from ports must go through this zone. The ice in the fairways is repeatedly

broken and through this thermo-mechanic action the rubble ice cover in the fairways grows. The thickest rubble ice occurs usually in the fairways leading to the ports of Oulu and Kemi; there the average thickness across the width can be in excess of 2 m.

3. THE OPERATIONAL PROFILE OF VESSELS

The operational performance of merchant vessels in the Baltic must be based on the most frequently encountered ice conditions and also on the operational profile in ice. As a background work for the Finnish-Swedish ice rules, an extensive field campaign to gather data about the encountered ice conditions and operational modes was carried out during years 1990-94. The observations were done by sending observers onboard ships navigating mainly in the northernmost Baltic. Ten vessels in IA Super and IA ice class were selected for observation. These vessels represent a wide variety of ship types; especially ships from lower and higher ice class were included. The vessels included in the study are described in Table 1 where the symbols are the following: α is the waterline entrance angle and φ the stem angle, L_{bow} is the length of the bow of the vessel, L_{pp} the length between perpendiculars of the vessel at the waterline, B breadth, T draught, P_S shaft power, D_{prop} propeller diameter and Δ the displacement of the vessel. A plot of the velocity and encountered ice profile was made from each voyage and these were matched with the operational events like icebreaker assistance, towing, getting stopped by ice, waiting for icebreaker escort etc.

The summary of the observations show that by far the most frequent ice condition encountered by merchant vessels is an old channel and the most frequent operational mode is navigating with the assistance of an icebreaker. These results are shown quantitatively in Fig. 1. Noticeable is that the relative distance navigated independently in the pack ice in the middle of the sea basins is small. Only MT Sotka and MS Finnfighter navigated in the pack ice, the former because of her exceptional icegoing capabilities and the latter because her voyage started from the Gulf of Finland and thus light ice conditions were included in the beginning of the icebound part of the voyage. MT Hamnö was the only vessel navigating independently during the 1993 observations. This was partly because she tried to reach the sea independently going out from Oulu harbour but was later stopped by ice and had to wait for an icebreaker. Other vessels waited for an icebreaker in the harbour.

Table 1. The particulars of vessels included in the observational programme.

Ship/ice class	α	ϕ	L_{bow}	L_{par}	L_{pp}	B	T	P_s	D_{prop}	Δ
	[°]	[°]	[m]	[m]	[m]	[m]	[m]	[MW]	[m]	[t]
ENVIK/IAS	29.0	39.0	25.6	38.0	96.0	16.2	5.2	2.74	3.05	5583.
KEMIRA/IAS	22.0	35.0	32.3	44.0	105.0	17.0	6.6	4.12	4.15	8565.
LINK STAR/IA	23.0	31.0	32.0	49.0	98.0	17.0	5.8	2.96	3.60	6877.
SOLANO/IA	23.0	31.0	33.4	51.0	116.3	21.0	6.2	5.52	3.80	10458.
TEBOSTAR/IA	19.0	47.0	33.5	37.0	105.3	17.6	6.6	3.68	3.7	7810.
SOTKA/IAS	24.0	29.0	32.4	77.0	150.0	21.5	9.5	11.47	5.45	22033.
AHTELA/IAS	19.0	35.0	43.1	50.0	112.0	19.0	6.1	5.92	3.7	9200.
AILA/IA	23.0	31.0	25.0	33.0	97.4	16.0	5.8	2.96	3.60	6320.
ARCTURUS/IAS	33.0	68.0	49.0	73.0	146.0	25.0	7.3	13.2	5.7	18000.
TERVI/IA	40.0	41.0	32.9	136.0	193.7	30.2	12.0	10.8	7.4	57300.

Instead of using the performance of individual vessels as the basis for efficiency of the Baltic winter navigation system, the definition of the required characteristics of merchant vessels could be based on the overall transport efficiency of the maritime transport system. This quantity is defined as

$$Q = \mathrm{dwt} \cdot \frac{v}{P_S} \qquad (1)$$

where dwt is the dead weight of the vessel and v the average speed through ice. The measured transport efficiencies are shown in Fig. 2. The variation in the transport efficiency is large and partly reflects the time used in waiting for icebreaker assistance. The transport efficiency should optimally be maximised when determining the requirements for merchant vessels. Too many uncertainties were deemed, however, to influence the transport efficiency making it difficult to base any decision on it.

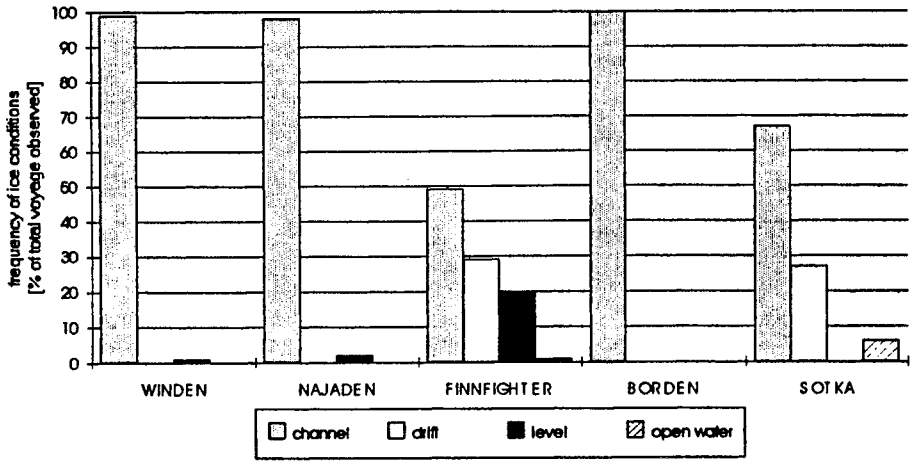

Fig. 1a. The observed frequency of encountered ice conditions in winter 1994 (Lehtinen 1994).

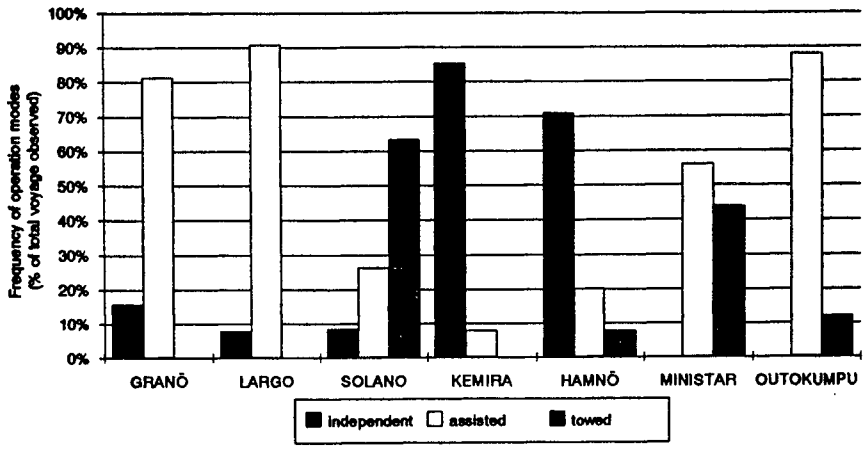

Fig. 1b. The observed operational modes used in winter 1993 (Lehtinen 1993).

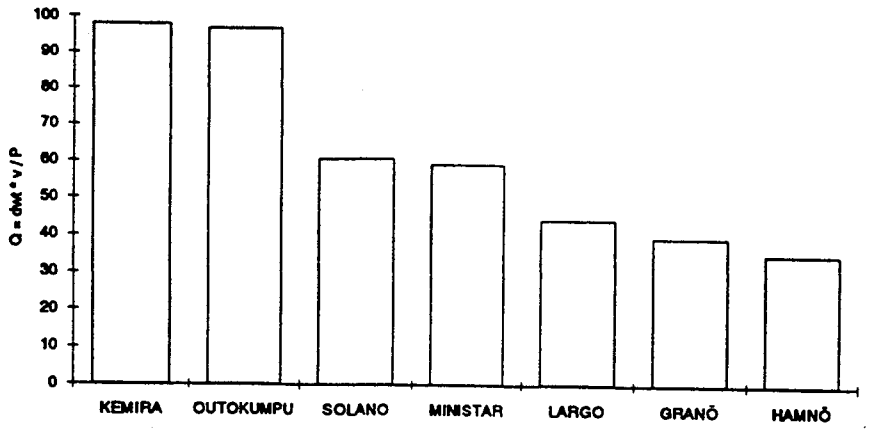

Fig. 2. The observed transport efficiencies observed during winter 1993 (Lehtinen 1993).

4. DEVELOPMENT OF THE ICE RESISTANCE FORMULATION

The ship observations showed that the most frequently encountered ice condition is an old navigation channel shown e.g. in Fig. 3. The ice in these channels can be described as brash ice. Brash ice is made of small rounded ice pieces, the diameter of which is mostly less than about 30 cm. The brash ice is formed by the frequent freezing-breaking cycles when ships navigate through the channels. The thickness growth of these channels is more rapid than that of the adjacent level ice. Figure 4 shows a typical cross section of an old channel close to harbour Kemi in the northern Baltic. The pronounced side ridges which can be several meters thick are clearly seen. The thickness at the middle of the channel is usually below 1 m but the average thickness is in excess of that. When ships do not pass through the channel, ice pieces freeze together. This consolidated layer makes the channel more difficult to navigate. When the air temperature is about -10^{o}C, the thickness of this layer will be about 10 cm after one day, assuming brash ice porosity of 20 % (Leppäranta 1993).

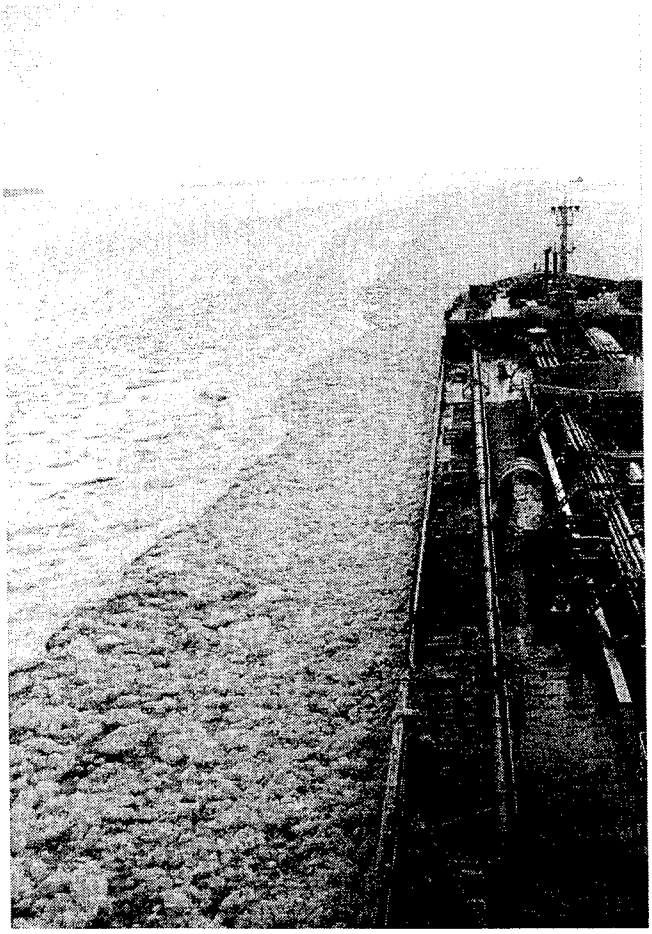

Fig. 3. MT Sotka in an old channel (photo M. Wilhelmson).

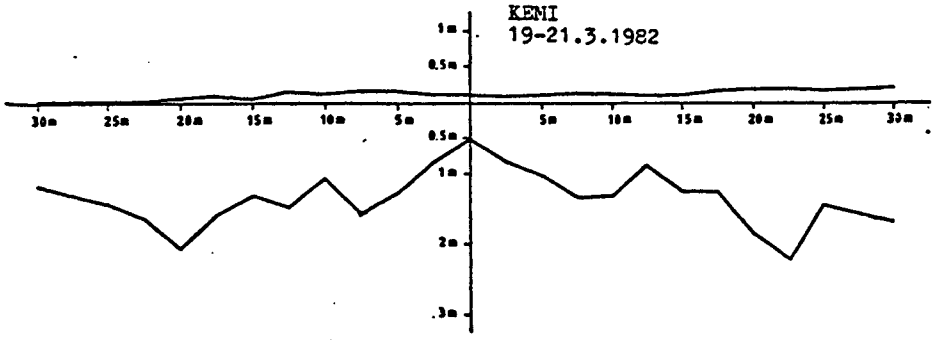

Fig. 4. Typical cross section of an old channel (Kannari 1982).

The ship performance in ice is commonly described by determining the speed that is reached in certain ice conditions using the propulsion power as a parameter. If the ice condition is level ice then the resulting plot is called h_i-v curve. This kind of performance curve may be determined also for an old channel using either the mean or the minimum thickness of the brash ice as the ice parameter. The limiting performance is now in principle given by the point of zero speed. This, however, is optimistic in practice as ships tend to stop when the speed falls below 4 knots as the ice resistance varies much and without much inertia the ship is stopped at any slightly higher peak in ice resistance.

Earlier ice class rules stipulated directly the required propulsion power level. This was given as a function of the displacement, breadth and stem angle. This formulation was deemed not to give proper description of the ice going capability of vessels and thus a more thorough description was sought for. The approach of setting the power level directly was not chosen in formulating the performance requirements but rather the approach of starting from the ice resistance leading to the propulsion power. This way a proper allowance may be given to more efficient systems changing power to thrust.

It was decided that ice channel is to be the design ice condition for the ice strengthened merchant vessels in the Baltic. The rationale behind this decision is that the vessels are always escorted through the ridged ice at sea but they must be able to proceed to ports from the beginning of the old channel. The decision to base the performance requirements on resistance requires a formulation for the channel resistance. In order to improve the existing formulations of the channel resistance, an extensive model test series was carried out. The first task in the model tests was to develop a method to model the old navigating channels. The challenge here is to produce in model scale fine enough brash ice - the ice pieces are typically round and about 30 cm in diameter in full scale. This leads to ice pieces of 1 - 2 cm diameter in model scale in the commonly used scales. Also the cross section of natural channels was to be reconstructed. The method developed produces very natural channels, see Fig. 5.

Fig. 5. The old channel produced in model scale (photo M. Wilhelmson).

The model test series was carried out using the basic model of MT Tervi with a variation of length and depth. A photograph from the tests is shown in Fig. 6. The test results were used to develop an equation for the pure channel resistance. The starting point in the improvement was the earlier formulation based on modelling the brash ice using soil mechanics (Malmberg 1983). The essential improvement compared to the earlier development was the modification of the channel thickness due to the ice displaced by the vessel, see Fig. 7. Also a velocity term was included in the channel resistance. The brash ice resistance was thus

$$R_{ch} = C_1 \cdot (H_F + H_M)^2 \cdot \left(B + 1.85 H_F - \frac{2H_F}{\tan\psi} \right) \cdot (0.15\cos\varphi_2 + \sin\psi \sin\alpha) + \\ + C_2 \cdot L_{par} \cdot H_F^2 + C_3 \cdot \left(\frac{L \cdot T}{B^2} \right)^3 \cdot H_M \cdot A_{wf} \cdot Fn^2 \quad (2)$$

where the angle φ_2 is the buttock line angle at the point y=B/4, ψ the flare angle, A_{wf} the water plane area of the bow ship and Fn the Froude number. The brash ice thickness at the ship side may be calculated based on geometry and it is

$$H_F = 0.26m + (H_M \cdot B)^2.$$

The constants in the equation are C_1=0.85 kN/m^3, C_2=0.04 kN/m^3 and C_3=1.2 kN/m^3. The results were validated using full scale observations of channel resistance in zero speed, see Fig. 8. A more detailed description of the derivation is to be found in Riska et al. (1997).

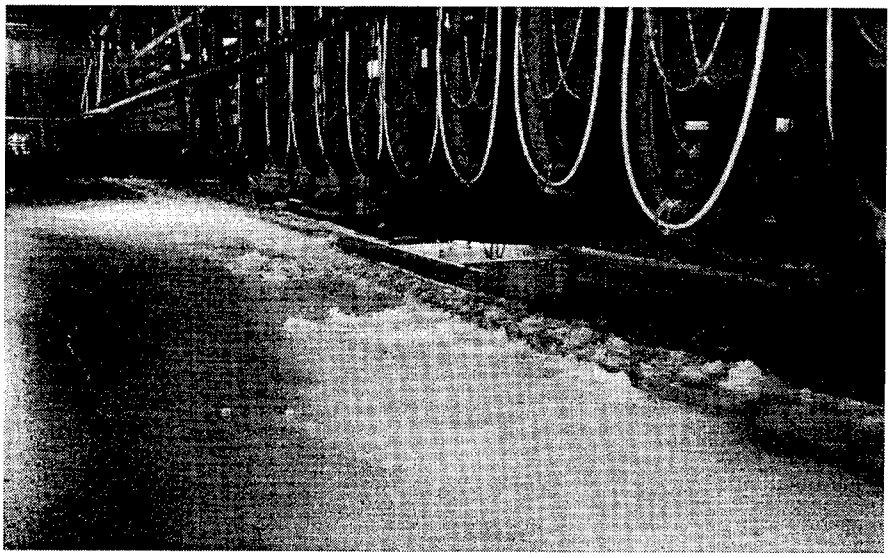

Fig. 6. MT Tervi in model tests (photo M. Wilhelmson).

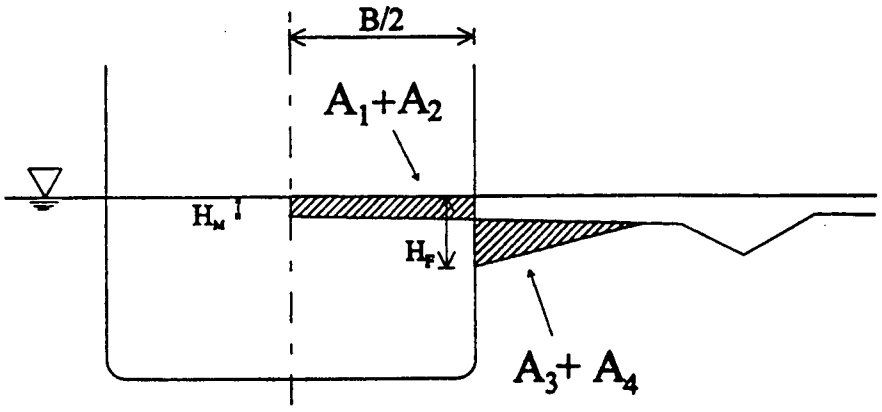

Fig. 7. The channel cross section modified by the ship, note especially the channel thickness at the ship side, H_F.

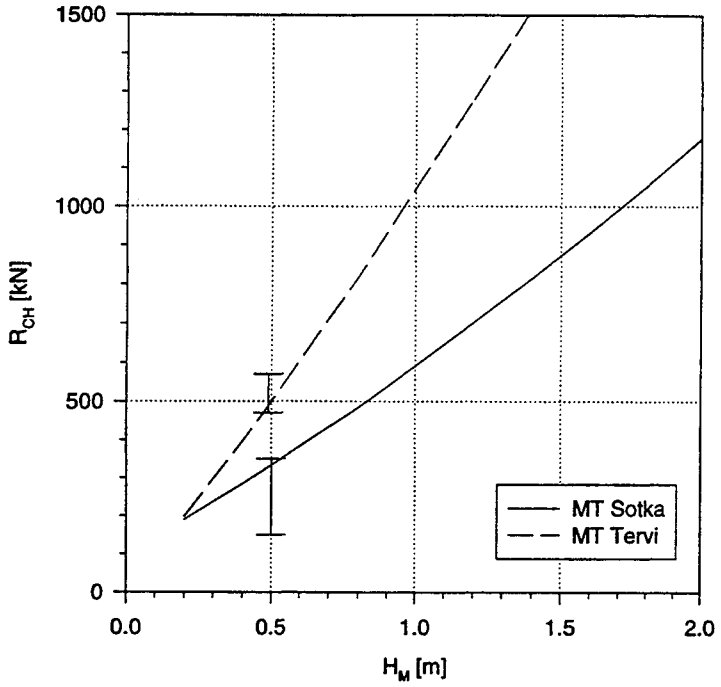

Fig. 8. The calculated low speed channel resistance for two vessels with some full scale results plotted versus the channel thickness at the centerline of the channel H_M (Riska et al. 1997).

5. FORMULATION OF POWERING REQUIREMENTS

The final task in developing the powering requirements to be included in the Finnish-Swedish ice class rules is to determine the required shaft power P_S from the ice resistance. For this purpose the resistance was first divided into two parts, one due to the consolidated layer forming on top of the brash ice in the channel ($R_{con}(h_{con},v)$) and one due to the pure channel resistance ($R_{ch}(H_M,v)$), where h_{con} is the thickness of the consolidated layer and v ship speed. The resistance due to the consolidated layer is assumed to be equal to the level ice resistance of the same thickness and the formulation for it is developed based on earlier research results, see e.g. Lindqvist (1989). The total ice resistance in these low speeds is, ignoring the open water component,

$$R_i(h_{con}, H_M, v) = R_{con}(h_{con}, v) + R_{ch}(H_M, v). \quad (3)$$

The thrust available to overcome the ice resistance is called sometimes the net thrust. This net thrust T_{NET} at any speed can be related to the bollard pull thrust T_{BP} by an approximate equation

$$T_{NET} = f(\frac{v}{v_{ow}}) \cdot T_{BP} \quad (4)$$

where v_{ow} is the open water speed of the vessel. The speed dependency is assumed here to be in form of the function f(.) which takes into account the open water resistance. This function is assumed to be of parabolic form:

$$f\left(\frac{v}{v_{ow}}\right) = 1 - \frac{1}{3} \cdot \frac{v}{v_{ow}} - \frac{2}{3} \cdot \left(\frac{v}{v_{ow}}\right)^2 \quad (5)$$

The propulsive power required at the bollard pull condition can be determined equating the zero speed ice resistance with the bollard pull. First, however, a relationship between ship power P_s and bollard pull must be found. This is given by an empiric bollard pull criterion (tornblad 1987)

$$T_{BP} = C \cdot (P_S D_P)^{2/3} \quad (6)$$

where D_p is the propeller diameter and the constant C is so called quality factor of the bollard pull. Units in equation (6) are kN, m and kW, respectively. The quality factor is usually for a single screw ice going vessel 0.85. Now, finally, the required propulsion power is obtained from these approximate relationships involving the bollard pull power and the net power available to overcome the ice resistance as

$$P_S(h_{con}, H_M, v) = K_e \left[1 - \frac{1}{3}\frac{v}{v_{ow}} - \frac{2}{3}(\frac{v}{v_{ow}})^2\right]^{-3/2} \frac{R_i(h_{con}, H_M, v)^{3/2}}{D_P} \quad (7)$$

where K_e is a constant which depends on the number of propellers

and type of machinery and propeller. For a single screw vessle its value is taken as 1.44 and for a double screw vessel as 1.18. This selection of the value for K_e corresponds to value of the quality factor, C=0.78; this reflects the fact that merchant vessel propellers are not optimised to bollard pull condition. The constant K_e may, however, be taken 10 % lower for better propulsion systems in ice like e.g. diesel-electric machinery or CP propeller.

The decision was made that the design situation for the ice class IASuper is an old channel the thickness of which is at he middle 1 m with a 10 cm thich consolidated layer on top of it. IASuper vessels are assumed to be able to proceed with 5 knots speed in heavy channels which have not been navigated during the last day (this allows the consolidated layer to grow). IA class vessels shall be able to proceed in old channels of 1 m thickness with a speed of 5 knots. These channels have not been consolidated i.e. a ship (icebreaker or other merchant vessel) has previously navigated through them breaking the consolidated layer. Thus the proposed power requirements are

IA Super $\mathbf{P_{S,Req} = P_S(10\ cm, 1\ m, 5\ knots)}$

IA $\mathbf{P_{S,Req} = P_S(0, 1\ m, 5\ knots).}$

The result of these requirements for existing vessels was checked. The result is shown in Fig. 9 where the result of the proposal is divided with the actual installed propulsive power of investigated vessel and plotted versus the dead weight of the vessel. It is noted that only for some of the smaller vessels, dead weight less than 4000 t, an increase in the propulsive power is foreseen. This, however, has already been anticipated in the navigational practice where restrictions to navigation are placed for IA vessels. These restrictions depend on the vessel dead weight and usually the limit goes up to 4000 tdw, and smaller vessels than the limit are not assisted into the ports.

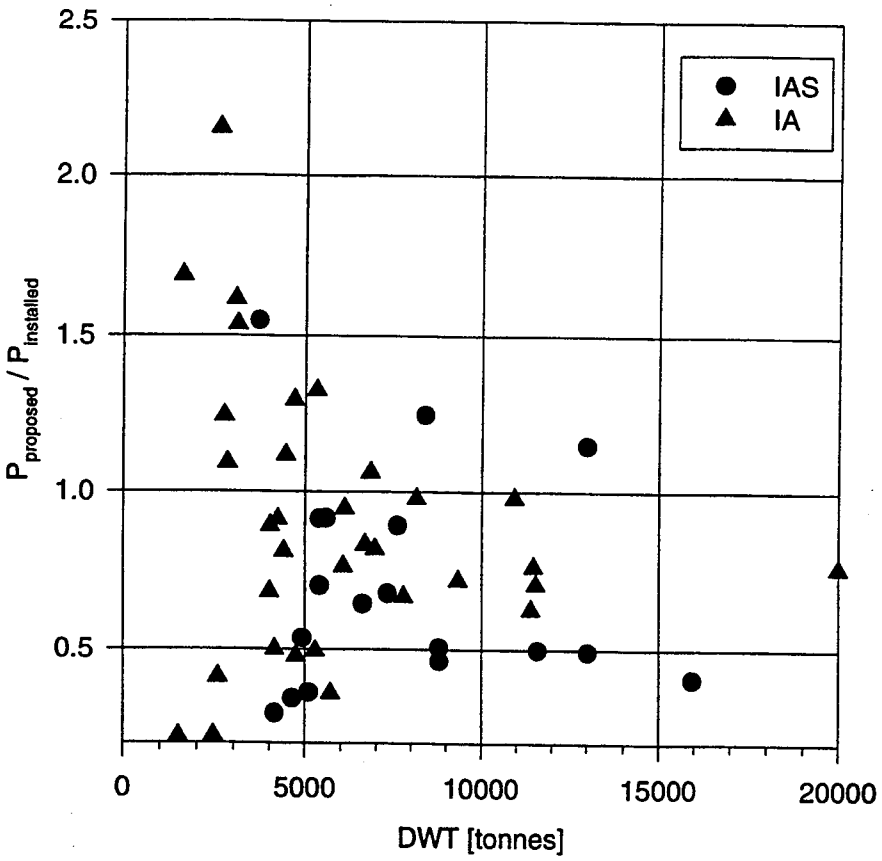

Fig. 9. The proposed power requirement divided by the installed one and plotted versus the dead weight calculated for a set of existing vessels (Riska et al. 1997).

6. CONCLUSION

The winter navigation in the Baltic may be investigated from a system point of view. The system is naturally driven by the import and export transportation where the flow of goods is carried by ice strengthened merchant vessels. In the system a balance between the number of required icebreakers, merchant vessel performance and number of winter ports should be found. The icebreakers ensure the continuous flow of vessels in and out of ports. As the assisting speeds and time for required assistance depend on the merchant vessel performance, some requirements must be placed on the propulsive power of them. This article described how these requirements were determined starting from the channel resistance of vessels.

The analysis of the channel resistance may be termed classic as it is based on the earlier formulations of the resistance. The main improvement is the inclusion of the speed dependency and a more thorough treatment of the channel thickness. The division into the bow and midbody resistance was, however, retained. An improvement to these formulations may be sought in analyzing the bow breaking resistance more thoroughly. Full scale observations suggest that the adfreeze between ice pieces plays an important role in ridge resistance - similarity could be drawn to brash ice resistance.

The ridged ice field where level ice and/or leads are dispersed with ice ridges was not selected to form the design point of merchant vessels. Icebreakers are assumed to be available once ridges are encountered. The question when icebreaker assistance becomes necessary for a merchant vessel is, however, an important one. This limiting point is determined by the size of ice ridges encountered. Thus the present investigation will be continued with analysis of ridge resistance and the need of icebreaker assistance.

Acknowledgements

The work to update the powering requirements was a team effort with the Finnish and Swedish maritime authorities and especially Mr. Gunnar Edelmann, Captains Jan Stenberg and Anders Backman acting as supervisors. The research team is very grateful of their unflinching encouragement. The team consisted of Ms. Päivi Lehtinen, Dr. Pentti Kujala, Mr. Max Wilhelmson, Kim Englund and Topi Leiviskä.

References

Kannari, P. 1982: Performance of a Product Tanker in Ice Channel [in Finnish]. Helsinki University of Technology, Ship Hydrodynamics Lab., Rpt M-100, 98 p.

Lehtinen, P. 1993: Performance of Ice-Navigating Ships in the Northern Baltic in Winter 1993. Helsinki University of Technology, Arctic Offshore Research Centre, Rpt M-182, Otaniemi, 50 p.

Lehtinen, P. 1994: Observations on Ice Navigation Performance of Ships in the Baltic in Winter 1994. Helsinki University of Technology, Arctic Offshore Research Centre, Rpt M-187, Otaniemi, 35 p.

Leppäranta, M. 1993: A Review of Analytical Models of Sea-Ice

Growth. Atmosphere-Ocean, 31(1993)1, pp. 123-138.
Malmberg, S. 1983: On the Mechanism of Getting Stuck in Ice [in Swedish]. M. Sc. Thesis, Helsinki University of Technology, 69 p.
Riska, K., Wilhelmson, M., Englund, K., Leiviskä, T: Performance of Merchant Vessels in Ice in the Baltic. Winter Navigation Research Board, Research Report No 52, The Finnish Maritime Administration & the Swedish Administration of Shipping and Navigation, Helsinki, 73 p.
Tornblad, J. 1987: Marine Propellers and Propulsion of Ships. KaMeWa, Sweden, 237 p.

FSA - A NEW METHODOLOGY TO PROMOTE SAFETY AT SEA

Risto Jalonen
Helsinki University of Technology, Ship Laboratory
Espoo, Finland

Tony Rosqvist
VTT Automation
Espoo, Finland

Summary

This paper gives an outline of the Formal Safety Assessment (FSA) process and its application to the regulatory process of the International Maritime Organisation (IMO). The backgrounds of the traditional and the new approach to the management of safety in shipping are reviewed. The five steps that form the framework of FSA are described and discussed in the following text as well as the concept of risk, which is the key element of this modern methodology. Some recent applications of FSA and their results are introduced. A discussion of the FSA-methodology is also presented, followed by some recommendations and, finally, the conclusions.

1 INTRODUCTION

Shipping is governed by several rules. The safety-related rules of today are predominantly prescriptive, quite often derived as a reaction to a disaster at sea. Thus, the traditional way of rule-making has lead to a multitude of rules. The cost-effectiveness of a new rule and its coherence with other rules have probably not been the leading thoughts in the rule-making process. As a result of public pressure and haste to make a change, the new rule may not be an optimal solution to the problem. The effects of some rules may be even questionable. In this respect, a new, more scientific way of thinking, i.e. a formal methodology supporting the regulatory process, might be more useful. This paper deals with FSA, which is a newly developed methodology striving for better regulation-making.

This paper describes first the traditional approach in regulatory work, the "Regulation by Disaster"-approach. Its positive results are presented in the light of some recent maritime accident statistics. Some negative features of the prevalent practice of regulatory work are highlighted, too. An outline of the FSA process, with its development and all its phases, is given. Some recent examples of the application of this new approach are also presented. The FSA methodology, its applications and the results are discussed in chapter 5. Some recommendations for future work and for the development of FSA are also given. Concluding remarks are given in the last chapter.

2 MARINE INCIDENTS, ACCIDENTS & DISASTERS AND THEIR REPERCUSSIONS

The fields of shipbuilding and shipping are regulated by a large number of rules. Some of them are based on the requirements of international (or regional) conventions, amendments and codes, while others are based on the rules developed by the classification societies. These rules may govern e.g. the design and workmanship of the structures of the ship in order to guarantee a hull, which will tolerate the loads and stresses exposed on the ship during its lifetime. The regulations form the minimum qualifications for safe shipping and insurance. The rules stem mainly, but not solely, from the motive to protect the property, i.e. the ship and its cargo. National and international rules have also been developed to safeguard human life and nowadays ever more often, to protect the environment. International rule-making for shipbuilding and shipping is concentrated at the International Maritime Organisation, IMO.

The prevalent practice of rule-making, which has been applied at nationally and internationally has traditionally been based on reactive work, promoted by major accidents. This methodology has lead to a continuously growing number of different kind of rules and regulations. International conventions like SOLAS, ICCL and MARPOL are examples of the results of IMO's safety-related work. The world-wide statistics of total losses from the last three decennials express a decreasing trend in loss rate (Fig. 1). Therefore, it is impossible to totally deny the benefits of the present rule-making methodology.

Most major marine accidents, such as the disasters of the passenger ships and passenger ro-ro ferries: Titanic (1912), Morro Castle (1934), Andrea Doria (1953), Scandinavian Star (1990) and Estonia (1994) as well as the tankers Torrey Canyon (1967), Amoco Cadiz (1978) and Exxon Valdez (1989), have had remarkable effects on the maritime legislation.

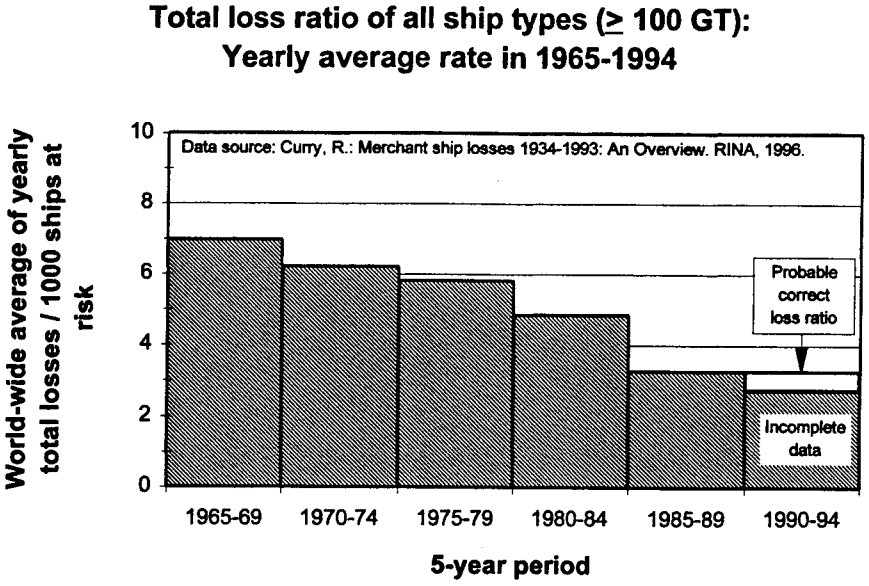

Figure 1. One indicator of the development of safety at sea. The yearly average rate of total losses (per 1000 ships year) in world shipping during the past 30 years, based on* [1] and [2].

However, this traditional rule-making methodology has been criticized too, due to several reasons. Some commentators have named it with the phrase "*Regulation by Disaster*". In principle, this prevailing methodology applied in rule-making can be described as a heuristic methodology. After each major accident a pressure in the society to develop new, better regulation arises. A change in legislation or some other outstanding acts by the authorities are often required in order to prevent similar accidents in future[1]. After the change, the society and the media usually will calm down, and start again to believe that the safety level is acceptable, at least until the next disaster happens.

There exists a big problem in setting an acceptable level of safety, if the only method to measure its efficiency is retrospective, e.g. counting of casualties. The views of the public, the media, the experts, the shipping companies, the authorities and other stakeholders may be different, when considering the acceptance of risks and the ability/willingness to pay for their reduction.

[1] The principle of prevention of accidents (and promoting safety in general) is mentioned in the law, which concerns the accident investigation in Finland (375/85). It is also written in the accident investigation reports prepared by the Accident Investigation Board.

A disaster-driven approach to rule-making may easily lead to inconsistency. The rules of one special area of interest, say fire protection, may become incompatible with the existing rules of some other area if all possible consequences of the new rules and the possible conflicting matters are not thoroughly considered (Fig. 2). If the public pressure, delivered, amplified or even generated by the media, is high enough, the negative contributions of this pressure (it has also positive contributions!) to regulators may increase the risk for new, not-thought-of consequences.

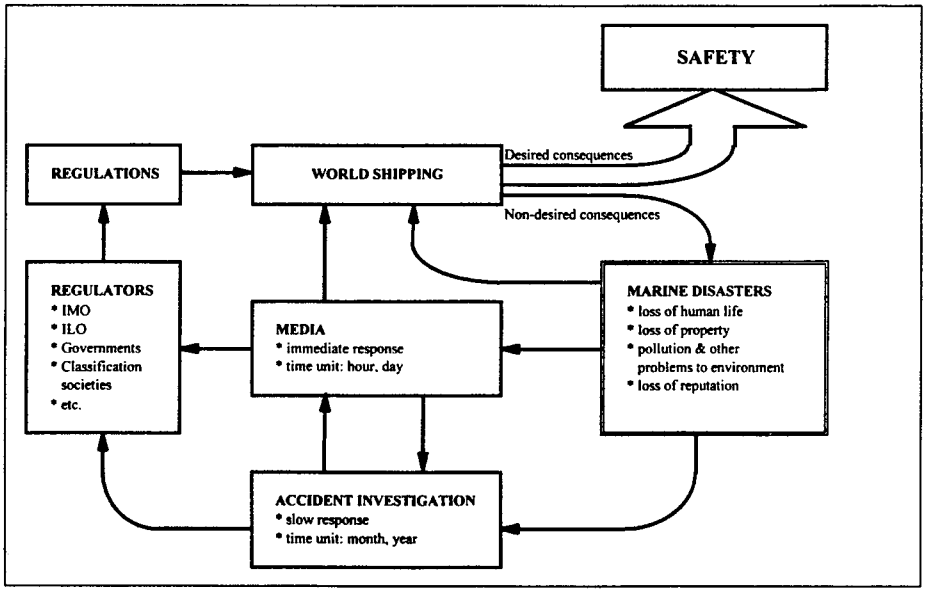

Figure 2. A sketch of the traditional, re-active type of rule-making process, "Regulation by Disaster". [2]

This approach may also lead to differences in national rules, because the political pressure for a change in rules is highest in the state where a recent major accident has happened or the citizens of which perished, whereas the economical counter force is usually much higher elsewhere. The OPA 90 rules in US waters, which followed the Exxon Valdez incident in 1989, have been named as one typical example of this kind of development. The lolling problems of some double-hulled tankers [3], for instance, have been pointed at, as an example of the non-desired consequences of these rules.

[2] This model is a modified version of the figure 1.1, "Årsaksstatistikkens rolle i et informasjonssystem", presented in: Wiencke, P.M.: Modeller og metoder for analyse av kollisjoner og grunnstotinger. Prosjekt: Årsakssammanhenger ved kollisjoner og grunnstotinger. DNV Forskningsdivisjonen, Rapport nr. 80-0080, 1980.

One completely different kind of problem within the accident-driven rule-making approach is that its result, a new rule, presumably does not give any protection against other, dissimilar types of hazards. A vast majority of the hazards is known by the sailors and even by shipping companies and classification societies. However, if no major accident have yet happened, the hazards, although often appearing in incidents, very seldom have had as dramatic an influence on the maritime legislation process or rules, as accidents. The reactive approach to safety seems to require major accidents and their dramatic consequences in order to function.

If our intention is to promote safety, it may be more effective to learn from the numerous incidents and minor accidents, than just from total losses and major accidents, the number of which is more limited (Fig. 3). A pro-active approach does not need realised human, environmental or economical losses to make things work. In this approach, the risk is the impetus.

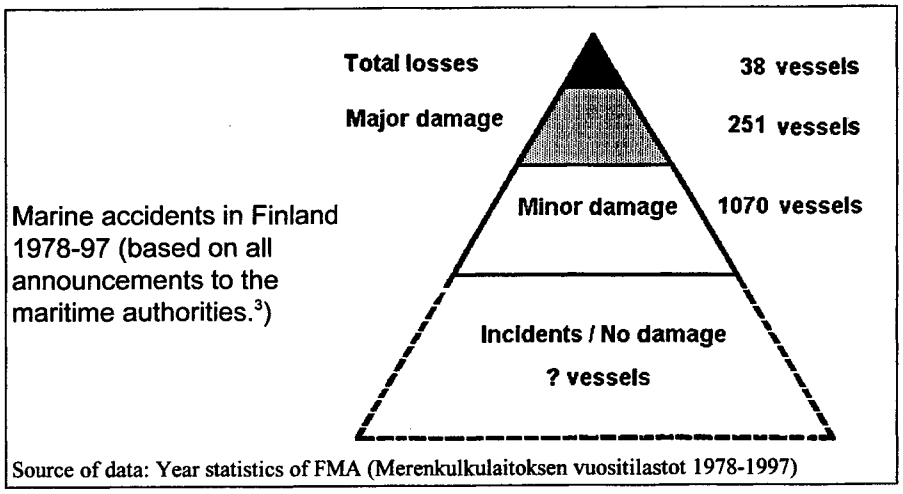

Figure 3. The accident triangle: total losses, major and minor damages.[3]

One of the most dramatic evidences of the negligence of the importance of incidents was presented in the final report concerning the capsizing of mv Estonia [4]. Several bow door failures or part-failures had occurred in the Baltic Sea and the North Sea before 1994, but they had only minor effects on the structures of the existing fleet of ro-ro ferries. The problems with the autopilot and stability of the ro-ro vessel Zenobia were well known by several incidents before the tragedy off Cyprus in 1981, but again, hardly

[3] This data is based on all marine accident announcements to the maritime authorities in Finland in 1978-1997, regarding all registered vessels (i.e. vessels with the following limitations: 1.11.1993- : $L \geq 15$ m, 1978-30.10.1993: $GT \geq 19$). [3]

anything had been done to reduce the risks [5]. These are just two examples of an unfortunately endless list of similar cases all over the world.

Almost every major accident seems to have a history of precursors, i.e. a number of incidents, which have given early warning signs of the apparent risk. Unfortunately, they are often not found until an exhaustive accident investigation is made. However, for one or more reasons, the necessary acts to reduce the risks have in such cases been neglected whether consciously or unconsciously. The list of incidents with bow door failures or part-failures in the final accident report of m/v Estonia [4] is very impressive, but one must remember that it was put together after the accident, when it is much easier to pick up these cases apart from the thousands of other minor accidents and incidents.

3 FSA - FORMAL SAFETY ASSESSMENT

Besides the traditional approach described above, a new, more systematic methodology in rule-making process has been recently introduced to the maritime regulators. This methodology, which is called the Formal Safety Assessment, was presented to the IMO by the United Kingdom in 1993 [6].

FSA was developed by the UK Marine Safety Agency (MSA) as a response to Lord Carver's report [7]. This report pointed to a scientific safety regulation, based on quantified assessment of risk, on analysis of costs and benefits and on international agreement as to what level of risk is acceptable. In essence, the report recommended a performance based approach to safety aspects in ship design and technology. It also presented a vision of a long term move to a so-called "safety case", which is a widely applied approach to safety in other industries, e.g. the chemical, nuclear and offshore industries. The apparent problems of creating an internationally governed, but still uniform concept of a "safety case" lead MSA to develop the idea further and to apply the same analytical processes to rule-making.

The FSA-concept has been suggested to be evaluated by the member states. Several trial applications of FSA have been performed, some of which are shortly described in this paper. It is anticipated, that this new, promising tool in the rule-making process in shipping will be introduced in the SOLAS convention in the near future [8].

Formal Safety Assessment is a risk-based, systematic and sturdy approach to safety management. It is a rather new methodology for rule-making, which applies a scientific approach of thinking. If correctly applied, FSA applications are transparent, traceable and repeatable. Recommendations for

rule-making prepared by independent FSA-teams on some area of interest should therefore not be contradictory. FSA acts in a pro-active way: it should put emphasis not only on risks which have lead to accidents, but also on risks which may have severe consequences. An ideal FSA has been characterised with the following attributes [9]:

- Well structured, systematic, comprehensive
- Objective, rational
- Auditible, repeatable, well documented
- Defensible, reliable, robust

FSA consists of the following five steps (Fig. 4):

1. Identification of hazards
2. Assessment of risks
3. Generation of risk control options
4. Cost benefit assessment of the risk control options
5. Decision making recommendations concerning the options available

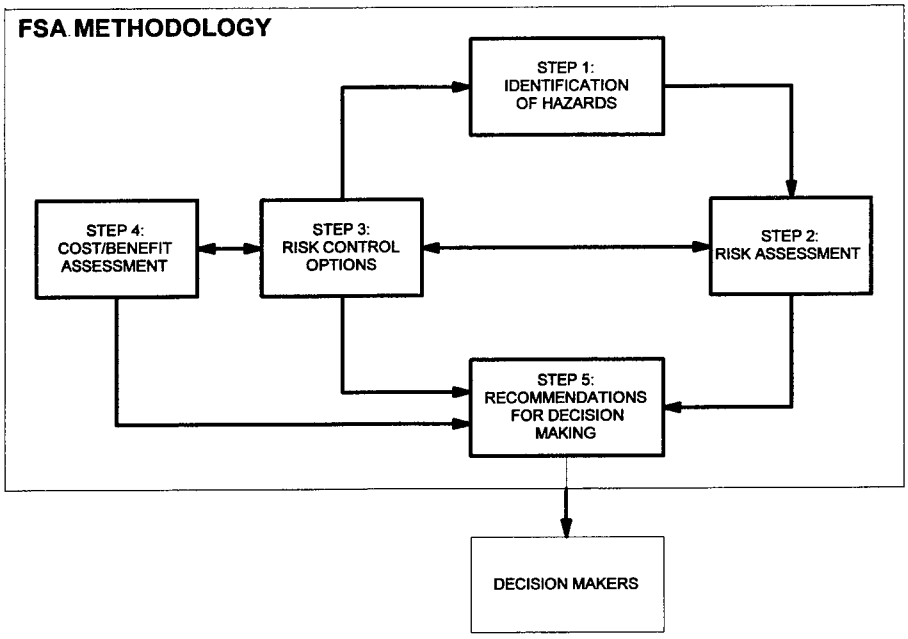

Figure 4. The structure of Formal Safety Assessment

All relevant grounds and arguments, models and data applied by the FSA-team leading to recommendations for decision making in regulatory work

are documented in a systematic way. Thus they can be discussed and, if necessary, revised if essential changes in the shipping take place.

The application of FSA should lead to cost-efficiency in rule-making, which probably leads to a better balance in the development of safety even if the funds available for this purpose are limited.

3.1 HAZARD IDENTIFICATION IN SHIPPING

The first phase of FSA, identification of hazards, is formed of two parallel parts. The first one is a description of the subject, e.g. a ship type. It should identify all essential features of this vessel type and include an understanding of the management features that are associated with the operation of the ship type [10]. Collection of relevant accident and incident & failure data as well as employing standard hazard identification technique(s) (e.g. structured brainstorming meeting) are used to identify all hazards involved, which may come into question with the subject undergoing the FSA study (e.g. a generic ship type).

The result of this phase is a list of all relevant accident scenarios. Peachey [11] makes it simple: the first phase of FSA should give a comprehensive answer to the question: *What can go wrong?*

3.2 THE ASSESSMENT OF RISKS

FSA is a risk-based approach to the management of safety. The risk is a combination of probability and consequences. These two contributors to each risk can be presented in a risk matrix (Fig. 5). The risk may be determined by its attributes qualitatively or quantitatively.

The purpose of the second step in the FSA process, risk assessment is to quantify the distribution of risk, i.e. to make the risk measurable or, at least comparable to other risks. Risk is composed of the probability or frequency of an occurrence and the severity of this occurrence. The frequency can be estimated by analysing accident data from databases and/or by expert judgement, if necessary.

The risk matrix is sometimes divided into three sections. The concept of acceptable risk and ALARP are then presented. Risks in the ALARP-area's higher risk zone (near the upper limit) can be tolerated only if it is impracticable to reduce the risk or if penalties involved are grossly disproportionate to the improvement gained. In the low risk zone, the risk can be considered as tolerable if penalties of reduction would exceed the improvement. The area in the upper right corner of figure 5 is composed of

such risks that cannot be tolerated. Some problems connected to the limits of the ALARP-region are discussed later, in chapter 5.

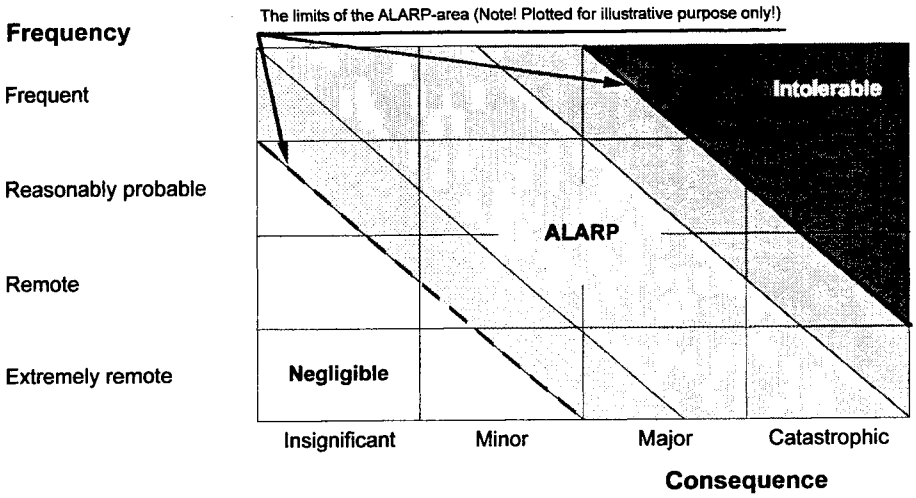

Figure 5. An example of a risk matrix.[3] *The ALARP-region*[4] *is restricted by its upper and lower limits. Note! The ALARP-limits are not included in IMO Guideline* [9]. *Such limits, if agreed upon and applied, will have far-reaching effects!*

The quantification of all risks in FSA makes it possible to concentrate on the high risk areas (i.e. the zones near the upper right corner in Fig 5) and to identify and evaluate the underlying factors which influence the levels of risk. These factors may include: design, maintenance, management, human elements, training, communication etc. Thus, the second step of FSA should identify and address systematically those factors which have a significant influence on the risk. Fault-tree and event-tree models can be constructed to obtain quantitative risk measures.

In simple terms, step 2 of FSA gives an answer to the questions: *How likely is it?* and *What consequences might it have?* [11]. The assessment of risks makes it possible to identify the principal risk contributors, thus enabling a systematic screening procedure and addressing of the most important factors influencing the risk. This important part of a systematic way of thinking has been missing from the traditional rule-making process.

---

[3] Note! The scales of consequence and frequency are qualitative in this risk matrix. A quantitative risk matrix has numerical scales for both consequence and frequency. The frequency may be presented as per one ship year, per 1000 ship years or alike.

[4] *ALARP = As Low As Reasonably Practicable*

The assessment of the risk contributors can be performed by constructing a fault- and event tree risk model. The output from the risk model can be presented in the form of a so-called F-N curve, which gives the relationship between consequence (N = number of fatalities) and likelihood of an occurrence (F = frequency) in a graphical form. F-N curves can also be constructed according to historical data on fatalities (Fig. 6).

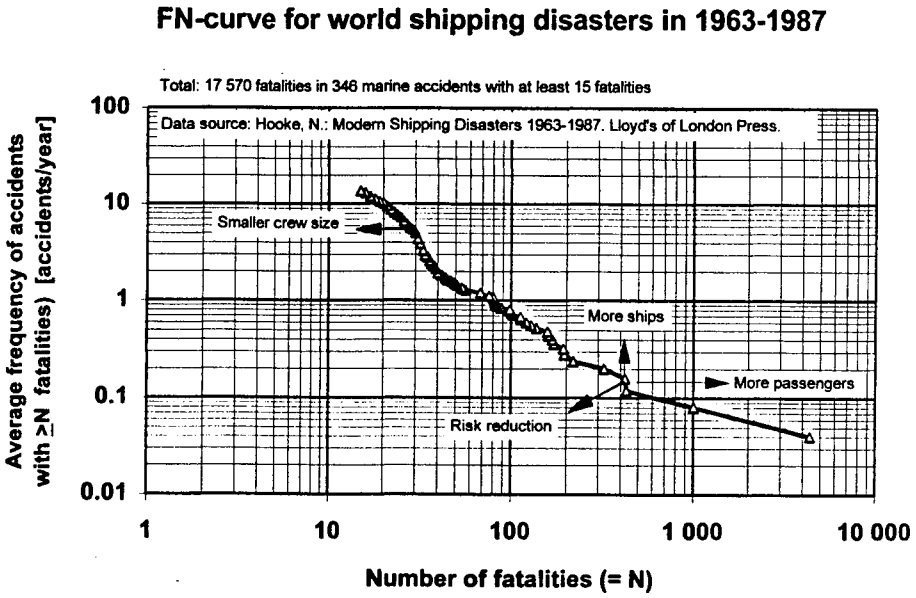

Figure 6. F-N curve presenting the distribution of fatalities in world shipping disasters (with $N \geq 15$) for the period 1963-1987.

3.3 DEVELOPMENT OF RISK CONTROL OPTIONS

The risks identified in step 2 can be divided into different categories by using the currency of risk. Some risks may be negligible, others may be high. It is most important to define the high risk areas and concentrate the safety management efforts there. In the third step of FSA different kind of risk control measures (RCMs) should be sought by considering systematically the possibilities of prevention, mitigation, active and passive, technical and procedural etc. alternatives. Thereafter, appropriate RCMs can be grouped together into risk control options (RCOs). The effectiveness of each option should then be assessed by repeating step 2, where the change in risk level can be estimated. Step 3 has been described [11] by asking: *What can be done in order to avoid it?*

3.4 COST BENEFIT ASSESSMENT

FSA differs from the traditional approach to risk management by regulation in two phases. One is the risk assessment (step 2) and the other is the cost-benefit analysis (CBA) (step 4). The fourth step of FSA is an established technique, which makes it possible to find out what are the most effective measures that are available to reduce the risks. This involves assigning a monetary value to the change of risk as well as to the costs of the risk control option.

The costs are composed of initial costs, running costs and cost of enforcement. The time span applied in CBA should be the lifetime of the vessel, so maintenance costs, if any, should be included. All benefits in different categories (averted statistical losses of life/property/environmental damage etc.) should also be considered when evaluating the potential benefits of the RCOs under comparison. Sensitivity analysis connected to the results of step 4 is an important part of the study, because it gives confidence *with respect to the* assumptions made.

Step 4 gives information concerning the questions: *How much do different risk control options cost?* and *How effective are the risk control options considered for the regulatory process?* [11]. The application of cost-benefit assessment makes FSA a more rational approach to rule-making, when compared to the traditional methodology.

3.5 RECOMMENDATIONS FOR DECISION-MAKING

FSA has to be considered as a tool for decision making, not a decision maker by itself. All the information generated in steps 1-4 should be used to help in decision making. The risks, costs and benefits may affect differently on the various persons, groups of persons or organisations in the context. Thus, all relevant aspects connected to the risk control option(s) under consideration have to be thoroughly considered, when performing the final stage of FSA.

The different groups of stakeholders should always be identified at the outset of each FSA procedure, and to some extent be included in the expert panel, to ensure comprehensive views in those FSA-analysis steps that rely on expert opinion. This is also the most important way of building up commitment to and understanding of the decisions made.[5] All the information gathered during the previous steps of FSA should be reviewed to identify the preferred regulatory option(s) in general, and then in more

[5] See chapter 5 for reference.

detail in order to reach a sufficient equability for each relevant stakeholder (e.g. passengers, crew, company etc.).

Thus, the final phase of FSA is shortly described by the question (and the answer): *What should the regulator do?* [11].

4 APPLICATIONS OF FSA - SOME RECENT EXPERIENCES

The following four sub-chapters present some recent trial applications of the Formal Safety Assessment:

4.1 BULK CARRIERS

The number of bulk carrier losses has been high for several years. The loss of life in these accidents within the time period 1971-1994 has, according to the information given in [12], been over 2700. A total of 99 bulk carriers and 654 people onboard have been lost in the period 1990 to mid-May 1997 [13]. Many of these ships have been lost without any survivors, so the causes and contributing factors to the accident may not have been found. This has made it more difficult to prepare well founded proposals for more efficient legislation preventing further losses.

Nevertheless, as a response to the high casualty rate of this ship type, several studies have been carried out to determine the best safety measures for bulkers. One of the studies performed was the analysis prepared by DNV[6] [14]. In this study the individual risk for seamen on bulk carriers was considered as not unacceptable[7]. However, the societal risk, which can be expressed by using F-N curves, of at least 15 years old bulk carriers exceeded the upper limit of the ALARP-region applied. Based on the F-N curve and the ALARP-limit, it was concluded that, considering the risk control options (RCOs), the focus should be put on the reduction of severe losses, i.e. such scenarios which can escalate quickly to total loss.

Water ingress to cargo hold no. 1, it's flooding and the subsequent failure and loss of the watertight integrity of the bulkhead between holds no. 1 and 2 and the following domino-effect ending with the sinking of the ship, was one of the scenarios studied. The implied cost of averting a fatality (ICAF =

---

[6] DNV = Det Norske Veritas

[7] The Fatal Accident Rate (FAR = number of fatalities per 10^8 hours) for bulk carriers for the period 1978-1995 was: FAR = 6.6. As a reference, the corresponding Fatal Accident Rate for oil and gas production for the period Apr 87-Mar 91 was: FAR = 30.9. [14]

Net annual cost of measure / Reduction in annual fatality rate) for the proposed RCO of upgrading the bulkhead between cargo holds no. 1 and 2, was calculated for bulk carriers of different size and age groups. As a result of this FSA-study it was concluded that the presented option was a cost effective safety measure for the majority of bulk carriers.

Another risk control option, the Enhanced Survey Programme, has also been effective to a certain extent. However, during February 1997, the first two bulk carriers subject to the ESP, *Albion Two* and *Leros Strength*, were lost. Even with these losses, it is stated that ESP will reduce the risk of ship loss by about 40 %. The applicability of the procedures used in FSA were demonstrated in this study [14].

Quite recently in 7-11 December 1998 the 70th session of the Maritime Safety Committee (MSC) has agreed with a United Kingdom proposal to carry out a FSA-study of bulk carriers, in order to help IMO decision-making on bulk carrier safety in future [15]. According to this reference, the FSA-study is, among other things, also likely to consider further, if the newly adopted SOLAS chapter XII on bulk carrier safety should also apply to bulk carriers which are shorter than 150 m in length or equipped with a double-skin.

4.2 HIGH SPEED PASSENGER CRAFT

The High Speed Catamarans and monohulls (HSC) represent a fast growing sector of shipping. It is a rather new sector of passenger traffic, which utilises many applications of new technology. As a newcomer, it suffers from a relatively limited time for experience. Thus, the evaluation of safety level of these HSC-vessels and an appropriate regulation for them is not an easy task. Two trial applications of FSA have been performed concerning HSC. The first one was submitted by MSA (UK) [16] and the other by Sweden. The former concentrated on catamarans, the latter, which was the result of the work of the Joint Nordic Project [17] had a wider scope, including monohulls.

In the MSA FSA the overall frequency for the worst case scenarios for large HSCs (with $N \geq 100$) was assessed to be $4.5*10^{-4}$ per ship year (with an uncertainty range from $2*10^{-4}$ to $10*10^{-4}$. This risk is high. It is located in the intolerable region, if the proposed criteria, presented in [17], are applied. Collision was identified as the principal risk contributor in the MSA FSA. The Nordic FSA, which also put emphasis on the variation between different craft and routes, made a somewhat lower estimate of the range of risk level, but it exceeded the upper limit of the proposed acceptance criteria (e.g. at $N \geq 100$, $F = \sim 0.1$ per 1000 ship/years) as well.

The MSA FSA [16] identified numerous Risk Control Measures, which were combined to Risk Control Options. The common RCO 3, which will enhance more effective procedures and better adherence to them by the operational staff, was ranked first in the list of three recommended RCOs in this study. The Potential Loss of Life (PLL) reduction of these RCOs varied between 0.025-0.042, when the basic risk level was 0.077, for the total risk, and 0.065 for collision. The estimated Cost per Unit Reduction in Risk (CURR) for the three recommended options varied in the range 0.17-0.55 million USD. The Nordic Joint Project ranked the factors having the greatest improvement potential: *Competence and Training* as the first factor among frequency reducing factors, *Passive Safety* and *Evacuation System and Procedures* as the main factors reducing consequences [16].

4.3 HELICOPTER LANDING PLATFORMS ON PASSENGER VESSELS

The third example of trial applications of FSA presented here was focused on Helicopter Landing Platforms (HLA) on non ro-ro passenger ships. The background of these studies lies in the requirement in SOLAS regulation III/28.3:

Passenger ships, other than ro-ro passenger ships, of 130 m in length and upwards, constructed on or after 1 July 1999, shall be provided with a helicopter pick-up area approved by the Administration having regard to the recommendations adopted by the Organisation.

The interesting point in this case is that this requirement has already been adopted as a SOLAS amendment. Thus, it differs from the general purpose to apply FSA as a tool of decision-makers before requirements are adopted. There has been two separate FSA studies on this subject, one performed jointly by Norway and ICCL [18], the other performed by Italy. Both FSA studies have been commented in the report of the Intersessional Correspondence Group on HLAs [19].

In the Norwegian FSA study [18] it was considered that the SOLAS regulation III/28.3 requiring HLAs is not recommended to be implemented for non ro-ro passenger ships. This conclusion seemed to be based on the cost efficiency of this safety measure, which was estimated to be more than one, possibly two, orders of magnitude less cost efficient than the normal level of commonly implemented safety measures in OECD countries.

According to the report [19], in principle, the approach adopted in both FSA studies is reliable. The Group also concluded that the Italian study,

although different in the scope and approach to the Norwegian FSA [18], broadly supports its conclusions. Nevertheless, the Group discovered *"considerable uncertainties in the evaluation of both the risk benefit likely to arise from using HLAs, and the costs of providing them"* [19] on the passenger ships.

So far, before MSC 71 (in May 1999), it is unclear how this issue will be pursued by the Member States. However, this requirement is one part of SOLAS.

4.4 TRANSPORTATION OF DANGEROUS GOODS ON PASSENGER/RO-RO CARGO VESSELS

This trial application of FSA was one part of the study programme "Safety Risks in Finnish Maritime Transportation", which was initiated by the Finnish Maritime Administration and carried out by the VTT Manufacturing Technology and the Ship laboratory of the Helsinki University of Technology. This trial application was also a first step in starting to build-up the expertise and experience, on a national level, required to carry out or audit formal safety initiatives [20].

The focus of this application was laid on the passenger/ro-ro cargo vessel, a ro-pax. This ship type has a growing popularity especially in the European waters and in short sea shipping. The reason for this is the increased cargo capacity for trucks, trailers and containers when compared to more traditional passenger car ferries. The level of risk implied to the passengers on a ro-pax vessel caused by cargo units containing dangerous goods as permitted by the IMDG Code and the SOLAS Convention was under scrutiny in this study.

As a result of the first structured expert group session, which was facilitated by a Group Decision Support System in a PC-network, over 80 accident scenarios were identified and the corresponding risks assessed (Fig. 7). The highest fatality risk to the passengers onboard was connected to a fire related to the IMDG cargo. The risk analysis performed, however, supports the impression that the fatality risk that IMDG cargo related fires impose upon the passengers of a ro-pax vessel, is reasonably low.

The most significant contribution to the estimated risk to passengers when considering the risks related to IMDG fires is represented by the possibilities of fires starting on the cargo decks and escalating to the IMDG-cargo units stowed on the decks. Temperature controlled cargo units (e.g. trailers equipped with refrigerator units) were found as the most likely single source of cargo deck fires.

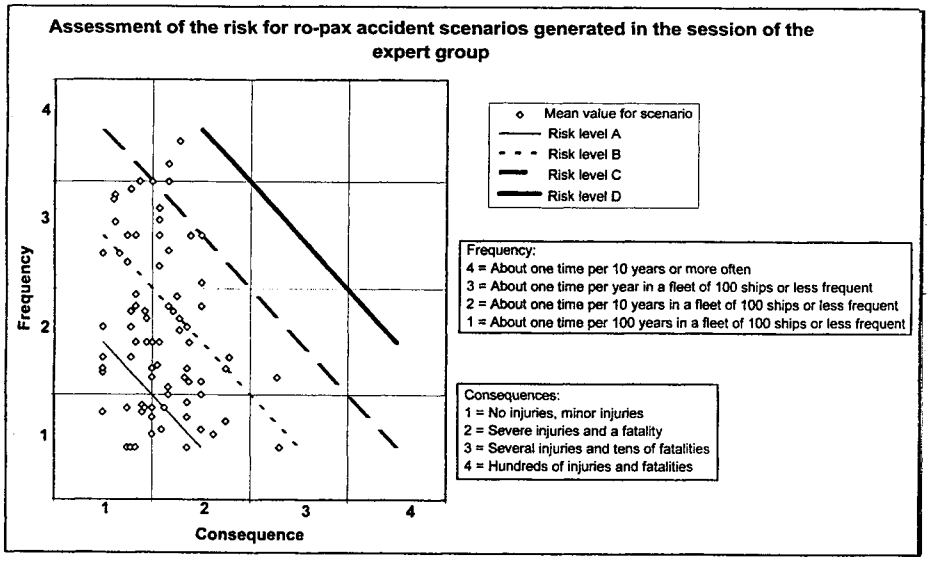

Figure 7. The risk matrix generated in the session of the expert group

Four different risk control options (RCOs) were derived and compiled for further assessment in this trial application of FSA. All of them belonged to the group of preventive measures against hazardous events. Preventive measures are usually considered more beneficial than mitigating measures due to the fact that the overall frequency of accidents can be reduced. The estimated total lifetime costs (for 20 years) of these RCOs varied in the range 0.1-0.5 million USD. Cost-benefit analysis ranked RCO3[8] as the most cost effective risk control option among the four options considered here. The estimated Cost per Unit Reduction in Risk (CURR) of this ranked most recommendable option was about 60 % of the CURR-value of the next cost effective option.

The results of this first national FSA-study in Finland have, quite recently, been submitted to the Finnish Maritime Administration who will continue with the issue by evaluating and considering the results.

5 DISCUSSION AND SOME RECOMMENDATIONS

Formal Safety Assessment seems to be a promising new method supporting the decision making for maritime regulations. FSA offers a more rational approach than the traditional "Regulation by Disaster"-method. The many

[8] RCO3: Inspection of the electrical and mechanical condition of the temperature controlled units before their loading onboard; development and procurement of an electrical tester unit.

advantages of FSA that were presented in the beginning of chapter 3 can be agreed upon. However, the FSA methodology is new, and therefore it may include some aspects that should be discussed further.

The acceptability of risk is a problematic question. However, in the five steps of FSA it is not specifically required to make judgements on the acceptability. If the limits of the ALARP-area are set, the acceptance limits are defined, but this is not a necessity for a complete FSA-process. At present FSA can be seen as a comparative method [22], but perhaps it may be developed to an absolute method in the near future.

Risk communication may also be a problematic issue. The terminology used in the FSA studies may not be easily understood and this may cause frustration or even misunderstandings. National and international work-shops, seminars, courses and lectures for persons involved in performing FSA or utilising its information are also recommended to reduce these kinds of problems. Unbiased and understandable risk communication is just one of the numerous needs for a successful implementation of the risk assessment process [23]. However, the future of FSA may depend on it.

The FSA procedure utilises expert judgements and expert sessions. It is important that all relevant stakeholders are identified at the beginning of the FSA-process and that the experts consider the views of all stakeholders in the sessions and in the judgements. The importance of selecting a sufficient group of suitable experts, so that it represents a required broad range of knowledge, domain experience and skills has been emphasised [11]. It should also be pointed out that the composition of the expert sessions should be such that the main results of its work would not change, even if a majority of its members would be changed.

The experts are often busy people and it is sometimes extremely difficult to make decision on a suitable day for a session. Weeks may pass very easily if it is necessary to have several persons available in the same meeting room at the same time. New information technology, Group Decision Support Systems, PC-networks, E-mail etc. are very useful and promising tools when such practical problems are to be solved.

Although there is some redundancy in the methods that can be applied, the need for probabilistic data supporting quantitative assessment has been repeated quite often (e.g. in [8]). Accident and incident data bases, if available, are in principle very useful in this respect. However, some problems may arise when considering the relevance of older data and data concerning distant occurrences. If some special type of accidents are rare the scope may have to be enlarged. It must still be remembered that

environmental conditions, cultural habits, e.g. adherence to rules and the applied requirements themselves may differ quite a lot between different areas and cultures of the world.

The reliability of information on losses of human life in accidents at sea is one example concerning the missing or incomplete data. Some sources of information (e.g. [2]) may present detailed information concerning total losses of ships ($\geq$ 100 GT). Total losses may often lead to a high number of fatalities, but numerous losses of life may also occur without the loss of the ship. The exact number of all world fleet fatalities per year and the corresponding accident types are unknown. The authorities should report to IMO all serious and very serious casualties on a standard format within six months, but several Flag States, e.g. Panama, Honduras, Malta, Philippines and Russia, seem not to be hasty in fulfilling this task [21]. Much more work is needed to develop more complete and reliable data bases serving questions on fatalities and other details in shipping accidents.

As a last recommendation it is suggested that the expertise and preparedness of the national FSA team should be maintained and developed further with other trial applications or reviews of FSA. Otherwise the experience and expertise gained may dry out.

6 CONCLUSION

FSA is not a solution to all safety problems in shipping. It is not intended to be a substitute for the established procedures at IMO. Nevertheless, it is an approach which may considerably influence the decision making process by introducing a new, more scientific and systematic methodology that applies modern techniques in risk assessment and cost-benefit analysis. FSA is a tool which can give decision makers the necessary information needed for well grounded rule-making. When correctly applied it gives also an opportunity to review or even inspect all the data, calculations, results and judgements, which together form the basis of the recommendations concerning new proposals for shipping regulation. This enforces all States to well prepared proposals for new rules. Thus, FSA has probably a great potential for promoting safety at sea.

REFERENCES

1. Curry, R.: Merchant Ship Losses 1934 - 1993 : An Overview. Trans. RINA, Vol. 138, pp. 1-20.

2. Lloyds Register Casualty Return 1993. Lloyds Register of Shipping, 1994.

3. Moore, C., Neuman, J. & Pippenger, D.: Intact Stability of Double Hull Tankers. Marine Technology, Vol. 33, No. 3, July 1996, pp. 167-182.

4. The Joint Accident Investigation Commission of Estonia, Finland and Sweden: Final report on the capsizing on 28 September 1994 in the Baltic Sea of the ro-ro passenger vessel mv Estonia. Edita Ltd, Helsinki 1997.

5. UTREDNINGSRAPPORT beträffande ro-ro/passagerarfartyget ZENOBIAs förlisning på redden utanför Larnaca, Cypern, den 7 juni, 1980. Den särskilda undersökningskommissionen, Sjöfartens haverikommission, Juli 1981.

6. IMO 1993: International Maritime Organisation, MSC62/24/3.

7. Lord Carver: Safety Aspects of Ship Design and Technology. House of Lords Select Committee on Science and Technology, February, 1992.

8. Emi, H. et al: Basic Investigation on Formal Safety Assessment - Risk Analysis of Fires in Ship Engine Rooms. NK TECH Bulletin, Vol. 15, 1997

9. Skjong, R.: Formal Safety Assessment, Analysis Tool For Shipping Safety and Economy, DNV Shipping Seminar, Helsinki 1998, April 29th.

10. Riding, J.: Formal Safety Assessment (FSA): putting the risk into marine regulations. Trans IMarE, Vol. 109, Part 2, pp. 185-192.

11. Peachey, J.: Formal Safety Assessment for Shipping: Developing its potential at the IMO. Jim H Peachey, 6th October 1997.

12. IMO and the safety of bulk carriers. Schip & Werf de Zee, Maart 1998, pp. 6-16.

13. Beech, E.: Don't balk at bulkers. Safety at Sea International, January 1996.

14. Cost Benefit Analysis of Existing Bulk Carriers. A Case Study on Application of Formal Safety Assessment Techniques. Det Norske Veritas, Paper series No. 97-P008, 1997.

15. Maritime Safety Committee - 70th Session: 7-11 December 1998: Maritime Safety Committee to further review bulk carrier safety. IMO News, 1998/4

16. Revision of the HSC Code, Formal Safety Assessment, Trial application to high speed passenger catamaran vessels, Final report. Submitted by the United Kingdom, IMO, DE 41/INF.7, 12 December 1997.

17 Joint Nordic Project for Safety Assessment of High-Speed Craft Operations. Final Report. Prepared for the Maritime Administrations in Denmark, Finland, Norway and Sweden. Co-ordinated by SSPA Maritime Consulting, October 1998. Report No 974125-1.

18. Report on Formal Safety Assessment of Helicopter Landing Area on Passenger Ships as a Safety Measure. Det Norske Veritas, Report No. 97-2053.

19. Formal Safety Assessment (FSA), Report of the Intersessional Correspondence Group on Helicopter Landing Areas (HLAs). Submitted by the United Kingdom, IMO, MSC 70/14, 11 September 1998.

20. Rosqvist, T., Tuominen, R., Jalonen, R., Salmikuukka, J & Reunanen, M.: Formal Safety Assessment - Trial Application of FSA to the Transportation of Dangerous Goods on Passenger Ro-ro Cargo Vessels. VTT Manufacturing Technology, Report VALB 353, 1998.

21. Middleton, I.: Small sinking somewhere: not many dead. Seatrade Review, October 1998, pp. 6-9.

22. Peachey, J: Overview of the 5 Steps of FSA. Formal Safety Assessment Seminar. International Maritime Organisation, 18th May 1995.

23. Reunanen, M. & Tuominen, R.: Assessment of Risks in Sea Transports by the Systematic Methods of Risk Analysis. Maritime Safety '97, VTT Symposium 176, Technical Research Centre of Finland, Espoo 1997.

AIS – The beginning of a new era in maritime safety?

Göran Granholm
VTT Manufacturing technology
Espoo, Finland

Abstract

The new functional specifications of a Universal AIS, as approved by the IMO, brings up a whole range of new possibilities when it comes to improving safety of maritime traffic. According to some experts, the Automatic Identification System, or AIS for short, will change the way we look at maritime communication. It may also become the most important safety improving technology since the introduction of the radar.

The system works on a dedicated VHF radio frequency on which a communication link is established completely autonomously without user involvement and without the need of a land based station to co-ordinate the radio traffic. This makes the communication services available both shore-to-ship and directly between ships where ever they meet. The underlying technology called STDMA (Self Organised Time Division Multiple Access) uses accurate GPS time as a common time reference for allocating individual transmission time slots. The objective is to incorporate the Universal AIS in SOLAS Chapter 5, making the equipment mandatory on ships fulfilling certain criteria. The Finnish and Swedish Maritime Administrations have been working hard to promote this technology and to make it the new standard internationally.

The core function is the basic position report containing identification, position, speed and heading broadcast from each vessel and available to all others within the reach of VHF radio. This message is updated with an interval of a few seconds to produce an accurate and up-to-date traffic image in the VTS or onboard other ships. In addition to the position report a number of other predefined messages have been defined. The possibility to construct new message structures based on free format binary data or text strings provides an attractive base for developing totally new services.

The AIS, when commonly in use will dramatically improve tracking and surveillance possibilities in VTS, improve the quality of the onboard traffic image and detail of traffic information. Automating routine tasks by means of AIS will decrease communication workload and risk of misunderstanding. All these benefits will in the long run most probably take the overall safety of navigation a great leap forward.

Introduction

The need to spot and positively identify targets participating in a specific traffic situation has always been a crucial part of safe navigation. When radar first was introduced and gradually became a one of the most important instruments on the bridge the possibilities to position the own ship in relation to other vessels, navigational aids and land especially in bad visibility were dramatically improved.

In order to resolve potential conflicts between two vessels a verbal communication has to be established between them. Because the radar only indicates the existence of a target the task still remains to establish the identity of the vessel to call. In a dense traffic situation it is of utmost importance to call the vessel by its identity to avoid confusion and unnecessary alerts on other vessels. By traditional means the identification process may take up valuable time and resources in a stressed situation.

As technology developed, many attempts were been made to solve the identification task including DSC and radar transponders etc. It was not until the developers succeeded in combining the GNSS, the VHF radio and the computer into one unit and in creating a communication protocol that made the use of the system reliable and easy to operate that the major break-through was made. The resulting technology that was later to be known as the Automatic Identification System, AIS. From the original idea to the final product the AIS has developed technologically and made its way through a range of standardisation and regulatory bodies. Gradually the AIS has gained acceptance to the point that it is now expected to become a globally requirement through the SOLAS convention. The milestones so far have been the approval of performance standards in IMO and technical specifications within ITU. These standards take the AIS a great step beyond just position and identification reporting. It makes it possible to implement numerous advanced safety-improving functions for use in both ship-to-shore and ship-to-ship communication. The first devices conforming to the approved ITU specifications have now hit he market.

1. Technology

The AIS device is an integrated hardware unit consisting of a GNSS receiver (GPS), a radio transceiver operating on VHF frequencies and of a computer module. The AIS automatically performs bi-directional data communication with other AIS units operating on the same radio frequency. The basic function of the AIS is to read geographical position from the integrated GPS receiver and to continuously transmit this together with identification information over the radio link. The AIS receives similar information from all other AIS units within the radio cell. The AIS in itself does not display received information. To make use of information from other targets and to take advantage of the more advanced functions the device must be connected to en external system, typically a computer based system such as an electronic chart display digital radar or a computer running dedicated communication software. Interaction between the AIS and external devices complies with the NMEA-0183 standard.

1.1 The radiolink communication protocol

The communication is based on the time division approach. In TDMA (Time Division Multiple Access) communication time is divided into slots of equal length. A number of slots build one frame. In the AIS system the frame consists of 2250 time slots and is one minute long. The can AIS use available time slots to transmit its data and the remaining time is spent receiving data from other units. The position report fits into one time slot. In order to synchronise transmission so that data collisions can be avoided a protocol called STDMA (Self-organised TDMA) is used. This protocol depends on a common time source for synchronisation of the time frame between the AIS units and a procedure in which the AIS attempts to occupy free time slots for data transmissions the synchronised time frame. Each AIS performs pre-allocation of time slots i.e. continuously informs the others about which slots it will use for transmission in the next frame. The time synchronisation source is the 1PPS pulse from the GNSS receiver. Because the protocol automatically resolves slot allocation conflicts a high level of message throughput and bandwidth efficiency can be maintained. The individual units will determine their own transmission schedule, the data link is automatically maintained without the involvement of a master stations. Land based AIS units can be defined as base stations but they will not control slot allocation of

remote units. They can however adjust reporting rates if required. Base station AIS units use FATDMA (Fixed Allocation TDMA) insisted of STDMA which makes it possible to link base stations together in a land based AIS network.

1.2 The interface and defined messages

The following description of AIS interfaces applies to the GP&C R3 AIS transponder. The AIS unit is interfaced through dedicated data ports. An auxiliary port is provided for connecting to external data sources for vessel motion and position. This also makes it possible to bypass the internal GNSS receiver for position information. Input messages supported by the GP&C AIS are:

GGA	Global Positioning System Fix Data
GSA	GPS DOP and Active Satellites
GSV	GPS Satellites in View
HDT	Heading - True
OSD	Own Ship Data
ROT	Rate of Turn
VTG	Track Made Good and Ground Speed
ZDA	Time and Date

High quality and redundant position sources can thus be used. A differential correction receiver can also be connected directly to the AIS. The message content is accessed through a data interface port using NMEA-0138/IEC 1162-2 compatible message format.

The message telegram has the following structure

$ PAIS , <Tgm Id> , <DATA> * <FCS><CR><LF>

The Telegram identification <Tgm Id> determines the type of message to follow in the data field. Messages can be input messages sent to the AIS for transmission by an onboard application or output messages received by the AIS from other stations. Most

important messages are presented in the table below. Same Tgm Id numbers are used both on input and output telegrams

Tgm Id	Telegram
.	
01	AIS standard Position - Own
02	AIS standard position - Remote
04	Addressed text telegram
05	Addressed text telegram - Acknowledgement
06	Broadcast text telegram
07	Addressed binary telegram
08	Addressed binary telegram - Acknowledgement
09	Broadcast binary telegram
0A	UTC date and time
0B	GNSS status
0C	Data link status
0E	Identification data
0F	Vessel data
10	SAR standard position
11	SAR standard position remote
...	
FF	

A number of messages related to data link management and backward compatibility are not shown in the list.

Position reports include vessel identification (MMSI number), rate of turn, Navigation status, Position, speed, course and heading, time stamp, accuracy indication, AIS operation mode, data terminal equipment and channel. Position is given as latitude-longitude values with a resolution of 1/10,000 degrees. Binary and text telegrams contain blocks of binary or 6-bit ASCII data. Maximum size per telegram is 156 characters or 114 bytes of binary data. The SAR messages are reserved for airborne vessels participating in search and rescue operations.

1.3 Capacity

The system capacity can be defined in different ways, e.g. number of messages or position reports per minute, number of vessels that can be handled simultaneously in one radio cell or the area that can be covered by one AIS unit. These capacity measures are dependent of each other in different ways. The time frame is divided into 2250 time slots. As one position report takes one time slot this number of position reports could theoretically be handled. In practice the throughput can be high but not 100% and there are also other types of messages transmitted. With export rates of once every minute up to 2000 vessels could share one radio frequency. The ITU specification does however include a dynamic reporting rate scheme that allows vessels to adjust the rate of position reports according to how they currently move. The reporting rate is changed automatically. This feature greatly increases the capacity in terms of number of ships.

I case the data link becomes overloaded a time slot reuse procedure is initiated. On a digested data link slot reuse can be either automatic or intentional. Automatic slot reuse occurs when a time slot pre-allocated by another AIS unit is unintentionally used. The units are then unaware of each other. A randomly varying slot offset is applied to ensure that unintentional collisions do not continue for the same pair of AIS sets. If the AIS detects that there are no free time slots available or the channel saturation exceeds a given limit the AIS may intentionally occupy a time slot already reserved by another AIS. The decision, which time slot to 'steal', is based on geographical distance from own position to the different AIS stations. This, in effect, decreases the radius of the current radio cell leaving always the closest targets visible. The data link will therefore never collapse due to overloading.

The different information types are valid for a different time period and thus need a different update rate. To make optimum use of the available bandwidth a reporting scheme has been agreed in which information is updated accordingly.

Table 1

Type of information	**Reporting rate**
Static Information	Every 6 minutes and on request.
Dynamic Information	Dependent on speed and course alteration according to Table 1
Voyage related information	Every 6 min, when data has been amended, and on request
Safety related message	As required

Vessels state of motion	**Reporting interval**
Ship at anchor	3 min
Ship 0-14 knots	12 sec
Ship 0-14 knots and changing course	4 sec
Ship 14-23 knots	6 sec
Ship 14-23 knots and changing course	2 sec
Ship > 23 knots	3 sec
Ship > 23 knots and changing course	2 sec

Ship Reporting Capacity - the system should be able to handle a minimum 2000 of reports per minute, to adequately provide for all operational scenarios envisioned.

2. Applications

Due to the autonomous operation the AIS performes both ship-to-shore and ship-to-ship communication without the assistance of specific base stations. Ship-to-shore applications typically have to do with Vessel Traffic Services (VTS) and are linked to tracking and surveillance tasks of the VTS while ship-to-ship applications are closer related to traffic situation awareness. Although it may, in practice, be difficult to find applications that strictly fit into one category the different types of AIS functions could be grouped as follows

- Surveillance applications
- Applications improving traffic situation awareness
- Communication applications
- Information service
- Search and rescue

In the following some important functions are described. Some of them are directly implemented in the AIS software; some rely on external software to present the content of standard messages and some base on new proprietary messages implemented on the text or binary messages.

2.1 Tracking and surveillance

The direct benefit from using AIS in connection to other navigation systems comes from the immediate identification and positioning of remote targets that allow automatic tracking of these targets onboard or in a VTS. Especially in a VTS a great part of the time on duty consists of identifying targets on the radar screens. AIS based tracking has some major advantages compared to traditional radar tracking. Firstly,

tracking is independent of environmental conditions such as weather, topography etc. Secondly, the system does not loose track of a target because tracking is not based on a set of previous observations but on single near real time position reports. AIS data can easily be recorded to produce an on-shore "black-box" of the AIS traffic in the area. Because the identification of the targets is reliable shore-based AIS data records can be used to trace back pollution sources.

Despite these advantages the AIS will not replace the radar but instead be used as complementary information source. This is because AIS is a co-operative tracking system and requires the tracked vessel to voluntarily report its identification and position whereas the radar can track targets not willing to reveal this information. Another reason is that not all vessels will be carrying transponders even in the future. A function has been developed that allow radar targets tracked in a VTS, for example, to be transmitted over the data link together with identification if known. These can then be received as if they were AIS targets by vessels carrying AIS. In the newest software release a new message based on the broadcast binary telegram has been developed to take care of this. Radar broadcasts can therefore be distinguished from true AIS targets.

2.2 Situation awareness

Frequently updated exact position, speed and course information help to produce more detailed and informative traffic situation displays. If turning rate is transmitted a curved 'path prediction' vector can be drawn for the target. The path prediction serves as an indicator of turning motion and pints to the position where the vessel would be in the near future if speed and turning rate remained unchanged. The 'path prediction' gives immediate visual information about the turn velocity and speed and eliminates the need to observe the target for long times before turning can be noticed.

2.3 Communication

Direct one-to-one communication is not expected to be performed over the data link partly because entering text using a keyboard is naturally much more time consuming and takes more attention than talking on the VHF and partly because of capacity

limitations. Pre-defined short messages could however easily be selected and transmitted to one or a group of receivers. If a standard vocabulary is adopted the messages could be number coded and appended with optional arguments. The message would then be decoded by the receiver application. This would shorten the message length and the message content could be presented in any language. The risk of misunderstanding because of language problems could be reduced.

2.4 Information service

The AIS is ideally suited to transmit short informative messages either directly to a specific receiver or broadcast to all vessels in a region. The function could be used by the VTS to broadcast notices to mariners, weather information etc. Tests are being made to equip weather buoys with AIS units.

2.5 Search and rescue

The new GP&C R3 transponder include messages that allow airborne and waterborne units to communicate with each other on the same frequency in a search and rescue operation. This gives totally new opportunities for the rescue control centre to organise the search and keep track of searched areas. Suggestions have been made that lifeboats should be equipped with AIS devices that would be activated in case of an emergency.

3. The Poseidon project

VTT participated in the European research project 'POSEIDON' sponsored by the European Commission and locally by the Finnish Maritime Administration. The project dealt with VTS (Vessel Traffic Services) integration and data networks and provides a logical basis for evaluating new communication systems such as the AIS.

The research work has focused on responding to a range of user requirements collected at specific user meetings organised within the project. The key message of these events was the need to reduce the overall work load of the VTS operators performing

their routine task of identifying and tracking vessels in the area. These tasks should be automated to allow the operator to concentrate on the developing of the traffic situation and to ensure safe transits. This could to a great extent be done by reducing VHF voice communication and automating identification and improving tracking functions. By introducing AIS technology these problems can be solved and at the same time the services can be made available directly onboard as well.

Within the Poseidon project a number of AIS installations were made. Two passenger car ferries, Ms Silja Serenade and ms Mariella were equipped with AIS sets connected to their integrated bridge systems and to an ECDIS software. Helsinki VTS got an AIS configured as a base station and the service ferry Ms Suomenlinna was equipped with a stand-alone AIS. Two AIS sets were installed within the Archipelago VTS. Additionally a land-based unit was installed at VTT. The equipment was delivered by GP&C Sweden.

3.1 Test Implementations

To make further use of the AIS possibilities, VTT took the task of developing new additional services. The new functions were presented and evaluated at an on-site demonstration 1-2 September this year as a part of the Poseidon project. The presentation started onboard Ms Silja Serenade on a trip from Stockholm to Helsinki and continued the next day in Helsinki. The event attracted some thirty experts from Scandinavia and the EU.

The first part of the demonstrator was devoted to ship-to-ship communication services. Onboard Silja Serenade the simultaneous departure of the own ship and ms Mariella as an AIS target was followed in real time. Demonstrated features were:

- **AIS tracking and identification.** Tracking and identification was demonstrated with a chart display based navigation software. This software directly supports the necessary AIS messages and produces a database of all received messages.

- **Path prediction**. The path prediction function is a display option intended to produce a more informative traffic image on a chart display. It consists of a trajectory forecast based on onboard measured speed, course, heading and turning

rate values. The frequently updated position broadcasts from each vessel makes it possible to produce such predictions some 1 or 2 minutes ahead

- **Passage plan exchange, ship-to-ship.** The passage plan exchange function consists of a set of waypoints picked from a predefined route plan and broadcast in an AIS message to be visualised on a chart display. The purpose of this function is to transmit data to other ships on the route plan currently in use on the vessel, so that the vessel's intentions are known to others in advance and encounter situations, for example, can be planned in more detail ahead of time

- **Exchange of text messages.** This function is based directly on the text message transmission capability of the AIS. In the future it is intended to put together a communication protocol based on standardised short messages, which will support a multilingual service in which the user can output a message in the chosen language.

- **Onboard AIS data recording and playback**. AIS data can easily be recorded and reproduced onboard or on shore, enabling e.g. a simple shore based black box.

The second day of the presentation was arranged together with Helsinki VTS and showed some VTS oriented services including:

- **Transmitting targets under radar surveillance using the AIS system.** Being a permanent radar installation, a VTS radar network can provide unbroken and wide coverage of the VTS area. AIS offers some major advantages that can be used to enhance radar-based traffic monitoring onboard. With this function, the location and identification data of the objects recognised in radar monitoring will be transmitted by the system just as if they were AIS subjects. As a result, objects need to be identified only once and other parties will be able to receive the object with their identification attached.

- **Transmitting differential corrections on the AIS network.** This is a function built into the system, by which a GPS correction signal can be transmitted on the AIS network. A DGPS-level positioning can thus be achieved on vessels without a differential receiver of their own. This correction signal, which is transmitted on

VHF, is also insensitive to weather interference, so it can be used as a backup on vessels, which normally use other differential receivers.

- **Transmitting wind data**. A mathematical model has earlier been made of the Helsinki harbour area based on wind tunnel measurements at VTT. With this model single wind measurement can be used to estimate the spatial distribution of wind speed and direction in the harbour area. The system is in use at the Helsinki VTS station and data can be obtained by vessels either by fax or over a separate radio link. Within the project the same data was transferred to the AIS, eliminating the need for further data transfer channels. In a similar way other meteorological data can be transmitted.

4. Standardisation

The technical development of the Universal AIS has been carried out under supervision of a range of regulatory bodies and performance standards and recommendations have been set. The following lists current status of the most important regulations:

IMO Resolution MSC.74(69), Annex 3, Recommendation on Performance Standards for an Universal Shipborne Automatic Identification Systems (AIS)

The 43rd session of the IMO Navigation Subcommittee, which met 14-18 July 1997, completed a draft performance standard on shipborne automatic identification systems. This performance standard describes the operational requirements for the device, but does not define the telecommunications protocol the device must use. The 69th Session of the IMO Maritime Safety Committee formally adopted that standard without change at its meeting in 11 May 1998.

ITU-R Recommendation M.1371, Technical Characteristics for a Universal Shipborne Automatic Identification System Using Time Division Multiple Access in the Maritime Mobile Band

The International Telecommunications Union Sector for Radiocommunications, Working Party 8B, met in Geneva in March 1998 to define the technology and

telecommunications protocol for this device. The draft recommendation was approved in Geneva on 7-8 July 1998. The Recommendation was formally adopted November 1998,

IEC Standard 61993-2 on AIS

On 27 July 1998, the International Electrotechnical Commission TC80/WG8-U.AIS committee began work on developing a performance, technical, operational and testing standard for the Universal AIS transponder. This standard will be developed on a fast track, with working group meetings held approximately four times per year. This standard will supersede IEC Standard 61993-1 on digital selective calling AIS transponders.

IMO Resolution MSC.74(69) Annex 3 describes the performance requirements for an AIS system, but does not define the technology used by such a system. Devices built only to MSC.74(69) will not necessarily be interoperable. ITU-R Rec. M.1371 does define the technology used by such a system, and devices built to that standard should be interoperable. However, no guarantee exists that they will be interoperable, without additional testing. IEC Standard 61993-2 will define the testing requirements, as well as interface requirements. AIS systems manufactured and sold commercially should meet all three standards described above.

ITU World Radio Conference Decisions

The 1997 ITU World Radio Conference (WRC97) designated two worldwide channels for AIS purposes. These AIS channels are 87B (161.975MHz) and 88B (162.025 MHz). WRC97 also decided to allow 12.5 kHz narrowband use in this band under certain conditions, and created two new channels 75 and 76, the old channel 16 guardband, for navigational purposes.

5. Conclusions

The new AIS concept has the potential of becoming one of the most safety improving technical aids since the radar. Its strength lies in the data transmission protocol that allows fully autonomous operation and in the strong integration of some of today's most important tools in navigation, the GNSS, the VHF and computer technology. When connected to integrated bridge systems, digital radar and electronic chart displays detailed, accurate and reliable up-to-date information is available without additional effort from the mariner. In fact, a more complete traffic image can be presented than before, leaving more time to focus on the navigation of the own vessel.

The final success of the AIS depends on how widely the technology will be adopted both as mandatory equipment and on voluntary basis. Taking again the more expensive radar as a reference case, the outlooks for the AIS seem quite favourable. An increasing number of countries, including the USA, have shifted their transponder policy in favour of the AIS.

Although the standardisation of the AIS technology has advanced, many of problems still remains to be solved before the vast possibilities can be fully exploited. Regional differences concerning traffic structure, environmental conditions etc. will call for different kinds of solutions and services. Regardless of the level of sophistication a minimum performance is ensured if a common standard can be agreed upon. The current plans aim at making AIS a requirement by the year 2002. How this will be achieved remains to be seen in the near future.

Published by

VTT

Vuorimiehentie 5, P.O.Box 2000, FIN-02044 VTT, Finland
Phone internat. +358 9 4561
Fax +358 9 456 4374

Series title, number and report code of publication
VTT Symposium 199
VTT-SYMP-199

Author(s)
Nyman, Tapio (ed.)

Title

Maritime Research Seminar '99

Abstract

This publication contains the papers given at the seminar 'Marine Research 99'. Seminar was organized by the Maritime Institute of Finland, which is the joint venture between Helsinki University of Technology and the Technical Research Centre of Finland. The aim of seminar was to present to the industry the latest results of the research work done at Otaniemi. This seminar continues and promotes the dialogue between maritime research and industry in Finland.

A modern and competitive ship designer needs today deep knowledge about physical problems in ship and marine structures as the ships are becoming technically more and more complicated. Application of design methods based on 'the first principles' are essential in order to decrease the over dimensioning. Important aspect in the implementation of new methods into the ship design process is that the designer has a clear picture of the contents of the methods and understands the limits of the capabilities of the methods. The iterative nature of the ship design process must be taken into consideration - the accuracy of the design converges stepwise. This means that the methods must accept the limited information at the beginning phase.

The contents of the papers given are divided into several items from ship performance in open water and also in ice to ship safety. The topics are based on the research work carried out during the past years in different research projects. The range of topics covered by the papers of the seminar is broad, which gives a good overview on the research activity in the Institute, but at the same time the broadness inevitably limits the depth of discussion on particular problems. The lecturers are thanked for their valuable contributions.

The seminar was held at Hanasaari in Espoo. The number of participants was about 50 persons. Mr. Martin Landtman, the director of Helsinki New Shipyard, Kvaerner Masa-Yards, gave the opening address. He emphasized the importance of the close contacts and co-operation between the industry and the institute. The discussions during the day gave us evidence that the general direction of the research work carried out in Otaniemi on marine technology is correct. We hope that the participants of the seminar gained some useful ideas. The participants from industry should be thanked for making the time to take part in the seminar.

Keywords
marine research, marine engineering, meetings, shipbuilding, ice, ships, safety, Finland, design process, ship hulls, fast planing boats

Activity unit
VTT Manufacturing Technology, Maritime and Mechanical Engineering, Tekniikantie 12,
P.O.Box 1705, FIN-02044 VTT, Finland

ISBN			Project number
951-38-5275-X			K7SU00066
Date	Language	Pages	Price
February 2000	English	141 p.	C
Name of project		Commissioned by	
		The Maritime Institute of Finland (Helsinki University of Technology, Technical Research Centre of Finland)	
Series title and ISSN		Sold by	
VTT Symposium 0357-9387		VTT Information Service P.O.Box 2000, FIN-02044 VTT, Finland Phone internat. +358 9 456 4404 Fax +358 9 456 4374	

VTT SYMPOSIUM

182 Fatigue design 1998. Vol. II. Espoo, Finland, 26 - 29 May, 1998. Ed. by Gary Marquis & Jussi Solin. Espoo 1998. 274 p.

183 Euromicro Summer School on Mobile Computing '98. Oulu, Finland, August 20 - 21, 1998. Ed. by Tapio Seppänen. Espoo 1998. 189 p. + app. 4 p.

184 BALTICA IV. International Conference on Plant Maintenance Managing Life & Performance. Vol. 1. Helsinki–Stockholm–Helsinki, 7 - 9 September, 1998. Ed. by Seija Hietanen & Pertti Auerkari. Espoo 1998. 340 p.

185 BALTICA IV. International Conference on Plant Maintenance Managing Life & Performance. Vol. 2. Helsinki–Stockholm–Helsinki, 7 - 9 September, 1998. Ed. by Seija Hietanen & Pertti Auerkari. Espoo 1998. 307 p.

186 Fresh novel foods by high pressure. Helsinki, Finland, 21 - 22 September, 1998. Ed. by Karin Autio. Espoo 1998. 199 p.

187 Functional Food Research in Europe. 3nd Workshop. Demonstration of the Nutrional Functionality of Probiotic Foods. FAIR CT96-1028, PROBDEMO. Haikko Manor, Finland, October 1 - 2, 1998. Ed. by Tiina Mattila-Sandholm & Tiina Kauppila. Espoo 1998. 124 p.

188 Käyttövarmuuden ja elinjaksotuoton hallinta. Espoo, 19.11.1998. Toim. Kenneth Holmberg. Espoo 1998. 130 s. + liit. 10 s.

189 RETU. The Finnish Research Programme on Reactor Safety 1995–1998. Final Symposium. Espoo 24.11.1998. Ed. by Timo Vanttola. Espoo 1998. 206 p. + app. 62 p.

190 RATU2. The Finnish Research Programme on the Structural Integrity of Nuclear Power Plants. Synthesis of achievements 1995–1998. Espoo 7.12.1998. Ed. by Jussi Solin, Matti Sarkimo, Merja Asikainen & Åsa Åvall. Espoo 1998. 333 p. + app. 42 p.

191 SIHTI 2. Energia- ja ympäristöteknologia. Tutkimusohjelman vuosikirja 1998. Projektiesittelyt. Toim. Maija Korhonen & Rabbe Thun. Espoo 1999. 487 s.

192 Power Production from Biomass III. Gasification and Pyrolysis R&D&D for Industry. Ed. by Kai Sipilä & Maija Korhonen. Espoo 1999. 416 s. + liitt. 6 s.

193 30th R^3-Nordic Contamination Control Symposium. Ed. by Gun Wirtanen, Satu Salo & Antti Mikkola. Espoo 1999. 503 p.

194 Proceedings of the 2nd CSNI Specialist Meeting on Simulators and Plant Analysers. Ed. by Olli Tiihonen. Espoo 1999. 600 p.

195 International Conference on Product Focused Software Process Improvement. Oulu, Finland, June 22 - 24, 1999. Ed. by Markku Oivo & Pasi Kuvaja. Espoo 1999. 662 p. + app. 4 p.

196 Käyttövarmuus ja käyttökunnon hallinta. Espoo, 18.11.1999. Toim. Kenneth Holmberg. Espoo 1999. 154 s. + liitt. 15 s.

197 15th European TRIGA Conference. Espoo, June 15 - 17, 1998. Seppo Salmenhaara (ed.). Espoo 1999. 229 p.

198 4th Workshop Demonstration of the Nutritional Functionality of Probiotic Foods. FAIR CT96-1028. Functional Foods for EU Health in 2000. Rovaniemi, Finland, February 25 - 28, 2000. Ed. by Minna Alander & Tiina Mattila-Sanholm. Espoo 1999. 106 p.

199 Maritime Research Seminar '99. Espoo, Finland, March 17th, 1999. Ed. by Tapio Nyman. Espoo 2000. 141 p.

Tätä julkaisua myy	Denna publikation säljs av	This publication is available from
VTT TIETOPALVELU PL 2000 02044 VTT Puh. (09) 456 4404 Faksi (09) 456 4374	VTT INFORMATIONSTJÄNST PB 2000 02044 VTT Tel. (09) 456 4404 Fax (09) 456 4374	VTT INFORMATION SERVICE P.O.Box 2000 FIN–02044 VTT, Finland Phone internat. + 358 9 456 4404 Fax + 358 9 456 4374

ISBN 951–38–5275–X ISSN 0357–9387